

A Study of Electrical Performance of Solar Cell Arrays Based on Piece-wise Linear Approximation

A Thesis

*Submitted in partial fulfilment of the
requirements for the degree of*

DOCTOR OF PHILOSOPHY

IN

ELECTRICAL & ELECTRONICS ENGINEERING

BY

MAN MOHAN SINGH ANAND

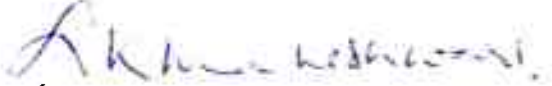
**BIRLA INSTITUTE OF TECHNOLOGY AND SCIENCE
PILANI (Rajasthan)**

MAY, 1982

BIRLA INSTITUTE OF TECHNOLOGY AND SCIENCE
PILANI (RAJASTHAN)

C E R T I F I C A T E

This is to certify that the thesis entitled "A STUDY OF ELECTRICAL PERFORMANCE OF SOLAR CELL ARRAYS BASED ON PIECE-WISE LINEAR APPROXIMATION" and submitted by Mr. M.M.S. Anand, ID No. 74E88501 for the award of Ph.D. degree of the Institute, embodies original work done by him under my supervision.


(L.K. Maheshwari)
Professor
Instrumentation Center

A C K N O W L E D G E M E N T

I am highly indebted to Dr. L.K. Maheshwari, Chief, Instrumentation Center, B.I.T.S., Pilani for his guidance and encouragement during this work.

I am thankful to Dr. C.R. Mitra, Director, Prof. N.K.N. Murthy, Administrative Dean, Prof. S.C. Rastogi, Group Leader, EEE Group and Prof. P.S.V.S.K. Raju, Chief, Information Processing Unit, B.I.T.S., Pilani for providing necessary facilities to carry out this work.

I am also thankful to Prof. M.M. Mukherji and Dr. A.P. Mathur, B.I.T.S., Pilani for their valuable suggestions. I also acknowledge my thanks to many other colleagues with whom I have had many valuable discussions.

I am thankful to Mr. G.R. Verma for typing the manuscript.


(M.M.S. Anand)

A B S T R A C T

A solar cell array consists of number of cells connected in series and shunt. The output voltage requirement decides the number of cells to be connected in series whereas the output current requirement decides the shunt connection of cells. The electrical behaviour of the array is decided by the V-I characteristics of each cell which forms the array. If the cells are identical the array V-I characteristics and thereby its parameters can be evaluated quite easily. The determination of the V-I characteristics of the array is not easy if the cells used in the array are nonidentical. The characteristics of the cells may not be identical due to the manufacturing spread or non-uniform illumination of the cells. Also the characteristic of the cells at the required environmental conditions may not be available. Therefore, one has to use the experimental characteristics of each cell and therefrom determine the characteristics of the array.

In order to analytically determine the characteristics of an array, each cell in the array is replaced by its equivalent model and the array is then analysed. The model of the cell in

common use at present involves a diode, series resistance and shunt resistance (Fig. 1.1). The relationship between the cell output voltage and current is thus nonlinear. Unless physical dimensions of each cell are available, the relationship can not yield accurate value of the voltage at a specified current. Also, since the model includes the series and shunt resistances, their values should also be known. Though many methods are available to determine these resistances, the values given by each method differ. Therefore, unless each cell characteristics are modelled accurately at the specified environmental conditions, the use of these models to determine the overall V-I characteristics does not yield accurate results. Moreover one has to handle nonlinear equations.

In the present work, a simple approach to analytically determine the solar cell array V-I characteristics has been presented. In this approach, the nonlinear experimental V-I characteristics of a cell is divided into three piece-wise linear segments and each segment is represented by a linear V-I relationship. Using the linearised characteristics, the performance of the array is analysed and the results are also experimentally verified. The problems of hot spot formation in series connection and power dissipation without any load in shunt connection are discussed. A general procedure to analytically determine the V-I characteristics of a solar cell array of any size is given and also experimentally verified for a 5×2 array.

The V-I characteristics of a solar cell and a solar cell array change with intensity and temperature. The variation of characterising parameters of a cell based upon the piece-wise linear approximation of its V-I characteristics is also discussed. The parameters describing the linear approximation are related with the parameters due to diode model of the cell (Fig. 1.1). Using the established variation of parameters of diode model with intensity and temperature, the variation of parameters due to linear approximation is explained and also experimentally verified. It is shown both qualitatively and experimentally that the solar cell array characterising parameters with intensity and temperature vary in a manner similar to that observed for a single solar cell.

The design of a 8085A microprocessor based system for the piece-wise linear characterisation of a solar cell/solar cell array characteristics is also presented. The hardware and software design of the system is given. The software design is verified using SDK-85. The assembly language conversion of the various algorithms is also given. The desired parameters of the cell/array can be selected through a key board and displayed using LED displays.

The operation of solar cell array coupled to fractional horse power DC motor and chargeable battery loads is studied. The solar cell array design taking into account the input intensity

variation is also presented. The design of regulated solar cell arrays delivering a constant-voltage or a constant-current/constant-voltage output is also given and experimentally verified.

The study is likely to be useful for applications of solar cell arrays in low power consumer applications.

+++++

TABLE OF CONTENTS

	<u>Page</u>
CERTIFICATE	ii
ACKNOWLEDGEMENT	iii
ABSTRACT	iv
LIST OF SYMBOLS	xii
CHAPTER 1 INTRODUCTION	1-25
CHAPTER 2 SOLAR CELL PERFORMANCE EVALUATION BASED ON PIECE-WISE APPROXIMATION	26-62
2.1 Introduction	28
2.2 Piece-wise Linear Approximation of a Solar Cell V-I Characteristics Employing Three Linear Segments	30
2.2.1 Maximum Power Output Evaluation	
2.3 Two Linear and One Nonlinear Segment Representation of Solar Cell V-I Characteristics	35
2.4 Experimental Study	36
2.5 Variation of Three Segment Parameters with Intensity and Temperature	41
2.5.1 Relations Between R_I , R_{II} , R_{III} and the Parameters of Fig.1.1.	
2.6 Experimental Study of Solar Cell Performance at High Intensity and High Temperature	43
2.6.1 Performance at High Intensity and Constant Temperature	
2.6.2 Performance at High Temperature and Constant Intensity	
2.7 Discussion	54
2.7.1 Parameters Variation with Intensity Keeping Temperature Constant	

	<u>Page</u>
2.7.2 Variation of Parameters with Temperature Under Constant Intensity	
2.8 Conclusions	57
References	59
CHAPTER 3 DETERMINATION OF SOLAR CELL ARRAY CHARACTERISTICS USING PIECE-WISE LINEAR APPROXIMATION	63-122
3.1 Introduction	64
3.2 Interconnection of Two Identical Cells	66
3.2.1 Series Connection	
3.2.2 Shunt Connection	
3.3 Interconnection of Two Nonidentical Cells	69
3.3.1 Series Connection	
3.3.2 Shunt Connection	
3.3.3 Experimental Study	
3.4 Analysis of Solar Cell Array (SCA)	96
3.4.1 Sub-array with Cells Connected in Series	
3.4.2 Determination of Solar Cell Array (SCA) Characteristics	
3.5 Variation of Array Parameters with Intensity and Temperature	109
3.5.1 Variation of R_I , R_{II} , R_{III} with Temperature Keeping Intensity Constant	
3.6 Conclusions	118
References	121
CHAPTER 4 A MICROPROCESSOR BASED SYSTEM FOR CHARACTERISATION OF SOLAR CELL ARRAYS	123-145
4.1 Introduction	124
4.2 Determination of Piece-Wise Linear Segments from the Given V-I Characteristics of the Cell	126
4.2.1 Evaluation of Segments I & III	
4.2.2 Evaluation of Segment II	

	<u>Pages</u>
4.3 Maximum Power and Fill Factor Evaluation	131
4.4 Microprocessor Based System	134
4.4.1 System Hardware	
4.4.2 System Software	
4.5 Design Verification	139
4.6 System Modification for the Characterisation of a Solar Cell Array	144
4.7 Conclusions	144
CHAPTER 5 PERFORMANCE ANALYSIS OF SOLAR CELL ARRAY COUPLED TO DIFFERENT LOADS	146-193
5.1 Introduction	147
5.2 SCA Coupled to R, L, C Loads	148
5.2.1 Experimental Study	
5.3 SCA Coupled to a Fractional Horse Power DC Motor	151
5.3.1 Characteristics of the Motor Load	
5.3.2 Considerations for the SCA Supplying the Motor Load	
5.3.3 Experimental Study	
5.4 Battery Charging using Solar Cell Array	166
5.4.1 Design of the Array	
5.4.2 Experimental Study	
5.5 Regulated Solar Power Supply	180
5.5.1 IC Regulated Solar Power Supply for Motor Load	
5.5.2 Constant-Current/Constant-Voltage Regulator Solar Power Supply for Battery Charging	
5.6 Conclusions	190
References	192

	<u>Page</u>	
CHAPTER 6	SUMMARY AND CONCLUSIONS	194-199
	6.1 Summary	195
	6.2 Conclusion	197
	APPENDICES	200-250
APPENDIX A	DESIGN OF HEAT SINK	202-208
	A.1 Design	202
	References	208
APPENDIX B	MAXIMUM POWER OUTPUT OF SHUNT AND SERIES CONNECTION OF TWO CELLS USING DIODE EQUIVALENT CIRCUIT OF FIG. 1.1	209-212
	B.1 Shunt Connection	209
	B.2 Series Connection	211
APPENDIX C	HARDWARE OF MICROPROCESSOR BASED SYSTEM	213-234
	C.1 System Design for the Characterisation of a Single Cell	213
	C.2 System Modification for the Characterisation of a Solar Cell Array	231
	References	234
APPENDIX D	ASSEMBLY LANGUAGE SYSTEM SOFTWARE DESCRIPTION	235-250
	D.1 Ports, Devices and Data Address Equates	235
	D.2 Subroutines	236
	D.3 Main Program	249

LIST OF SYMBOLS

A	-	area of crossection
A	-	diode quality factor
A/D, ADC	-	analog to digital converter
ϵ	-	deviation
E_b	-	back emf
E_g	-	band gap
EPROM	-	erasable programmable read only memory
FF	-	fill factor
\bar{h}	-	average heat transfer coefficient
I_F	-	forward bias current
I_M	-	current at maximum power point
I_O	-	reverse saturation current
I_R	-	reverse bias current
I_S	-	photogenerated current
K	-	thermal conductivity
k	-	Boltzmann's constant
L	-	length of the duct
LED	-	light emitting diode
λ	-	AkT/q
μ_b	-	viscosity at mean bulk temperature
μ_P	-	microprocessor
μ_S	-	viscosity at average heat sink temperature
\bar{N}_{UD}	-	average Nusselt number

P_M	- maximum power output
P_P	- maximum power output of shunt connection of cells
P_r	- Prandtl number
P_S	- maximum power output of series connection of cells
q	- charge
q	- heat transfer rate
R_e	- Reynold number
R_f	- forward resistance
R_L	- load resistance
R_M	- load resistance for maximum power output
R_r	- reverse resistance
R_S	- series resistance
R_{Sh}	- shunt resistance
R_I	- resistance offered by segment I
R_{II}	- resistance offered by segment II
R_{III}	- resistance offered by segment III
RAM	- random access memory
ρ_b	- density of the fluid
SCA	- solar cell array
T	- temperature
T	- torque
T_b	- mean bulk temperature
T_S	- average heat sink temperature
T_w	- water temperature
V_F	- forward bias voltage
V_R	- reverse bias voltage

- (V_1, I_1) - intersection point of segments I & II
- (V_2, I_2) - intersection point of segments II & III
- v - velocity of water flow

+++++++

CHAPTER 1

I N T R O D U C T I O N

CHAPTER 1

I N T R O D U C T I O N

A solar cell is a device which converts sunlight into electrical power. The power can be extracted by connecting a load to the solar cell.¹ The power available from a single cell is very small. The open circuit voltage of a silicon solar cell is about 0.6 volts whereas the short circuit current depends upon the area of the cell and so far the silicon cells in use have short circuit current of the order of 1 Ampere. Therefore, to get large power, voltage and current outputs from a supply using solar cells, number of cells are to be connected in series and shunt. This forms a solar cell array. The output voltage requirement decides the number of cells to be connected in series whereas the output current requirement decides the shunt connection of the cells.

The solar cell arrays have been used extensively as source of power in space programs. The usefulness of the solar cell arrays for terrestrial applications is even greater. The feasibility of large scale generation of electric power using solar cells has been emphasised by Loferski.² Efforts

are being made to use solar cell arrays economically for terrestrial applications.³⁻⁴²

To design a solar cell array for any application or to study the performance of a solar cell array, at least the following electrical parameters for the given environmental conditions and intensity are specified.

- a) Open circuit voltage, V_{OC}
- b) Short circuit current, I_{SC}
- c) Maximum power output, P_M
- d) Voltage and current at the maximum power output, V_M and I_M
- e) Load resistance to be connected to the array for maximum power output, R_M

All these parameters can be determined from the V-I characteristics of the array. As the array consists of series and shunt connection of number of cells, the V-I characteristics of the array depends upon the V-I characteristics of each cell forming the array. In order to determine the V-I characteristics of the array, each cell in the array is replaced by its electrical equivalent and the complete equivalent circuit of the array is then analysed using known circuit analysis techniques.

Various equivalent models of solar cells reported in the literature are discussed below and limitations in using the

particular model for the array analysis are also presented.

The equivalent circuit of a solar cell in common use¹ is shown in Fig. 1.1. In this model I_S is the photogenerated current, diode represents the p-n junction, R_S and R_{Sh} are series and shunt resistances. If load resistance R_L is connected across the output terminals, the current I_L through the load is given by

$$I_L = I_S - I_D - \frac{V_L + I_L R_S}{R_{Sh}} \quad \dots 1.1$$

where the diode current I_D is,

$$I_D = I_0 \left(e^{\frac{q(V_L + I_L R_S)}{AkT}} - 1 \right)$$

Here I_0 is the diode reverse saturation current, k is the Boltzmann's constant, T is the temperature, q is the charge of electron and A is the diode quality factor.

It is obvious from eqn. 1.1 that the load current depends upon I_S , I_0 , A , R_S and R_{Sh} . All these terms depend upon the fabrication specifications of the cell. I_S also depends upon the incident photon intensity. Therefore, the analytical determination of the load current requires the knowledge of the cell fabrication details. Eqn. 1.1 has also been obtained using the V-I characteristics of the solar cell and curve fitting techniques.⁴³

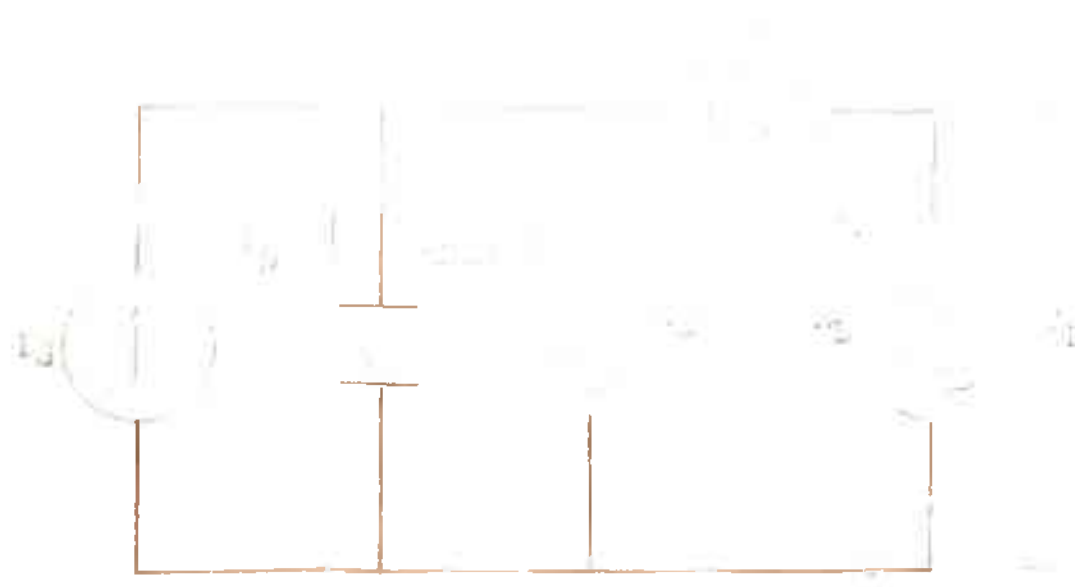


Fig. 1.1 Equivalent circuit of a solar cell

Numerous techniques for the evaluation of various parameters of the solar cell with reference to eqn. 1.1 have been reported in the literature.⁴⁴⁻⁵⁵ Since each method is based upon particular assumptions, the parameter values calculated using these methods have resulted in different numerical values even for the same solar cell.

Many other equivalent circuits like distributed constants model, second order lumped constants model, etc.⁵⁶ have also been put forth. But because of their complexity they have not received wide acceptance.

In view of the fact that the cell is generally used near or at the maximum power point, it has been suggested that instead of R_S one should use the internal resistance, R_{iM} given by the slope of the V-I characteristics of the cell at the maximum power point. The optimum value of the load, R_{oM} has to be equal to $V_M \cdot I_M$ for maximum efficiency of operation of the cell.⁵⁷

The equivalent circuit of solar cell given in Fig. 1.1 and represented by eqn. 1.1 has the following drawbacks:

a) The eqn. 1.1 is a nonlinear equation and when number of cells are connected in an array, the analysis using this model becomes quite difficult. Complexity further increases if the cells are not identical to start with or their characteristics differ because of different operating conditions.

b) The parameters in eqn.1.1 depend upon the fabrication specifications of the solar cell in addition to their dependence on intensity and temperature.

c) No simple method exists to find out the parameters like R_s , R_{sh} , I_0 , A etc.

d) The equivalent circuit does not take into account the operation of the cell under positive and negative over voltages which are the likely conditions in any array.

Some work has been done to study the effect of variation of solar cell parameters on the array output using the above equivalent circuit and probability theory.⁵⁸⁻⁶⁴ The analysis of an array using this approach becomes quite involved when nonidentical cells form the array.

Another difficulty one faces is that as the V-I characteristics of the array depends upon the individual cell V-I characteristics, one needs the V-I characteristics of each cell at the operating intensity and temperature. These V-I characteristics of the cells may differ from the one given by the manufacturer. Infact, the difference in the actual V-I characteristics of the cell may also be due to the manufacturing spread. Thus for an accurate analysis of the array, the actual V-I characteristics of each cell at the desired operating intensity and temperature must be known. The analysis based on these V-I characteristics of each cell is more meaningful.

A new equivalent circuit put forth by Slonim⁶⁵ has been used in reliability simulation of a large solar battery⁶⁶ using identical solar cells. This equivalent circuit is based on the actual experimental V-I characteristics of the cell. The V-I characteristics is divided into two linear segments. Each segment is expressed by a linear V-I relationship. The cell has been modelled on the basis of these linear equations. The model also takes into account the positive and negative over voltages.

However, no attempt has been made to analyse the solar cell array using nonidentical cells involving the linear segment equations or the equivalent circuit based upon these equations.

The motivation of the present work has been to analytically determine the characteristics^{of} solar cell arrays employing both identical and nonidentical cells.

The scope of the present work is mentioned in the next section.

Scope of the Present Work

In the present work, the analytical determination of a solar cell array V-I characteristics is carried out using piece-wise approximation. The V-I characteristics of individual cell is approximated to be piece-wise linear and is represented by

a three linear segment approximation. Each segment is expressed by a simple linear equation. Using this approximation, the complete array characteristics is determined. The features of the piece-wise approximation are given below.

- a) Each segment is represented by a linear V-I relation which is easier to deal with in comparison with the V-I relation of the cell given by eqn. 1.1.
- b) The determination of the parameters used in the linear equations is straight forward and does not require any fabrication specifications or the manufacturer's V-I characteristics.
- c) The determination of the parameters used in eqn. 1.1 like R_s , R_{sh} , I_0 etc. is not needed as the equations specifying the V-I relation for a segment do not involve these parameters.
- d) Representation of the V-I relations in the form of the equivalent circuit used by Slonim is not needed in the analysis of the solar cell array.
- e) The behaviour of a solar cell under positive and negative over voltages is also taken care of by this approximation as the reverse and forward characteristics of each cell are also considered.

The validity of the piece-wise approximation is discussed and a piece-wise linear approximation of the solar cell V-I characteristics employing three linear segments is used for the analysis of a solar cell array. The parameters to characterise a solar cell based upon this approximation are defined and their

relationship with the parameters based upon the equivalent circuit of Fig. 1.1 is established. As the variation of the parameters like R_S , R_{Sh} , V_{OC} , I_{SC} , I_0 etc. with intensity and temperature is known, the above relationships are used to discuss the variation of the characterising parameters based upon three linear segment approximation with intensity and temperature. This knowledge of the variation of parameters also helps in estimating the performance of solar cell array with intensity and temperature.

Three piece-wise linear segment approximation of V-I characteristics of a cell is used to determine analytically the V-I characteristics of a solar cell array. The procedure for analysing a solar cell array is first illustrated by using a combination of two identical and also two nonidentical cells. It is shown that given the characterising parameters of solar cells, the evaluation of the V-I characteristics of the combination of two cells is straight forward and easy even when non-identical cells are used. This approach also clearly explains the formation of hot spot in series connection⁶⁷ and dissipation of energy in the shunt connection even without any load. A general procedure is then presented to analytically determine the V-I characteristics of a solar cell array of any size. The analysis being dependent only on the three piece-wise linear approximation of individual cell forming the array does not require any complicated mathematical manipulations to characterise a solar cell array using nonidentical cells.

For the analysis of a large array, the determination of characterising parameters of each cell is quite time consuming. The manual evaluation of parameters of each cell is avoided by designing a microprocessor based system which displays the desired parameters of a cell. The system designed is based on 8085A microprocessor and its associated hardware. The microprocessor has already been used in the design of systems for the measurement of energy, battery charging, tracking, etc. by some authors.^{68,69} The software and hardware design of the system is presented.

The present work also includes the study of the performance and design of a solar cell array coupled to different types of loads. The various loads are simple resistor, inductor, capacitor and their combinations. A fractional horse power dc motor commonly used in tape recorders and a chargeable battery as loads to the solar cell array are also studied. It is shown that for battery charging a constant current/constant voltage type supply is suitable. This type of supply is designed using regulators coupled to solar cell arrays.

In Chapter 2, the piece-wise approximation of a solar cell is presented. The experimentally obtained nonlinear V-I characteristics of the solar cell is approximated using three piece-wise linear segments and two

piece-wise linear and one non-linear segment. It is shown that the three linear segment approximation of the characteristics is optimum. The conclusion is based upon the experimental and analytical results which show that the error in using three piece-wise linear segments as compared to two piece-wise linear and one nonlinear segment approximation is quite small. The selection of three piece-wise linear segments rather than large number of linear segments is also discussed.

Based upon three piece-wise linear approximation of a solar cell, the characterising parameters of the cell are defined. The relationship between these parameters and the parameters due to the model of Fig. 1.1 is established. The variation of characterising parameters due to three piece-wise linear approximation with intensity and temperature is discussed using the known variation of cell parameters of Fig. 1.1. The variation is experimentally verified.

Chapter 3 illustrates the procedure for the determination of a solar cell array V-I characteristics based upon three piece-wise linear segment approximation of the solar cell V-I characteristics. Combination of two nonidentical cells is taken first. To find the V-I characteristics of the combination, the resultant short circuit current and open circuit voltage are first determined. The method to determine resultant

I_{SC} and V_{OC} both for series and shunt connections is given and verified experimentally. From this method, hot spot formation in series connection and energy dissipation in shunt connection becomes obvious. The overall V-I characteristics of the combination is then obtained. This procedure is illustrated using examples and is also experimentally verified.

When more than two nonidentical cells are connected in series or shunt, the procedure to evaluate the overall V-I characteristics of the combination is taken next. Here the resultant characteristics of two cells are determined first. As the cells are nonidentical, the resultant characteristics may contain more than three piece-wise linear segments. Therefore, the resultant characteristics of two cells is first converted to three linear segments and then the resultant characteristics of this combination and the third cell is obtained. The method to convert the resultant V-I characteristics of the combination of two cells into three segments is illustrated. This method is used in the computer analysis of the complete array.

The general procedure to determine V-I characteristics of the array consisting of m number of shunt connection of sub-arrays employing n number of series connected nonidentical cells is then presented. The characteristics of a 5×2 array using the above procedure is: analytically determined and the performance of the array is also experimentally studied. The

experimentally determined V-I characteristics of this array matches very well with those obtained analytically.

The performance of solar cell arrays with increase in intensity and temperature is studied. The variation of the characterising parameters of the array with intensity and temperature is measured experimentally. This variation is then discussed using the variation of the characterising parameters of a single cell. It is observed that the array parameters follow an identical variation as obtained in the case of a single cell.

The analysis of a solar cell array requires the characterising parameters of each cell forming the array. The design of a 8085A microprocessor based system to characterise each cell is presented in Chapter 4. Voltage and current data points corresponding to the cell V-I characteristics are obtained in the system. The characterising parameters are evaluated by a suitable manipulation of these data points. The desired parameters of the cell are selected through a key board and displayed on seven segment displays. The display also indicates any error in manipulations of the data or wrong interconnection of the cell with the system. The algorithms for calculating the maximum power output and fill factor are presented. The hardware design of the system is discussed and the details of the design are presented in Appendix C. In this design, the system accepts maximum values of the input

voltage and current. The output of a solar cell array may exceed these limits. The system modification for this purpose is also dealt with. The various algorithms for computing the cell parameters are verified using the experimental data points as the input. The algorithms are translated in the assembly language and the corresponding machine language codes are generated for each instruction. The design of the software is also verified. The assembly language conversion of various subroutines is presented in Appendix D.

In actual practice, a solar cell array is coupled to different loads. The performance of solar cell arrays coupled to different types of loads is analysed in Chapter 5. Two main types of loads considered are, a fractional horse power dc motor used in cassette tape recorders and a chargeable 6 volt lead acid battery. For each type of load the design criterion of the solar cell array is presented. The design also takes into account the effect of variation of intensity on the array performance. The design is verified experimentally. For the completion of study, other types of loads such as resistive, inductive, capacitive and their combinations are also studied. Many applications require regulated dc power supply. In such applications, the array output directly cannot be used because the V-I characteristics of the array changes with intensity and temperature. The design of regulated solar power supplies using discrete and integrated circuit components is presented

and experimentally verified.

The summary and conclusions of the present work are presented in Chapter 6.

.....

REFERENCES

1. Prince, M.B., "Silicon Solar Energy Converters," J. Appl. Phys., Vol. 26, 1955, p 534.
2. Loferski, J.J., "Large-Scale Solar power via Photovoltaic Effect", Mech. Engg., Vol. 95, Dec 1973, p 28.
3. Ralph, E.L., "A Commercial Solar Cell array design", Solar Energy, Vol. 14, 1972, p 279.
4. Bhaskara Rao, A., "Terrestrial solar cell power stations", Indian J. Phys., Vol. 48, 1974, p 973.
5. Alvarado, E.L. and Eltimsahy, A.D., "Direct coupling of solar cell arrays to electric power networks", IEEE Trans. on Industry Applications, Vol. 1A-12, 1976, p 90.
6. Kirpich, A. and Buerger, E., "Performance and cost assessment of Photovoltaic system concepts", Conference records of 12th IEEE Photovoltaic specialists conference, Louisiana, 1976, p 673.
7. Pittman, P.F. et al, "Technical and Economic results of solar photovoltaic power systems analysis", Conference records of 12th IEEE Photovoltaic specialists conference, Louisiana, 1976, p 681.
8. Bartels, F.T.C. and Kelber, C.C., "Photovoltaic system design and analysis application to a shopping center", Conference records of 12th IEEE Photovoltaic specialists conference, Louisiana, 1976, p 691.

9. Shepard, N.F. and Landes, R., "The conceptual design and analysis of a photovoltaic powered experimental residence", Conference records of 12th IEEE Photovoltaic specialists conference, Louisiana, 1976, p 705.
10. Burgess, E.L. and Edenburn, M.W., "One Kilowatt Photovoltaic subsystem using Fresnel Lens concentrators", Conference records of 12th IEEE Photovoltaic specialists conference, Louisiana, 1976, p 774.
11. Cherdak, A.S. and Haas, G.M., "A Data Acquisition System for In Situ measurements of Terrestrial photovoltaic array performance", Conference records of ^{12th} IEEE Photovoltaic specialists conference, Louisiana, 1976, p 794.
12. Yekutieli, G., et al, "A solar cell system for concentrated sunlight", Proceedings of International Photovoltaic Solar Energy Conference, Luxembourg, 1977, p 370.
13. Redfield, D., "Method for minimizing the cost/watt of complete photovoltaic systems and applications", Proceedings of International Photovoltaic Solar Energy Conference, Luxembourg, 1977, p 1202.
14. Feber, R.R. et al, "Minimum array structure for solar photovoltaic power plants, "International Solar Energy Congress, New Delhi, Extended Abstracts, Vol. 1, 1978, p 504.
15. Santala, T. et al, "Optimized Solar Module Design", Conference records of 13th IEEE Photovoltaic specialists conference, Washington, 1978, p 733.

16. Redfield, D., "Cost criterion for low efficiency solar cells to make system power cost competitive with that of high efficiency cells", Conference records of 13th IEEE Photovoltaic specialists conference, Washington, 1978, p 911.
17. Roy, A.S., "Model for comparing cost of flat-array and concentrator photovoltaic solar cell systems", Conference records of 13th IEEE Photovoltaic specialists conference, Washington, 1978, p 914.
18. Hamilton, R.C. and Witt, C.E., "Terrestrial Concentrating Photovoltaic Systems Comparative Performance and Costs", Conference records of 13th IEEE Photovoltaic specialists conference, Washington, 1978, p 980.
19. Borden, C.S., "Lifetime cost and performance model for photovoltaic power systems", Conference records of 13th IEEE photovoltaic specialists conference, Washington, 1978, p 925.
20. Hein, G.F. et al, "Impact of Balance of system (BOS) costs on photovoltaic power systems", Conference records of 13th IEEE photovoltaic specialists conference, Washington, 1978, p 930.
21. Roesler, D.J., "A 60 KW solar cell power system with peak power tracking and utility interface", Conference records of 13th IEEE photovoltaic specialists conference, Washington, 1978, p 978.
22. Pickrell, R.L. et al, "An inverter/controller subsystem optimized for photovoltaic applications", Conference records of 13th IEEE photovoltaic specialists conference, Washington, 1978, p 984.

23. Federmann, E.F. et al, "Potential for stand-alone photovoltaic on-site total energy residential systems", Conference records of 13th IEEE photovoltaic specialists conference, Washington, 1978, p 1004.
24. Burgess, E.L. and Pritchard, D.A., "Performance of a One KW concentrator photovoltaic array utilizing active cooling", Conference records of 13th IEEE photovoltaic specialists conference, Washington, 1978, p 1121.
25. Donovan, R.L. et al, "Ten KW photovoltaic concentratic array", Conference records of 13th IEEE photovoltaic specialists conference, Washington, 1978, p 1125.
26. Castle, J.A., "10 KW photovoltaic concentrator system design", Conference records of 13th IEEE photovoltaic specialists conference, Washington, 1978, p 1131.
27. Luque, A. et al, "Project of the 'Ramon Areces' concentrated photovoltaic power station", Conference records of 13th IEEE photovoltaic specialists conference, Washington, 1978, p 1139.
28. Jones, G.J. and Schueler, D.G., "Status of the DOE photovoltaic systems engineering and analysis project", Conference records of 13th IEEE Photovoltaic Specialists Conference, Washington, 1978, p 1160.
29. Linn, J.K., "Optimization of Terrestrial Photovoltaic power systems", Conference records of 13th IEEE photovoltaic specialists conference, Washington, 1978, p 1166.
30. Kirpich, A.S. et al, "Regional analysis of residential photovoltaic system concepts", Conference records of 13th IEEE photovoltaic specialists conference, Washington, 1978, p 1171.

31. Chobotov, V. and Stegel, B., "Analysis of photovoltaic total energy system concepts for single-family residential applications", Conference records of 13th IEEE photovoltaic specialists conference, Washington, 1978, p 1179.
32. Tsou, P. and Stolte, W., "Effects of design on cost of flat-plate solar photovoltaic arrays for terrestrial central station power applications", Conference records of 13th IEEE photovoltaic specialists conference, Washington, 1978, p 1196.
33. Lyon, E.F., "A 100 KW peak photovoltaic power system for the natural bridges national monument", Proc. of the international solar energy society, Georgia, SUN II, Vol.3, 1979, p 1732.
34. Sala, G. et al, "The Ramon Areces concentration photovoltaic array", Proc. of the international solar energy society, Georgia, SUN II, Vol. 3, 1979, p 1737.
35. Blevins, B., et al, "A 20 KW photovoltaic flat panel power system in EL PASO, Texas", Proc. of the international solar energy society, Georgia, SUN II, Vol. 3, 1979, p 1749.
36. Matlin, R.W., "PV-Powered Microirrigation Systems", Proc. of the international solar energy society, Georgia, SUN II, Vol. 3, 1979, p 1754.
37. Luque, A. et al, "Quasi-Static concentrated array with double side illuminated solar cells", Proc. of the international solar energy society, Georgia, SUN II, Vol. 3, 1979, p 1813.
38. Pizzini, S. et al, "Development of 1 pKW photovoltaic module with concentration", Proc. of the international solar energy society, Georgia, SUN II, Vol. 3, 1979, p 1818.

39. Basu, P. et al, "Solar Photovoltaic Systems for Village Usage", Proc. of National Solar Energy Convension, Annamalainagar, 1980, p 400.
40. Mukhopadhyay, K. et al, "Solar Powered Village Energy Centre - A Field Experience", Proc. of National Solar Energy Convention, Bangalore, 1981, p 10.018.
41. Edenburn, M.W. et al, "Computer simulation of photovoltaic systems", Conference records of 12th IEEE Photovoltaic Specialists Conference, Louisiana, 1976, p 667.
42. Goldstein, L.H. and Cage, G.R., "PVSS - A Photovoltaic System Simulation Program", Solar Energy, Vol. 21, 1978,p 37.
43. Luque, A. et al, "Connection losses in Photovoltaic Arrays", Solar Energy, Vol. 25, 1980, p 171.
44. Wolf, M., "Limitations and Possibilities of Improvement of Photovoltaic Solar Energy Converters", Proc. of I.R.E., Vol. 48, 1960, p 1246.
45. Wyszocki, J.J., "The Effect of Series Resistance on Photovoltaic Solar Energy Conversion", RCA Review, Vol. 22, 1961, p 57.
46. Chelnokov, Y. Ye, "Method for measuring series resistance of diffusion silicon photoelements of large area", Radio Engg. and Electronics Physics, Vol. 8, 1963, p 892.
47. Handy, R.J., "Theoretical Analysis of the Series resistance of a solar cell", Solid State Electronics, Vol. 10, 1967, p 765.
48. Imamura, M.S. and Portscheller, J.I., "An evaluation of the

methods of determining solar cell series resistance",
Conference record of the 8th IEEE Photovoltaic specialists
conference, Washington, 1970, p 102.

49. Rao, A.B. and Prasad S., "Series Resistance of a Silicon Solar Cell at Very Low Intensities", Indian Journal of Phys., Vol. 45, Sept. 1971, p 391.
50. Rao, A.B. and Nath P., "Internal Resistance of a Silicon Solar Cell", Indian Journal of Pure and Applied Physics, Vol. 10, May 1972, p 351.
51. Evdokimov, V.M., "Calculations of Series and Shunt Resistances on the Basis of the Volt-Ampere Characteristics of a Solar Cell," Applied Solar Energy, Vol. 8, No. 6, 1972, p 63.
52. Rao, A.B. and Padmanabhan, G.R., "A method for estimating the optimum load resistance of a silicon solar cell used in terrestrial power applications", Solar Energy, Vol. 15, 1973, p 171.
53. Bordina, N.M. et al, "Determining the parameters of a photo-converter current-voltage characteristics", Applied Solar Energy, Vol. 13, 1977, p 13.
54. Bobbio, S. and Califano, F.P., "On the series resistance of Solar Cells", Conference Records of 12th IEEE Photovoltaic Specialists Conference, Louisiana, 1976, p 71.
55. Boone, J.L. and Van Doren, T.P., "Solar Cell Design based on a Distributed Diode Analysis," IEEE Trans. on Electron Devices, Vol. ED-25, 1978, p 767.

56. Wolf, M. and Rauschenbach, H., "Series Resistance Effects on Solar Cell Measurements", Advanced Energy Conversion, Vol. 3, 1963, p 455.
57. Murthy, B.S. et al, "Some comments on the Evaluation of Electrical Parameters of a Solar Cell", Journal of the Institution of Electronics and Telecommunication Engineers, Vol. 21, 1975, p 359.
58. Rauschenbach, H., "Electrical output of shadowed solar arrays", IEEE Transactions on Electron Devices, Vol. ED-18, 1971, p 483.
59. Wathins, J.L. and Burgess, E.L., "The Effect of Solar Cell Parameter Variation on Array Power Output", Conference records on 13th IEEE Photovoltaic Specialists Conference, Washington, 1978, p 1061.
60. Luque, A. et al, "Connection losses in Photovoltaic Arrays", SUN II, Proc. of the International Solar Energy Society, Georgia, 1979, p 1051. Also Solar Energy, Vol. 25, 1980, p 171.
61. Luque, A. and Lorenzo, E., "The effect of dispersion of the characteristics of solar cells in large systems", Solar Energy, Vol. 22, 1979, p 187.
62. Bany, J. et al., "The influence of parameter dispersion of electrical cells on the array power output", IEEE Trans. on Electron Devices, Vol. ED-24, 1977, p 1032.
63. Lahiri, R. et al, "The Experimental Study of Series Combination of Solar Cells", Conference records on 13th IEEE Photovoltaic Specialists Conference, Washington, 1978, p 1080.

64. Bhaduri, A. et al, "Electrical characteristics of solar cell series/parallel combinations", Proc. of National Solar Energy Convention, 1980, p 406.
65. Slonim, M.A., "New Equivalent Diagram of Solar Cells (Engineering point of view)", Solid State Electronics, Vol. 21, 1978, p 617.
66. Bogomolny, B. et al, "Reliability simulation of a large solar battery", Proc. of International Photovoltaic Solar Energy Conference, Luxembourg, 1977, p 1261.
67. Watkins, J.L. and Burgess, E.L. "The effect of Solar Cell Parameter Variation on array power output", Conference records on 13th IEEE Photovoltaic Specialists Conference, Washington, 1978, p 1061.
68. Dixon, A.E. and Leslie, J.D., Solar Energy Conversion: An Introductory Course, Pergamon Press, 1979, p 953.
69. Rao, N.V.S. et al, "A Microprocessor Based Tracking System for Linear Focussing Solar Energy Concentrators", Proc. of National Solar Energy Convention 1981, IISc, Bangalore, Jan. 1982, p 11.014.

CHAPTER 2

SOLAR CELL PERFORMANCE EVALUATION BASED ON PIECE-WISE APPROXIMATION

- 2.1 Introduction
- 2.2 Piece-wise Linear Approximation of a Solar Cell
V-I Characteristics Employing Three Linear Segments
 - 2.2.1 Maximum power output evaluation
- 2.3 Two Linear and One Nonlinear Segment Representation
of Solar Cell V-I Characteristics
- 2.4 Experimental Study
- 2.5 Variation of Three Segment Parameters with
Intensity and Temperature
 - 2.5.1 Relations Between R_I , R_{II} , R_{III} and the
Parameters of Fig. 1.1
- 2.6 Experimental Study of Solar Cell Performance at
High Intensity and High Temperature
 - 2.6.1 Performance at High Intensity and Constant
Temperature
 - 2.6.2 Performance at High Temperature and
Constant Intensity

2.7 Discussion

2.7.1 Parameters Variation with Intensity

Keeping Temperature Constant

2.7.2 Variation of Parameters with Temperature

Under Constant Intensity

2.8 Conclusions

References

CHAPTER 2

SOLAR CELL PERFORMANCE EVALUATION BASED ON PIECE-WISE APPROXIMATION

2.1 Introduction

In order to evaluate the performance of solar cells analytically, various equivalent circuits representing the solar cell behaviour are available.¹⁻³ The equivalent circuit in common use has already been given in Fig. 1.1 (Ch. 1). The V-I relation of the solar cell represented by this model is non-linear and depends upon the various physical parameters of the device which may not be readily available. Techniques for the evaluation of various parameters have been reported in the literature.⁴⁻¹⁵ However the parameters evaluated using different techniques are not always same. Further, the actual V-I characteristics of the cell may differ from the one given by the manufacturer because of manufacturing spread, operation under different intensities and temperatures etc. When nonidentical cells are connected to form an array, it is possible that some of the cells may operate under positive and negative over voltages. The model does not represent the behaviour of the

cell under these conditions. It also becomes very difficult to evaluate the performance of the array analytically using this model.

A new equivalent circuit given by Slonim^{16,17} is based on the actual experimental V-I characteristics of the cell. In this model, the V-I characteristics is divided into two linear segments which are in turn expressed by linear V-I relations. The model also accounts for the abnormal operating conditions of the cell when used in an array.

V-I characteristics representation using only two linear segments does not accurately represent the actual characteristics of the cell. Using more number of segments in turn increases the complexity of the equivalent representation.

In this chapter, the piece-wise approximation of a solar cell V-I characteristics is presented. The starting point is the actual experimental V-I characteristics of the cell to be used. In general, the nonlinear V-I characteristics can be approximated by number of linear segments or a combination of linear and nonlinear segments. The selection of the number of segments depends upon a compromise between the desired accuracy and ease of calculations. Three linear segment representation of the V-I characteristics of a cell is introduced and a comparison with an approximation involving two linear and one nonlinear segment is made. V-I characteristics representation using three

piece-wise linear segments is considered to be optimum if the cells are to be used in an array.

The performance of a solar cell has been experimentally studied and three linear segments approximation of the V-I characteristics is given. The solar cell parameters are evaluated using the piece-wise linear approximation and the comparison with the actual characteristics is given. The performance of the cell under high intensity and high temperature is also experimentally studied. The design of the heat sink to be used with the cell is illustrated in Appendix A. The variation of parameters characterising the three linear segments at high intensity and high temperature is presented using the known variation of conventional solar cell model parameters under these conditions. The variations of these parameters with temperature and intensity can be used to predict the nature of variation of the array characteristics under these operating conditions.

2.2 Piece-wise Linear Approximation of a Solar Cell V-I Characteristics Employing Three Linear Segments

A typical V-I characteristics of a solar cell is plotted in Fig. 2.1. The V-I characteristics is approximated by three linear segments as shown. The linear segments I and III are drawn to cover maximum number of data points near V_{OC} and I_{SC} respectively. Segment II intersects segment I at (V_1, I_1) and segment III at (V_2, I_2) points. The criterion to draw segment II in addition to cover maximum number of data points is that this

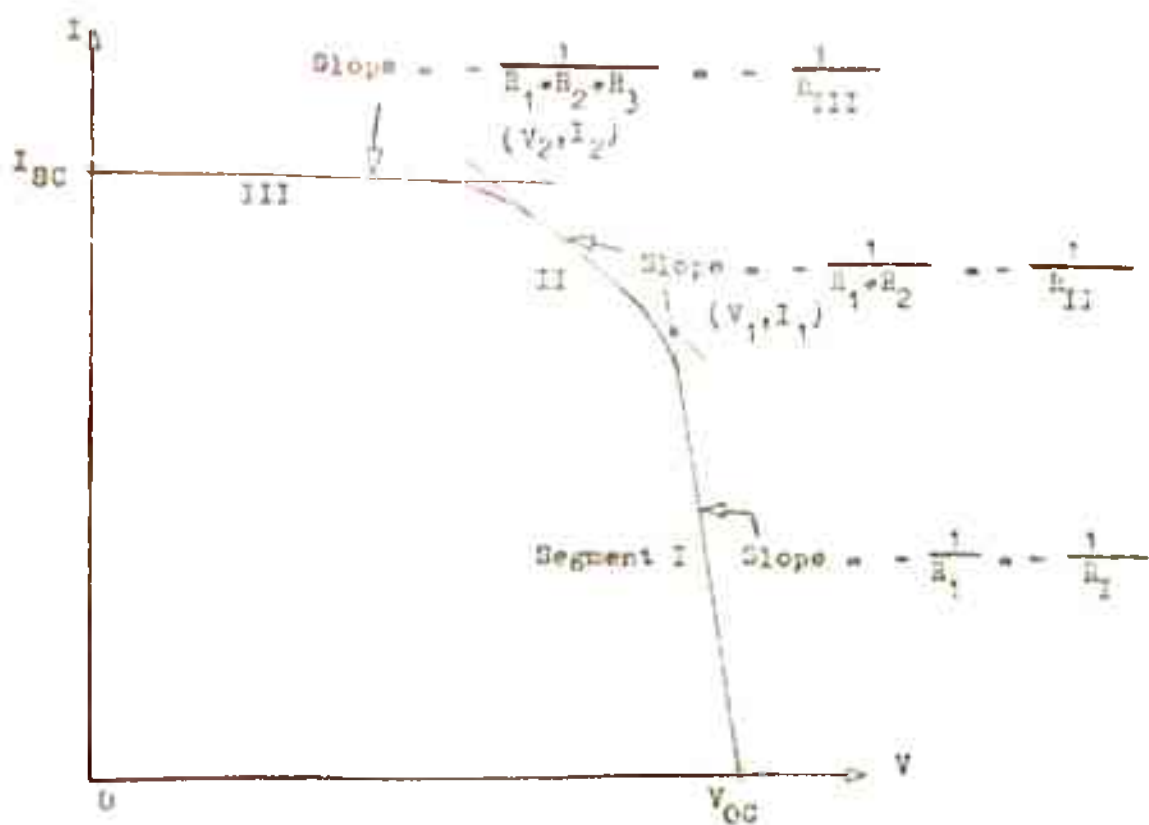


Fig. 2.1 Three Segment Approximation of V-I Characteristics of a Solar Cell.

segment is drawn so as to have almost equal distance from the intersection points to the nearest data points on the characteristics i.e.

$$\text{Distance of } (V_1, I_1) \text{ from its nearest data point} \approx \text{Distance of } (V_2, I_2) \text{ from its nearest data point}$$

In this way the segment II is symmetrically drawn. In most of the cells, the maximum power point lies in segment II. The figure also indicates the slopes of each segment in terms of the resistances offered by the straight lines joining two intersection points.

The equations representing these segments in terms of the resistances and intersection points can be found from the basic straight line equation joining any two points. The equations governing each segment are

$$\text{Segment I, } V = V_{OC} - R_1 I \quad \dots 2.1a$$

$$\text{Segment II, } V = V_{OC} + I_1 R_2 - (R_1 + R_2) I \quad \dots 2.1b$$

$$\text{Segment III, } V = V_{OC} + I_1 R_2 + I_2 R_3 - (R_1 + R_2 + R_3) I \quad \dots 2.1c$$

$$\text{where } R_1 = \frac{V_{OC} - V_1}{I_1}, \quad R_1 + R_2 = \frac{V_1 - V_2}{I_2 - I_1}, \quad R_1 + R_2 + R_3 = \frac{V_2}{I_{SC} - I_2}$$

These equations, being simple linear equations, can be manipulated with a great ease in comparison to the nonlinear equation of the cell.

2.2.1 Maximum Power Output Evaluation

One of the most desired parameter of a cell is the maximum power available from the cell. The calculation of the maximum power output of the cell is quite easy using piece-wise linear segment representation of the characteristics as compared to the nonlinear model.

The segment equation 2.1 can be written in the following general form

$$V = K_1 - K_2 I \quad \dots 2.2$$

where K_1 and K_2 are constants decided by the segment.

Power P is given by

$$P = VI = K_1 I - K_2 I^2 \quad \dots 2.3$$

Differentiating and equating the result to zero gives the value of the current, I_M for the maximum power

$$I_M = \frac{K_1}{2K_2} \quad \dots 2.4$$

Substituting eqn. 2.4 in eqns. 2.2 and 2.3, the value of the voltage, V_M at maximum power and the maximum power, P_M are given by

$$V_M = \frac{K_1}{2} \quad \dots 2.5$$

and

$$P_M = \frac{K_1^2}{4K_2}$$

The load resistance, R_M to be connected to the cell for the maximum power output is given by $R_M = K_2$.

In general the maximum power point can lie in any of the three segments. Also there is only one maximum power point on the V-I characteristics of the cell. Keeping in mind the above, the following procedure is used to evaluate the maximum power output.

V_M and I_M are calculated for segment I using eqns. 2.4 and 2.5 and substituting K_1 and K_2 values for this segment. The segment I lies between (V_1, I_1) and $(V_{OC}, 0)$ points. If V_M and I_M values lie within this range, $P_M (= V_M \cdot I_M)$ is the maximum power output. Otherwise, as the power increases with increasing values of the current from point $(V_{OC}, 0)$, $V_M = V_1$ and $I_M = I_1$ such that $P_M = V_1 \cdot I_1$.

The above method is repeated for segment II also and V_M and I_M values are checked with the limits of segment II viz. (V_2, I_2) and (V_1, I_1) . If these lie within the range, $P_M (= V_M \cdot I_M)$ is the maximum power output. Otherwise the power $P_M = V_2 \cdot I_2$ is checked with $V_1 \cdot I_1$ product and maximum of the two values gives the maximum power output.

For segment III also V_M and I_M are determined using eqns. 2.4 and 2.5, if these lie within the limits of segment III viz. $(0, I_{SC})$ and (V_2, I_2) . This is the maximum power point. Otherwise $P_M = V_2 \cdot I_2$. Knowing V_M and I_M ; $R_M (= \frac{V_M}{I_M})$ is also determined.

2.3 Two Linear and One Nonlinear Segment Representation of Solar Cell V-I characteristics

The solar cell V-I characteristics can also be transformed into two linear and one nonlinear segment. Segments I and III are approximated to be linear segments and are drawn using the same criterion as discussed for the three linear segment representation. Segment II is considered as a nonlinear segment. The equation governing V-I relation is derived using empirical results.

This representation can also be used to simulate the solar cell characteristics and analyse the solar cell array. But as this representation uses nonlinear empirical equation, it has the same drawbacks as the nonlinear equation of the cell. Also as this representation requires the empirical equation for the nonlinear segment which varies with slight change in the characteristics of the cell and replacement of a cell by another cell, the approach tends to be of little interest.

It may also look that in three linear segment representation, the maximum power output may be quite different from the two linear and one nonlinear segment representation, because of approximation of nonlinear curve with linear segment. However, it is shown that the maximum power difference in two representations is very small. The V-I characteristics of a cell is experimentally obtained and represented by piece-wise approximation in the next section.

2.4 Experimental study

For the purpose of experimental studies presented in the thesis two types of solar cells manufactured by CEL, India have been employed. The specifications of the cells at 1 SUN and 27^oC are given below:

Cell I (Small area cell, 5 cm²)

$$I_{SC} = 142 \text{ mA}, \quad V_{OC} = 0.58 \text{ volts}, \quad P_M = 65 \text{ mW}$$

Cell II (Large area cell, 20 cm²)

$$I_{SC} = 500 \text{ mA}, \quad V_{OC} = 0.58 \text{ volts}, \quad P_M = 260 \text{ mW}$$

The data points corresponding to the V-I characteristics of a small area cell (Cell I) are measured experimentally using the set up shown in Fig. 2.2. Using these data points V-I characteristics of the cell is plotted in Fig. 2.3. This characteristics is divided into three linear segments using the procedure outlined earlier. The various parameters estimated from the three linear segment piece-wise approximation are given in Table 2.1.

Table 2.1

V_0 (Volts)	I_{SC} (Amperes)	V_1 (Volts)	I_1 (Amperes)	V_2 (Volts)	I_2 (Amperes)
0.5400	0.0770	0.4000	0.0600	0.2550	0.0755



Fig. 2.2 Experimental Set up.



Fig. 2.3 V-I Characteristics of Solar Cell

The maximum power as calculated is 24 mW.

The experimental data points are also used to get two linear and one nonlinear segment representation of the V-I characteristics. The empirical equation for the nonlinear segment II using the curve fitting technique is given by

$$I = 0.072 + 0.09V - 0.32V^2 \quad \dots 2.6$$

The derivation of this equation is based on the assumption that the nonlinear segment II is of the form¹⁹

$$\frac{I - I_a}{V - V_a} = a' + b'V$$

where I_a and V_a correspond to the intersection of segment I and II. For the cell under observation, the segment II corresponds to the observations given in Table 2.2.

Table 2.2

V (Volts)	I (Amperes)
0.410	0.056
0.380	0.061
0.340	0.066
0.300	0.071
0.234	0.074
0.162	0.076

The coefficients a' and b' are determined from the observations.

For the maximum power calculations, eqns. 2.4 and 2.5 are modified for segment II. From equation 2.6

$$P = VI = 0.072V + 0.09V^2 - 0.32V^3$$

Differentiating and equating to zero, we obtain

$$V_M = 0.38V \quad \text{and} \quad -0.19V$$

As $V_M = -0.19V$ is not within the range of segment II, $V_M = 0.38V$ is accepted. For this V_M ,

$$P_M = 22.8 \text{ mW}$$

$$\text{and} \quad I_M = 0.06A$$

The parameters obtained using this representation are given in Table 2.3.

Table 2.3

V_{OC} (Volts)	I_{SC} (Amperes)	V_1 (Volts)	I_1 (Amperes)	V_2 (Volts)	I_2 (Amperes)
0.5400	0.0770	0.4100	0.0560	0.1620	0.0760

It can be seen from the maximum power output in the two cases, the error is only 5%. This shows that the three linear segments can be used without much error to approximate the V-I characteristics of the solar cell.

2.5 Variation of Three Segment Parameters with Intensity and Temperature

The variation of various parameters of the solar cell model of Fig. 1.1 viz. I_{SC} , V_{OC} , R_S etc. with intensity and temperature has been studied by many authors. Variation of the resistances offered by each linear segment of the piece-wise approximation (Fig. 2.1) with intensity and temperature is presented here. It is assumed that

- a) Schockley's equations are valid.
- b) Segment I is drawn as a tangent at point V_{OC} and segment III as a tangent at I_{SC} .
- c) The maximum power point lies in segment II.
- d) "A" does not vary with intensity and temperature²⁰ in the range of interest.

Since the variation of intensity is considered to be within the limits of low level injection, the first assumption is generally valid. The requirements for drawing segments I and III are not much different from drawing tangents at points V_{OC} and I_{SC} respectively and also as has been pointed out earlier, the maximum point lies in segment II, assumptions b) and c) are quite satisfactory. The validity of assumption 'd' is already established.²⁰

2.5.1 Relations Between R_I , R_{II} & R_{III} and the Parameters of Fig. 1.1

Neglecting the effect of R_{Sh} ²¹ nonlinear equation of the cell

becomes

$$I_L = I_S - I_0 \left(e^{\frac{1}{\lambda} (V_L + I_L R_S)} - 1 \right), \quad \text{where } \lambda = \frac{AkT}{q}$$

Differentiating this equation

$$dI_L = -I_0 \left(\frac{1}{\lambda} e^{\frac{V_L + I_L R_S}{\lambda}} dV_L + \frac{R_S}{\lambda} e^{\frac{V_L + I_L R_S}{\lambda}} dI_L \right)$$

$$\text{or } \frac{dV_L}{dI_L} = -\frac{\lambda}{I_0} e^{-\frac{V_L + I_L R_S}{\lambda}} - R_S \quad \dots 2.7$$

Eqn. 2.7 gives the slope at any value of V_L and I_L .

At $I_L = 0$ where $V_L = V_{OC}$, eqn. 2.7 reduces to

$$\left. \frac{dV_L}{dI_L} \right|_{I_L=0} = -\left(R_S + \frac{\lambda}{I_0} e^{-\frac{V_{OC}}{\lambda}} \right)$$

This is also equal to $-R_I$. So

$$R_I = R_S + \frac{\lambda}{I_0} e^{-\frac{V_{OC}}{\lambda}}$$

Also $V_{OC} = \lambda \ln \left(\frac{I_S}{I_0} + 1 \right)$ from nonlinear equation of the cell

$$\therefore R_I = R_S + \frac{\lambda}{I_S + I_0} \quad \dots 2.8$$

At $V_L = 0$ where $I_L = I_{SC}$, eqn. 2.7 becomes

$$\left. \frac{dV_L}{dI_L} \right|_{V_L=0} = - \left(R_S + \frac{1}{I_0} e^{-\frac{I_{SC} R_S}{V_L}} \right)$$

which is equal to $-R_{III}$. So

$$R_{III} = R_S + \frac{1}{I_0} e^{-\frac{I_{SC} R_S}{V_L}} \quad \dots \quad 2.9$$

As the maximum power point lies in segment II,

$$V_M = \frac{V_{OC} + I_1 R_2}{2}, \quad I_M = \frac{V_{OC} + I_1 R_2}{2(R_1 + R_2)}$$

$$\text{Hence, } R_{II} = R_1 + R_2 = \frac{V_M}{I_M} = \frac{P_M}{I_M^2} \quad \dots \quad 2.10$$

Eqns. 2.8 - 2.10 give the required relationship.

2.6 Experimental Study of Solar Cell Performance at High Intensity and High Temperature

2.6.1 Performance at High Intensity and Constant Temperature

The performance of a solar cell at high intensity is experimentally studied using the set up shown in Fig. 2.4. The small area cell is used for the study. While the intensity is varied the temperature of cell is kept constant by a proper heat sink design and active cooling by varying the flow rate of cold water. The heat sink design is presented in Appendix A. Increase in intensity is obtained by using a Fresnel's Lens²² (M.P. 12) of

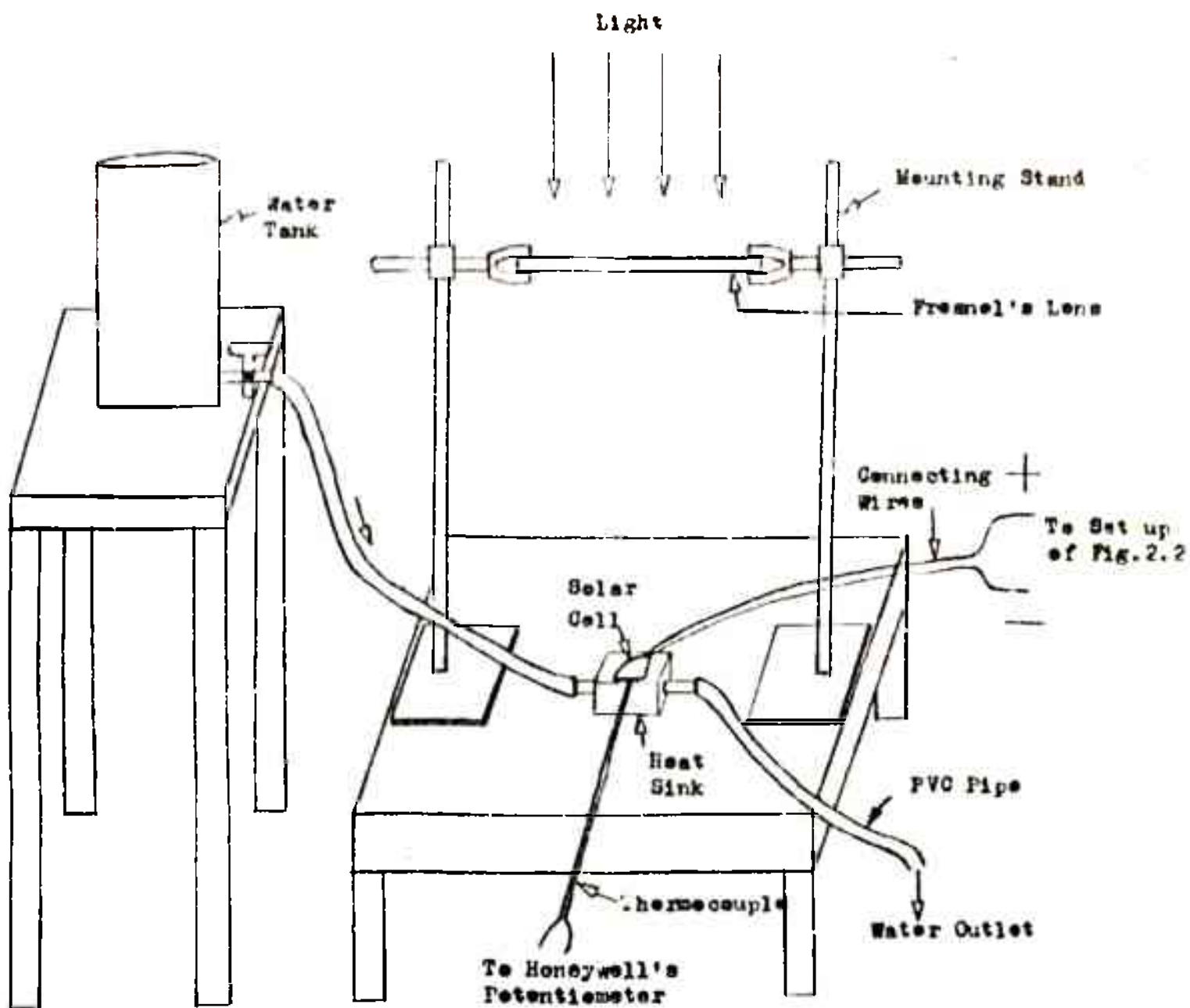


Fig. 2.4 Experimental Set up

focal length 34.3 cm and diameter 35.6 cm (obtained from I.I.Sc., Bangalore). The temperature is monitored using a copper constant thermocouple in conjunction with Honeywell's potentiometer. The characteristics of the cell is measured at different intensities. Each characteristics in turn is linearized using three segment piece-wise approximation. Figs. 2.5 to 2.7 show the piece-wise linear V-I characteristics of the cell at various values of intensity (Intensity proportional to I_{SC}) keeping the temperature fixed. The variation of V_{OC} , R_I , R_{II} , R_{III} , P_M and I_M with intensity is shown in Figs. 2.8 to 2.12.

2.6.2 Performance at High Temperature and Constant Intensity

The set up of Fig. 2.4 is also used to determine the solar cell performance at high temperatures keeping the intensity constant and the variation of R_I , R_{II} and R_{III} with temperature is derived. The temperature is increased by keeping the cell in a high temperature ambient. In all the measurements with different temperatures, the change in short circuit current is negligible. Fig. 2.13 gives the linearized V-I characteristics of the cell at three temperatures and Fig. 2.14 shows the variation of V_{OC} with temperature. The resistances offered by each segment, maximum power output P_M , the voltage and current at maximum power output, V_M and I_M and the values of P_M/I_M^2 are given in Table 2.4.

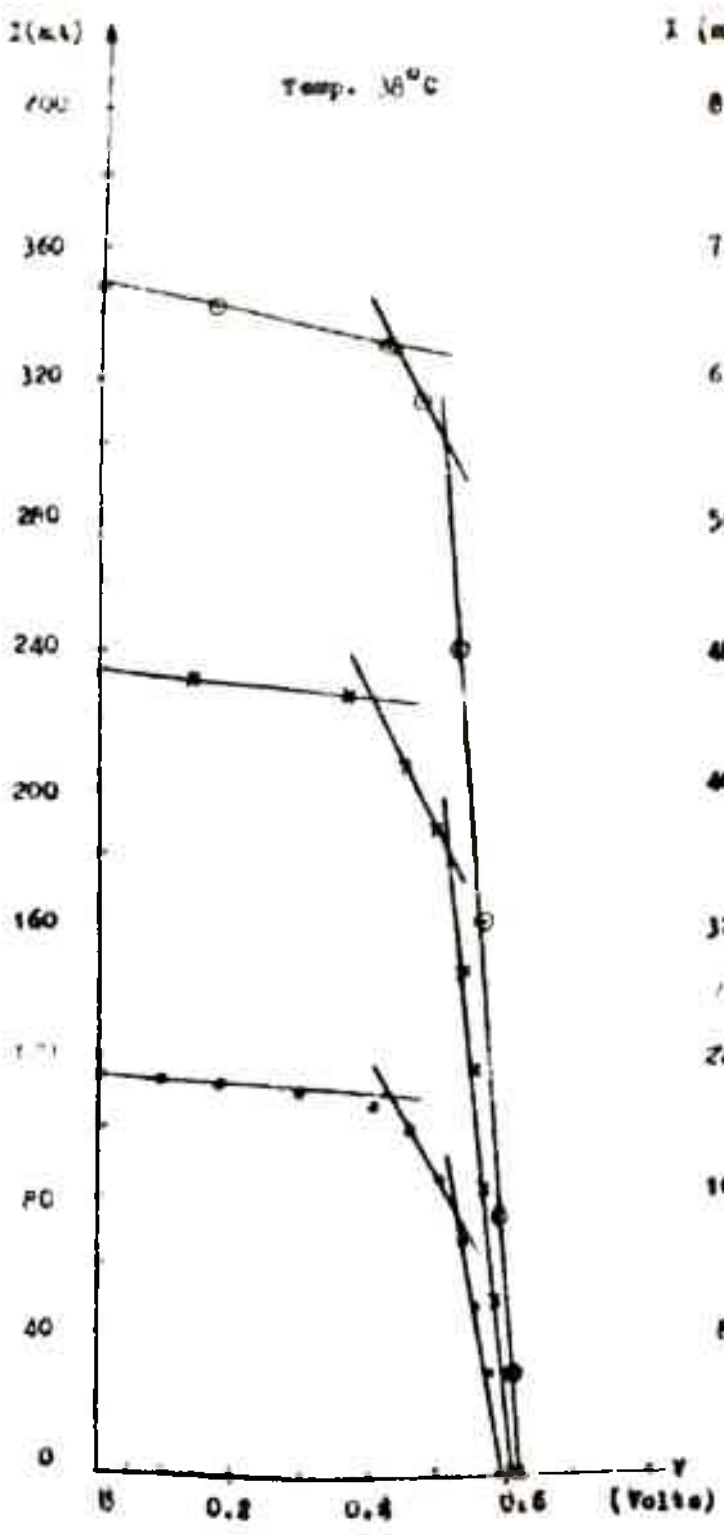


Fig. 2.5 Piece-wise linear V-I Characteristics of Solar Cell

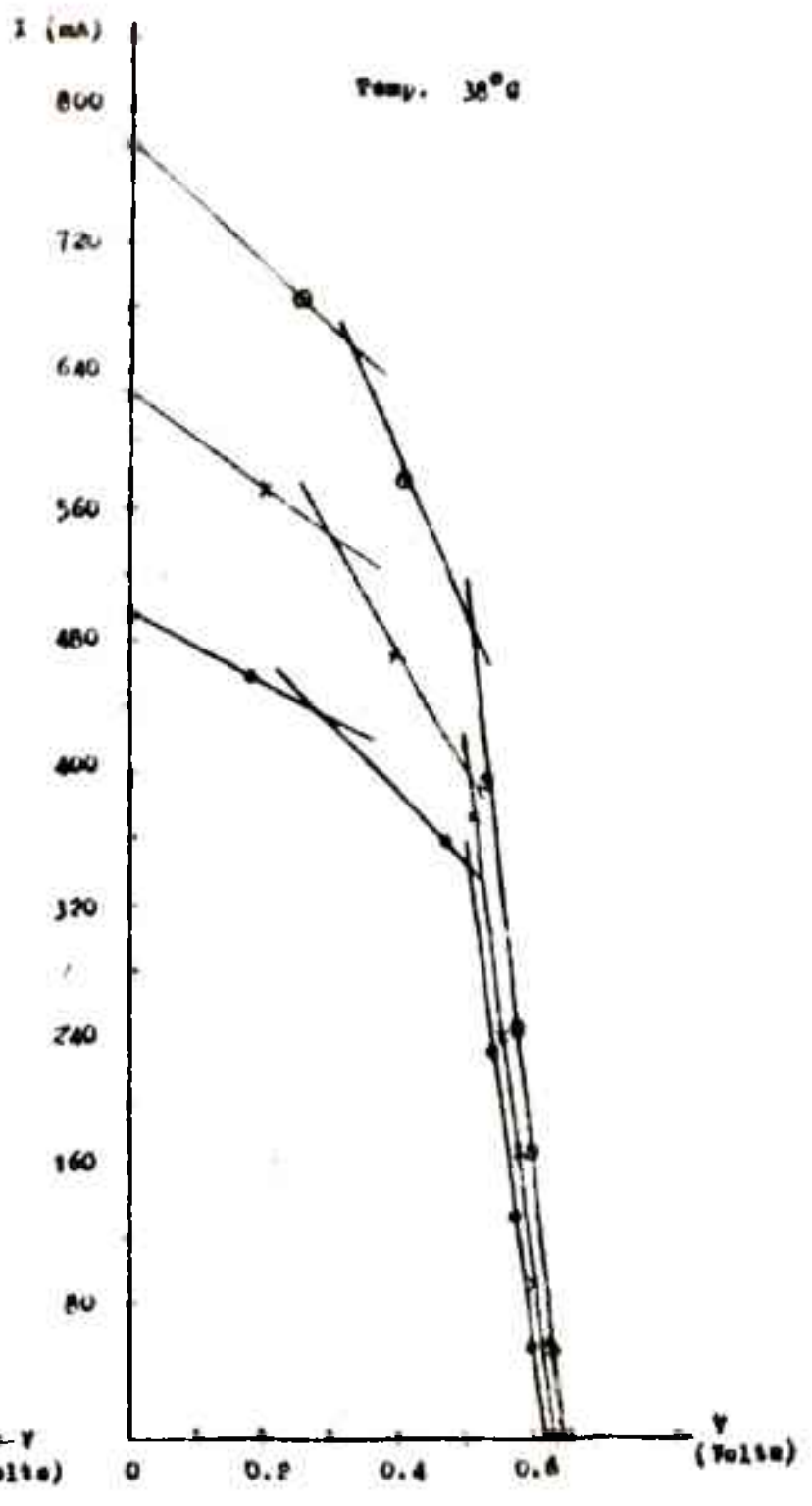


Fig. 2.6 Piece-wise linear V-I Characteristics of Solar Cell

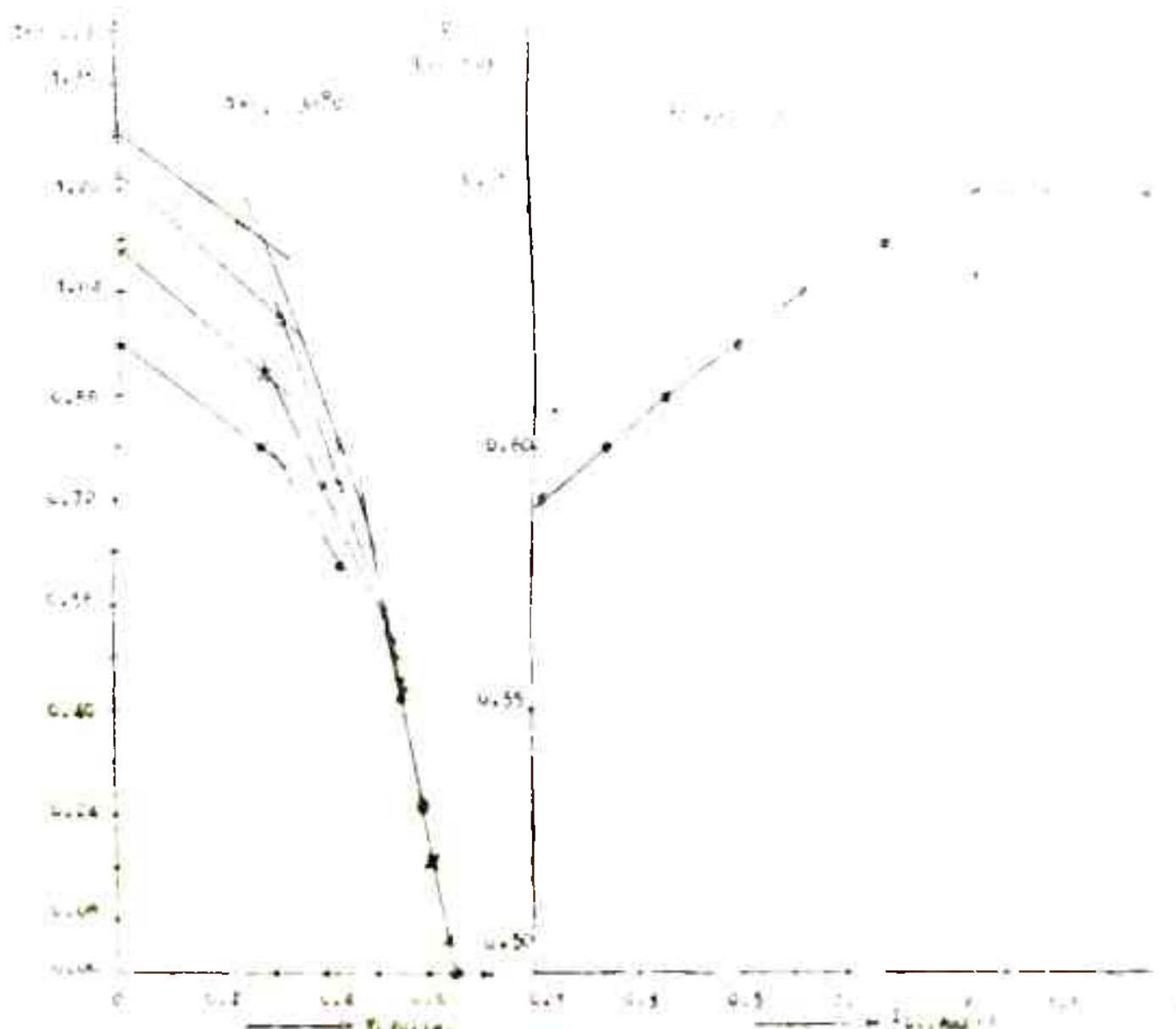


Fig. 2.7 Piece-wise linear I-V Characteristic of Solar Cell.

Fig. 2.8 Variation of V_{OC} with intensity.

10. 17. 64

11. 18. 64

12. 19. 64

13.

14.

15.

16.

17.

18.

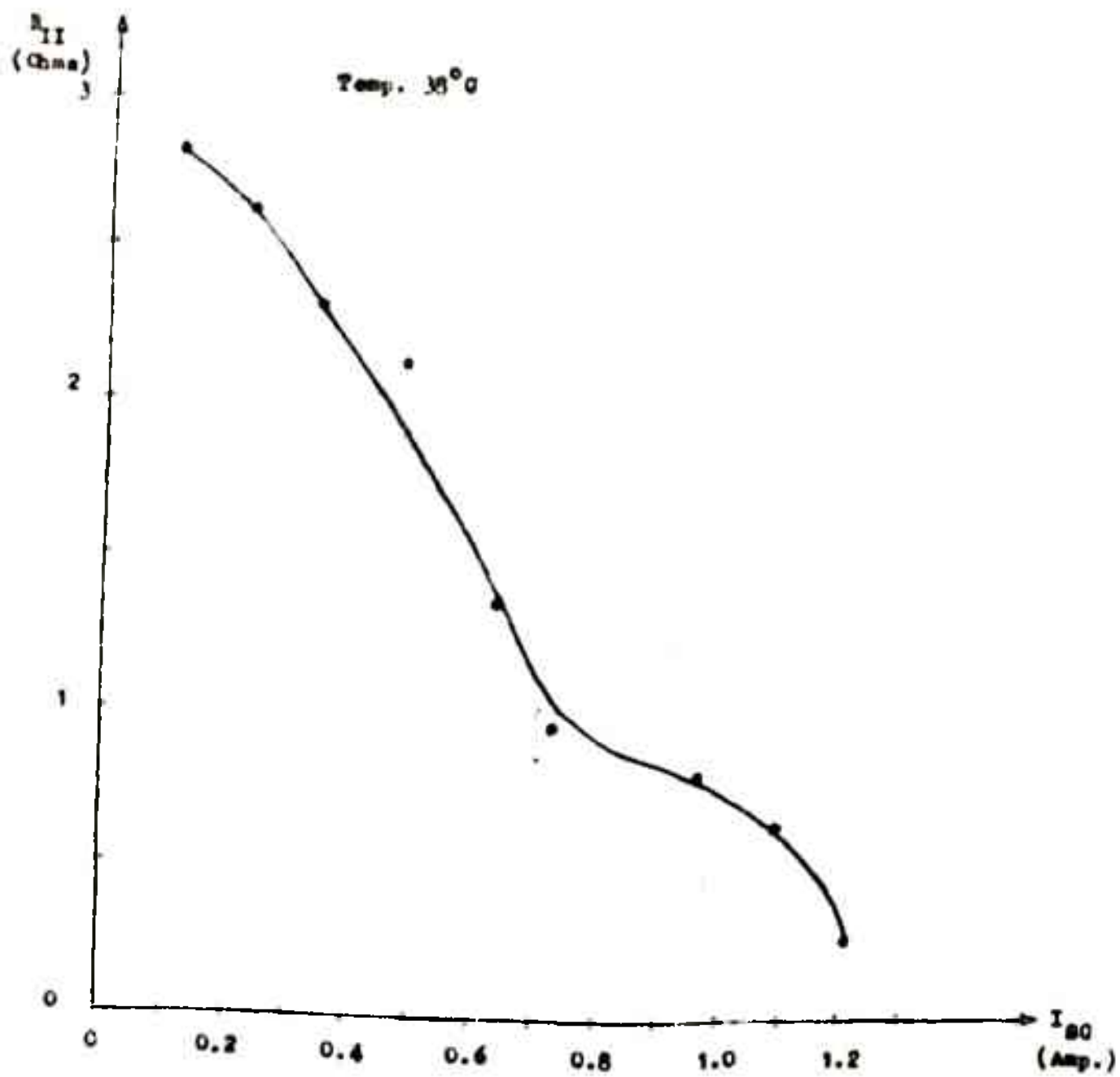


Fig. 2.10 Variation of R_{II} with intensity.

■

■

■

■

■

■

■

■

I_M P_M
(Amp.) (Watts)

1.5 0.9

1.5 0.8

1.4 0.7

1.2 0.6

1.0 0.5

0.7 0.4

0.6 0.3

0.4 0.2

0.2 0.1

0.0 0.0

Temp. 30°

—•— I_M
--- I_M

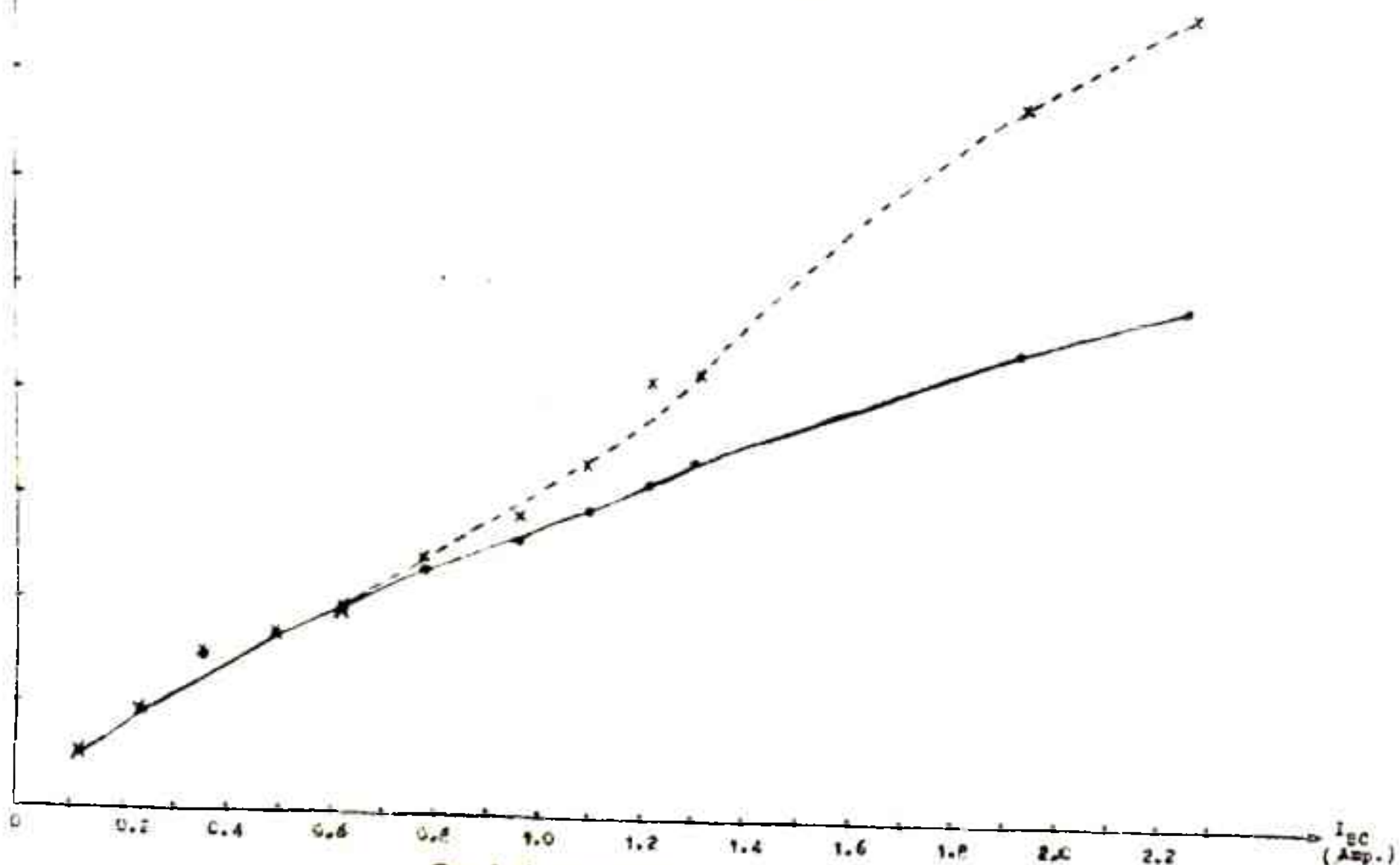


Fig. 2.12 Variation of I_M and P_M with intensity.

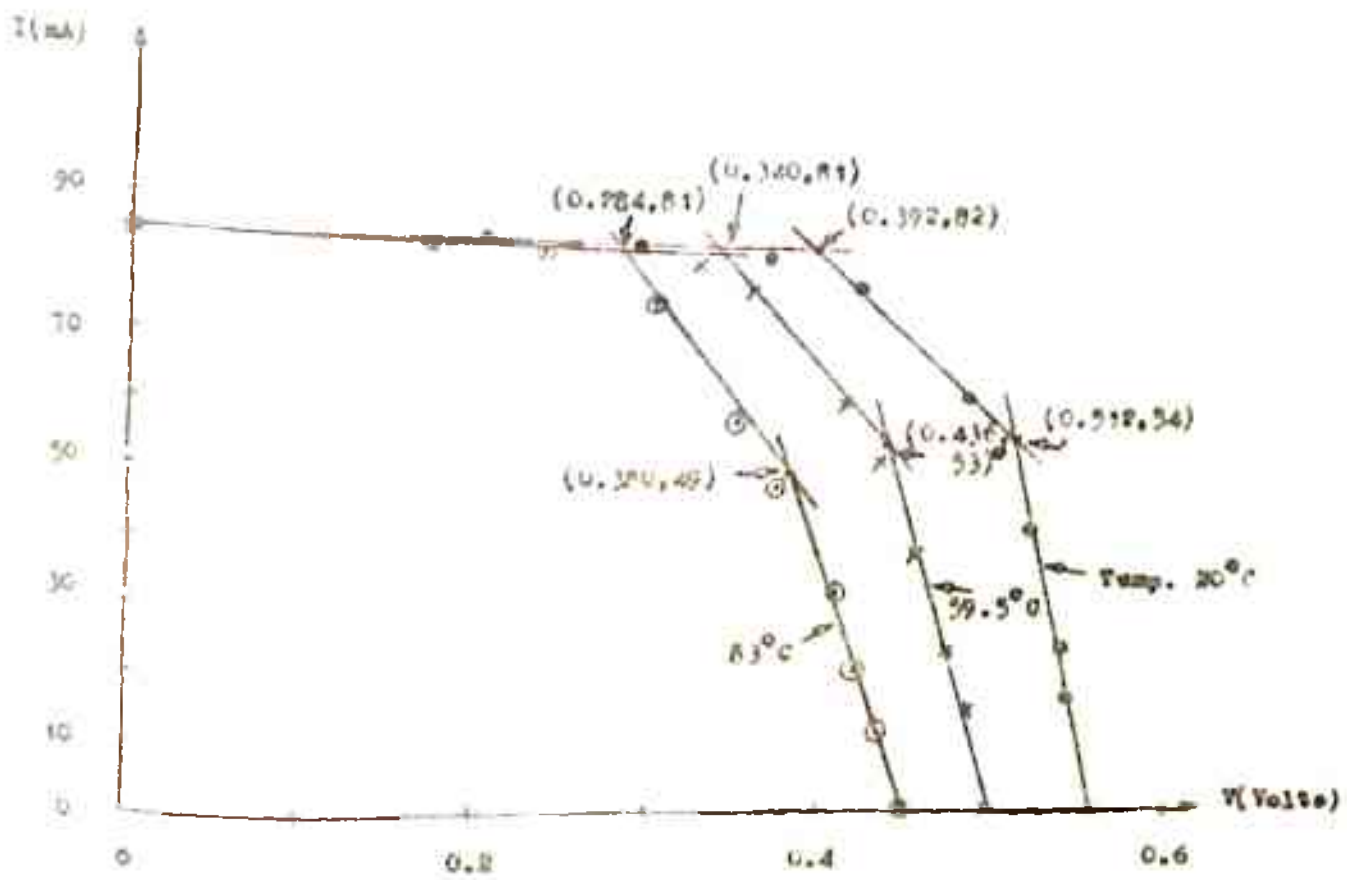


Fig. 2.13 Piece-wise Linear Characteristics of Solar Cell.

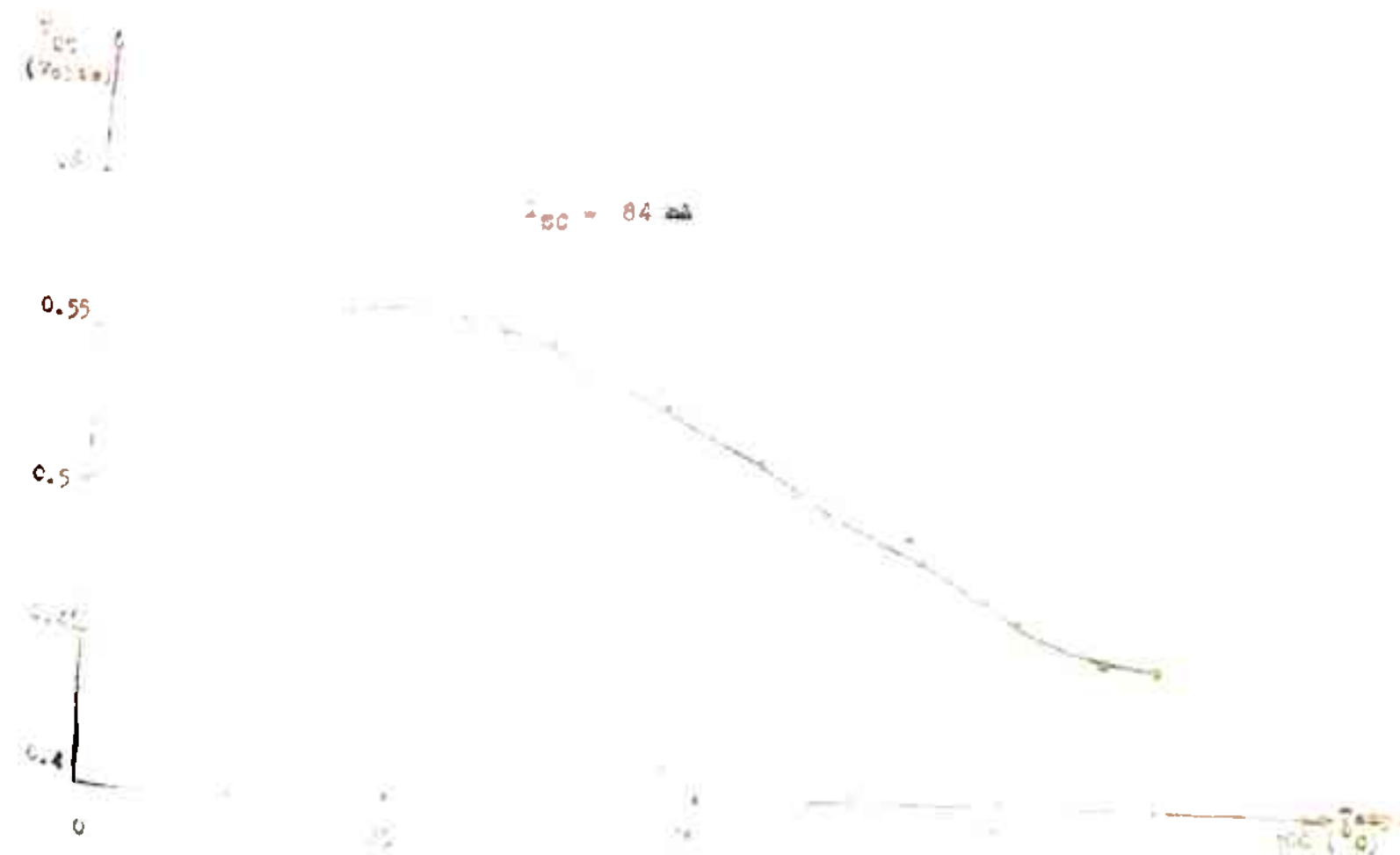


Fig. 2.14 Variation of V_{CE} with Temperature.

Table 2.4

Temp. (°C)	R_I (Ohms)	R_{II} (Ohms)	R_{III} (Ohms)	P_M (Watts)	V_K (Volts)	I_M (Amperes)	$\frac{P_M}{2 I_M}$ (Ohms)
20	0.8704	4.2859	196.0000	0.0321	0.3920	0.0820	4.7805
59.5	1.1320	3.4286	109.3333	0.0275	0.3400	0.0810	4.1975
83	1.3870	3.0000	94.6667	0.0230	0.2840	0.0810	3.5067

2.7 Discussion

The nature of variation of three segment parameters viz. R_I , R_{II} and R_{III} with intensity and temperature can be explained from the theoretical relations (eqns. 2.8 to 2.10).

2.7.1 Parameters Variation with Intensity Keeping Temperature Constant

Figs. 2.9 to 2.11 show that R_I , R_{II} and R_{III} decrease with intensity. This decrease can be explained from eqns. 2.8 to 2.10. R_I decreases nonlinearly as the photo generated current I_S increases linearly with intensity. Infact, if we assume R_S , λ and I_0 independent of the intensity, the variation of R_I with intensity is essentially hyperbolic. However, even if the variation of R_S and I_0 with intensity¹⁸⁻²⁰ is taken into account, R_I still decreases with intensity.

The variation of R_{III} with intensity is essentially going to be dependent on the increase in I_{SC} . Since I_{SC} increases linearly with intensity in the range of interest, R_{III} shall decrease exponentially with intensity as seen from eqn.2.9.

The variation of R_{II} with intensity depends on the change of P_M and I_M with intensity (eqn. 2.10). There is an increase in both P_M and I_M with increase in intensity. However, P_M increase with intensity is slow because of increasing drop across R_S which in turn decreases V_M^{23} . Further, the denominator being I_M^2 , R_{II} decreases nonlinearly with intensity.

2.7.2 Variation of Parameters with Temperature Under Constant Intensity

It is clear from the experimental observations that R_I increases and R_{II} and R_{III} decrease with temperatures. The variation of these parameters can be explained using the eqns. 2.8 to 2.10. In these equations the major factor which controls the variation is I_0 and it is well established that I_0 increases exponentially with temperature.^{21,24,28}

The short circuit current does not vary much with temperature.²⁵⁻²⁷ But V_{OC} decreases with temperature^{21,25-27} which is shown in Fig. 2.14. This is obvious from the nonlinear equation of the cell which when written for $I_L = 0$ gives

$$V_{OC} = \lambda \ln \left(\frac{I_S}{I_0} + 1 \right)$$

where $\lambda = \frac{AkT}{q}$

The dominant parameter in this equation is again I_0 .

Though R_S also varies a bit with temperature in the eqn. 2.8 and 2.9, the dominant term is the second term. Also as $I_S \gg I_0$,

$$R_I = R_S + \frac{\lambda}{I_S}$$

I_S remains constant with temperature, As λ increases linearly with temperature, R_I also increases. Experimentally this increase is also observed.

The decrease in R_{III} with temperature can be explained by examining the second term in eqn. 2.9 which is

$$\frac{\lambda}{I_0} e^{-\frac{I_{SC} R_S}{\lambda}}$$

This is proportional to ²⁴

$$\frac{1}{T^2 e^{-E_g/kT}} e^{-\frac{I_{SC} R_S}{\lambda}}$$

This term decreases with increase in temperature, thereby R_{III} also decreases.

The variation of R_{II} with temperature can be seen from the variation of P_M and I_M with temperature. Both P_M and

I_M decrease with temperature.²⁵ The decrease of P_M is much more as compared to the decrease of I_M . Infact I_M may not change much with temperature²⁷ and as the area under the V-I curve decreases with temperature²¹, V_M also decreases. Hence P_M decreases with increase in temperature resulting into decrease of R_{II} with temperature.

2.8 CONCLUSIONS

In this Chapter, piece-wise approximation of the V-I characteristics of a solar cell has been presented. It has been shown on the basis of experimental results that three piece-wise linear segment approximation of the V-I characteristics of the cell is most suited. The procedure of drawing three linear segments has been presented. Thereby, the characteristic parameters of three segment linearised V-I characteristics has been defined.

The performance of a solar cell at high intensity and temperature has been experimentally studied. It has been observed that the three segment parameters R_{II} and R_{III} decrease both with increase in intensity and temperature whereas R_I decreases with increase in intensity but increases with increase in temperature. The variation of these parameters with intensity and temperature has been explained on the basis of known variation of parameters of a conventional model of a cell.

In Chapter 3, the three piece-wise linear segments approximation of V-I characteristics of a single cell is used to analytically determine the V-I characteristics of a solar cell array. The variation of three segment parameters of a single cell with intensity and temperature is extended to study the behaviour of solar cell array at high intensity and temperature.

REFERENCES

1. Prince, M.B., "Silicon Solar Energy Converters", J. Appl. Phy., Vol. 26, 1955, p 534.
2. Wolf, M. and Rauschenbach, H., "Series Resistance Effects on Solar Cell Measurements", Advanced Energy Conversion, Vol. 3, 1963, p 455.
3. Luque, A. et al, "Connection Losses in Photovoltaic Arrays", Solar Energy, Vol. 25, 1980, p 171.
4. Wolf, M., "Limitations and Possibilities of Improvement of Photovoltaic Solar Energy Converters", Proc. of I.R.E., Vol. 48, 1960, p 1246.
5. Wysocki, J.J., "The Effect of Series Resistance on Photovoltaic Solar Energy Conversion", RCA Review, Vol. 22, 1961, p 57.
6. Chelnokov, Y. Ye, "Method for Measuring Series Resistance of Diffusion Silicon Photoelements of Large Area", Radio Engg. and Electronics Physics, Vol. 8, 1963, p 892.
7. Handy, R.J., "Theoretical Analysis of the Series Resistance of a Solar Cell", Solid State Electronics, Vol. 10, 1967, p 765.
8. Inamura, M.S. and Portscheller, J.I., "An Evaluation of the Methods of Determining Solar Cell Series Resistance", Conference Record of the 8th IEEE Photovoltaic Specialists Conference, Washington, 1970, p 102.
9. Rao, A.B. and Prasad, S., "Series Resistance of a Silicon Solar Cell at Very Low Intensities", Indian Journal of Physics, Vol. 45, Sept. 1971, p 391.

10. Rao, A.B. and Nath, P., "Internal Resistance of a Silicon Solar Cell", Indian Journal of Pure and Applied Physics, Vol. 10, May 1972, p 351.
11. Evdokimov, V.M., "Calculations of Series and Shunt Resistances on the Basis of the Volt-Ampere Characteristics of a Solar Cell", Applied Solar Energy, Vol. 8, No. 6, 1972, p 63.
12. Rao, A.B. and Padmanabhan, G.R., "A Method for Estimating the Optimum Load Resistance of a Silicon Solar Cell used in Terrestrial Power Applications", Solar Energy, Vol. 15, 1973, p 171.
13. Bordina, N.M., et al., "Determining the Parameters of a Photoconverter Current-Voltage Characteristics", Applied Solar Energy, Vol. 13, 1977, p 13.
14. Bubbio, S. and Califano, F.P., "On the Series Resistance of Solar Cells", Conference Record of the 12th IEEE Photovoltaic Specialists Conference, Louisiana, 1976, p 71.
15. Boone, J.L. and Van Doren, T.P., "Solar Cell Design based on a Distributed Diode Analysis", IEEE Trans. on Electron Devices, Vol. ED-25, 1978, p 767.
16. Slonim, M.A., "New Equivalent Diagram of Solar Cells (Engineering point of view)", Solid State Electronics, Vol. 21, 1978, p 617.
17. Bogomolny, B., et al., "Reliability Simulation of a Large Solar Battery", Proceedings of International Photovoltaic Solar Energy Conference, Luxembourg, 1977, p 1261.
18. Joshi, S.P. et al., "Development of Silicon Solar Cells for Concentrated Sunlight", Proc. National Solar Energy Convention, IIT Bombay, 1979, p 293.

19. Davis, D.S., *Nomography and Empirical Equations*, Reinhold Publishing Corp., 1962, p 30.
20. Otterbein, R.T. et al., "A Modified Single Diode Model for High Illumination Solar Cells for Simulation Work", Conference Records of 13th IEEE Photovoltaic Specialist Conference, Washington, 1978, p 1074.
21. Hovel, H.J., *Semiconductors and Semimetals, Solar Cells*, Vol. 11, Academic Press, 1975.
22. Pardhasaradhi, T.V. and Ramakishana Rao, M., "Some Problems in the Fabrication of Fresnel Lenses", Proc. National Solar Energy Convention, IIT, Bombay., 1979, p 465.
23. Agarwal, A., "Response of Solar Cells to High Intensity, Concentrated Radiation", Ph.D. Thesis, BITS, Pilani, 1979.
24. Sze, S.M., *Physics of Semiconductor Devices*, John Wiley & Sons., 1969.
25. Wysocki, J.J. and Rappaport, P., "Effect of Temperature on Photovoltaic Solar Energy Conversion", *J. App. Phys.*, Vol. 31, March 1960, p 571.
26. Rule, T.T. et al, "The Testing of Specially Designed Silicon Solar Cells Under High Sunlight Illumination", Conference Record of 12th IEEE Photovoltaic Specialists Conference, Louisiana, 1976, p 744.
27. Yasui, R.K. and Schmidt, L.W., "Performance Characteristics of Ti-Ag Contact N/P and P/N Silicon Solar Cells", Conference Record of the 8th IEEE Photovoltaic Specialists Conference, Washington, 1970, p 110.

28. Bachus, C.E. et al., "The Performance of Silicon Solar Cells under Concentrated Sunlight", SUN II, Proc. of the International Solar Energy Society, Georgia, Vol. 3, 1979, p 1798.

+++++++

CHAPTER 3DETERMINATION OF SOLAR CELL ARRAY CHARACTERISTICS
USING PIECE-WISE LINEAR APPROXIMATION

- 3.1 Introduction
- 3.2 Interconnection of Two Identical Cells
 - 3.2.1 Series Connection
 - 3.2.2 Shunt Connection
- 3.3 Interconnection of Two Nonidentical Cells
 - 3.3.1 Series Connection
 - 3.3.2 Shunt Connection
 - 3.3.3 Experimental Study
- 3.4 Analysis of Solar Cell Array (SCA)
 - 3.4.1 Sub-array with Cells Connected in Series
 - 3.4.2 Determination of Solar Cell Array (SCA) Characteristics
- 3.5 Variation of Array Parameters with Intensity and Temperature
 - 3.5.1 Variation of R_I , R_{II} and R_{III} with Intensity Keeping Temperature Constant
 - 3.5.2 Variation of R_I , R_{II} and R_{III} with Temperature Keeping Intensity Constant
- 3.6 Conclusions
- References

CHAPTER 3

DETERMINATION OF SOLAR CELL ARRAY CHARACTERISTICS USING PIECE-WISE LINEAR APPROXIMATION

3.1 Introduction

A solar cell array consists of large number of cells connected in series and shunt in a matrix form. The V-I characteristics of the array depends upon the V-I characteristics of individual cell forming the array. To estimate the V-I characteristics of the array, individual cells can be replaced by their equivalent models and the complete analysis can be carried out.¹⁻⁵ A widely used model of the cell is the diode model as shown in Fig. 1.1. The analysis of the array is rather easy when the cells are identical. In practice it is quite likely that the cells are not identical to start with or there may be unequal change in the characteristics of individual solar cells forming the array. The effect of solar cell parameter variation on array output has been studied by various investigators.^{1,2,4-9}

When nonidentical cells are connected in series or if some of the cells in the series connected combination are shadowed, a large reverse voltage may appear across the cell with minimum

value of short circuit current, thus forming the hot spots. Such problems can be removed by using the shunt diodes.^{7,10}

Detailed method for the analytical determination of V-I characteristics of a solar cell array using nonidentical cells is not available in literature. In this chapter, the procedure for analytical determination of V-I characteristics of a solar cell array employing nonidentical cells is presented. The procedure is based upon the three segment piece-wise linear approximation of V-I characteristics of each cell and thereby determining the overall V-I characteristics of the array using the linear equations for the three segments.

Using the established variation of parameters like R_S and R_{Sh} of the equivalent circuit of Fig. 1.1 of individual cell, with intensity and temperature, the variation of R_I , R_{II} and R_{III} of single cells with intensity and temperature has already been discussed in Chapter 2. The variation of R_I , R_{II} and R_{III} for the array with intensity and temperature are expected to follow the variation obtained in the case of a single cell.

The chapter discusses the interconnection of two identical solar cells both in series and shunt and thereby the maximum power output in each case is evaluated. This is followed by the detailed study of the analytical determination of V-I characteristics of series and shunt connected two nonidentical cells.

Maximum power output in each connection is also evaluated. Experimental verification is also presented both for series and shunt connected cells.

As the array consists of large number of cells connected in series and shunt, the analytical evaluation of the V-I characteristics of the array starting from the experimental individual cell V-I characteristics is the next study performed. The performance is also verified experimentally. The variation of the characterising parameters based on three segment linear approximation of the V-I characteristics of the array with intensity and temperature is also discussed and experimentally verified.

3.2 Interconnection of Two Identical Cells

The cells in a solar cell array can be connected in series or in shunt. Analytical determination of the V-I characteristics of both types of connections using piece-wise approximation is given below.

3.2.1 Series Connection

When two exactly identical cells operating under same conditions of intensity and temperature are connected in series, the overall V-I characteristics of the series connection of solar cells can be predicted easily. In each segment, voltage is calculated at a particular value of the current due to each cell.

The overall voltage at this value of the current is sum of the two voltages. As the cells are identical, the overall voltage is simply double of the single cell voltage. This way the overall V-I characteristics can be predicted analytically. The V-I characteristics thus obtained has intersection points as $(V_1' + V_1'', I_1')$ and $(V_2' + V_2'', I_2')$, open circuit voltage $V_{OC} = V_{OC}' + V_{OC}'' = 2 V_{OC}'$ and short circuit current $I_{SC} = I_{SC}' = I_{SC}''$. Here (V_1', I_1') and (V_2', I_2') are intersection points for cell 1 and (V_1'', I_1'') and (V_2'', I_2'') are intersection points for cell 2. Because the cells are identical, $I_1' = I_1''$, $I_2' = I_2''$. For the overall characteristics, the resistances offered by each segment are

$$R_I = \frac{V_{OC} - (V_1' + V_1'')}{I_1'} = \frac{V_{OC}' - V_1'}{I_1'} + \frac{V_{OC}'' - V_1''}{I_1''}$$

$$= R_I' + R_I'' = 2R_I'$$

Similarly,

$$R_{II} = 2R_{II}'$$

$$R_{III} = 2R_{III}'$$

Maximum Power Output

As discussed in Chapter 2, the maximum power output point can lie in any segment. In most of the cases, it lies in segment II.

The maximum power output

$$P_M = \frac{K_1^2}{4K_2}$$

where $K_1 = V_{OC} + I_1 R_2$ and $K_2 = R_1 + R_2 = R_{II}$

in the segment II.

$$\text{Therefore, } P_M = \frac{(V_{OC} + I_1 R_2)^2}{4 R_{II}}$$

$$\text{or } P_M = \frac{(V'_{OC} + I'_1 R'_2)^2}{2R'_{II}}$$

Thus P_M is double the maximum power output due to single cell as expected.

3.2.2 Shunt Connection

If two identical cells are connected in shunt, to predict the overall characteristics, for each segment the current is calculated at a particular voltage for each cell. The overall characteristics contains current equal to sum of the currents due to individual cell at that value of voltage. Because cells are identical total current is double of the single cell current at that voltage. Using this procedure, each segment of the overall characteristics can be determined. The intension points are $(V'_1, I'_1 + I''_1)$ and $(V'_2, I'_2 + I''_2)$, open circuit voltage, $V_{OC} = V'_{OC} = V''_{OC}$ and shunt circuit current

$I_{SC} = I_{SC}' + I_{SC}'' = 2I_{SC}'$. The resistances offered by each segment are

$$R_I = \frac{V_{OC}' - V_1'}{I_1' + I_1''} = \frac{V_{OC}' - V_1'}{2I_1'} = \frac{R_I'}{2}$$

Similarly, $R_{II} = \frac{R_{II}'}{2}$

and $R_{III} = \frac{R_{III}'}{2}$

Maximum Power Output

Again assuming that the maximum power point lies in segment II, we have

$$P_M = \frac{(V_{OC}' + I_1' R_2')^2}{4R_{II}'}$$

$$\text{or } P_M = \frac{(V_{OC}' + I_1' R_2')^2}{2R_{II}'}$$

Thus in this case also P_M is double the maximum power output due to single cell.

3.3 Interconnection of two nonidentical cells

The analytical determination of overall V-I characteristics of two identical cells connections is straight forward. In practice when an array is fabricated the cells may not be identical to begin with or their characteristics may differ due to different

operating conditions. Therefore the determination of the array characteristics using nonlinear cell model is quite involved. In this section, series and shunt connections of two nonidentical cells are considered. The overall V-I characteristics determination using piece-wise linear approximation is presented and some of the problems faced are indicated.

3.3.1 Series Connection

Let us assume that cells have different values of short circuit currents and open circuit voltages. Let the short circuit current be I_{SC}^I and open circuit voltage be V_{OC}^I for cell 1 and corresponding values be I_{SC}^{II} and V_{OC}^{II} for cell 2. Let us also assume that $I_{SC}^I < I_{SC}^{II}$ and $V_{OC}^I < V_{OC}^{II}$.

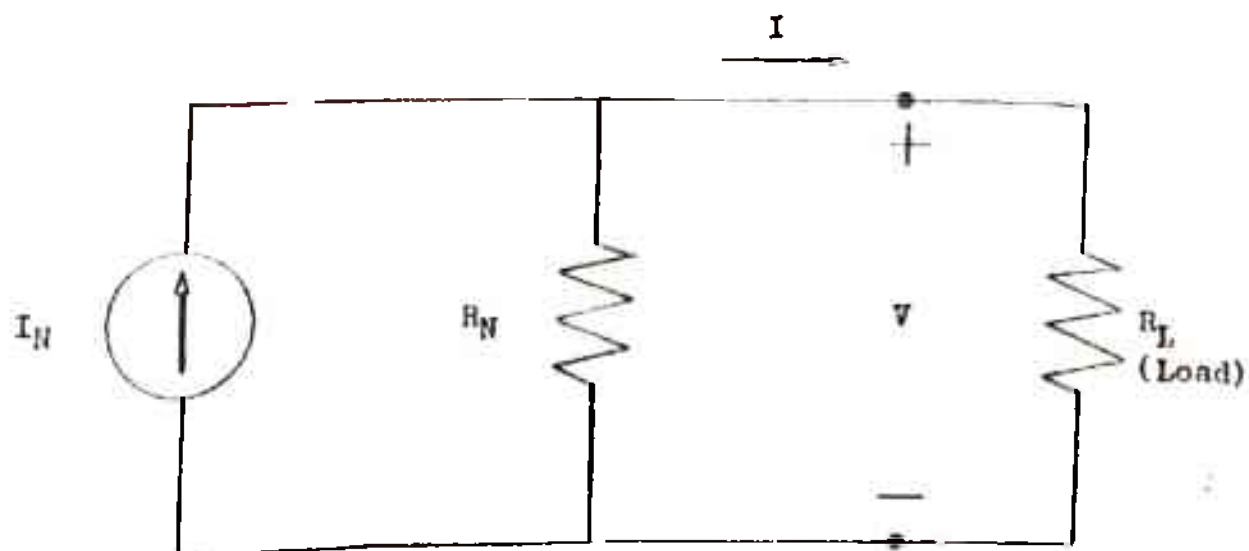
For a single cell, each segment equation can be represented by an equivalent circuit shown in Fig. 3.1.

$$\text{For segment I, } I_N = \frac{V_{OC}^I}{R_I}, \quad R_N = R_I$$

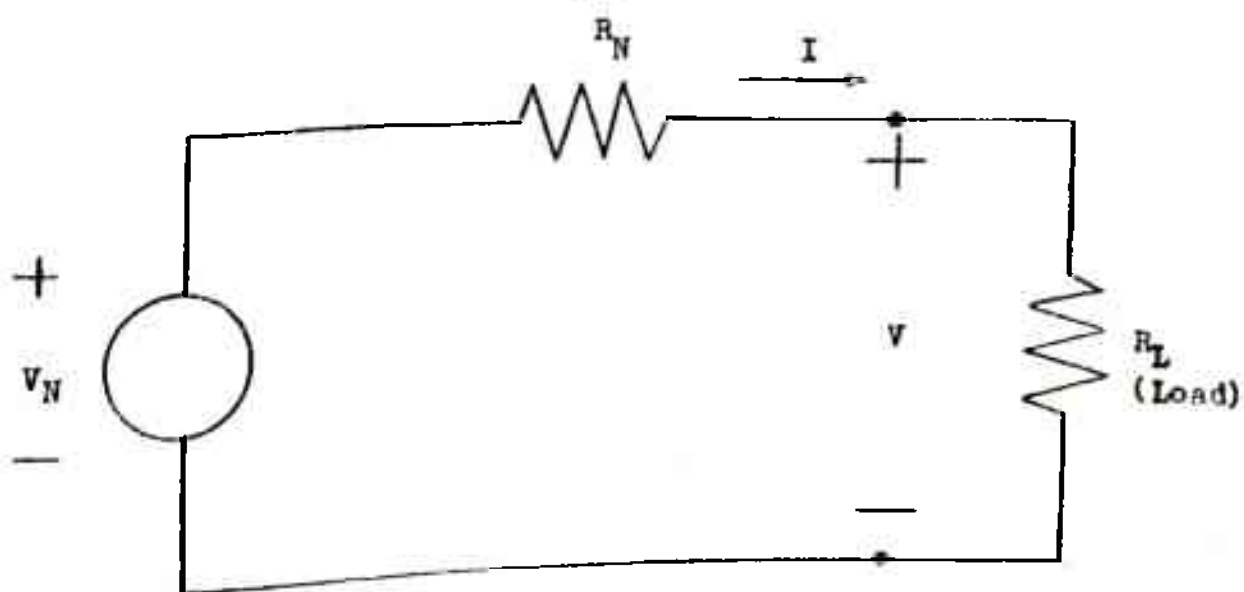
$$\text{For segment II, } I_N = \frac{V_{OC}^I + I_1 R_2}{R_{II}}, \quad R_N = R_{II}$$

$$\text{and for segment III, } I_N = \frac{V_{OC}^I + I_1 R_2 + I_2 R_3}{R_{III}}, \quad R_N = R_{III}$$

For the series connection of two nonidentical cells, the overall equivalent circuit is shown in Fig. 3.2. The short circuit current of the series combination is determined as follows. In segment III of each cell, $I_N^I = I_{SC}^I$, $I_N^{II} = I_{SC}^{II}$. Under the short circuit condition, $R_L = 0$,



(a)



$$V_N = I_N \cdot R_N$$

(b)

Fig. 3.1 Equivalent Circuit Representation of the Linear Segment Equations (a) Current Source Representation (b) Voltage Source Representation

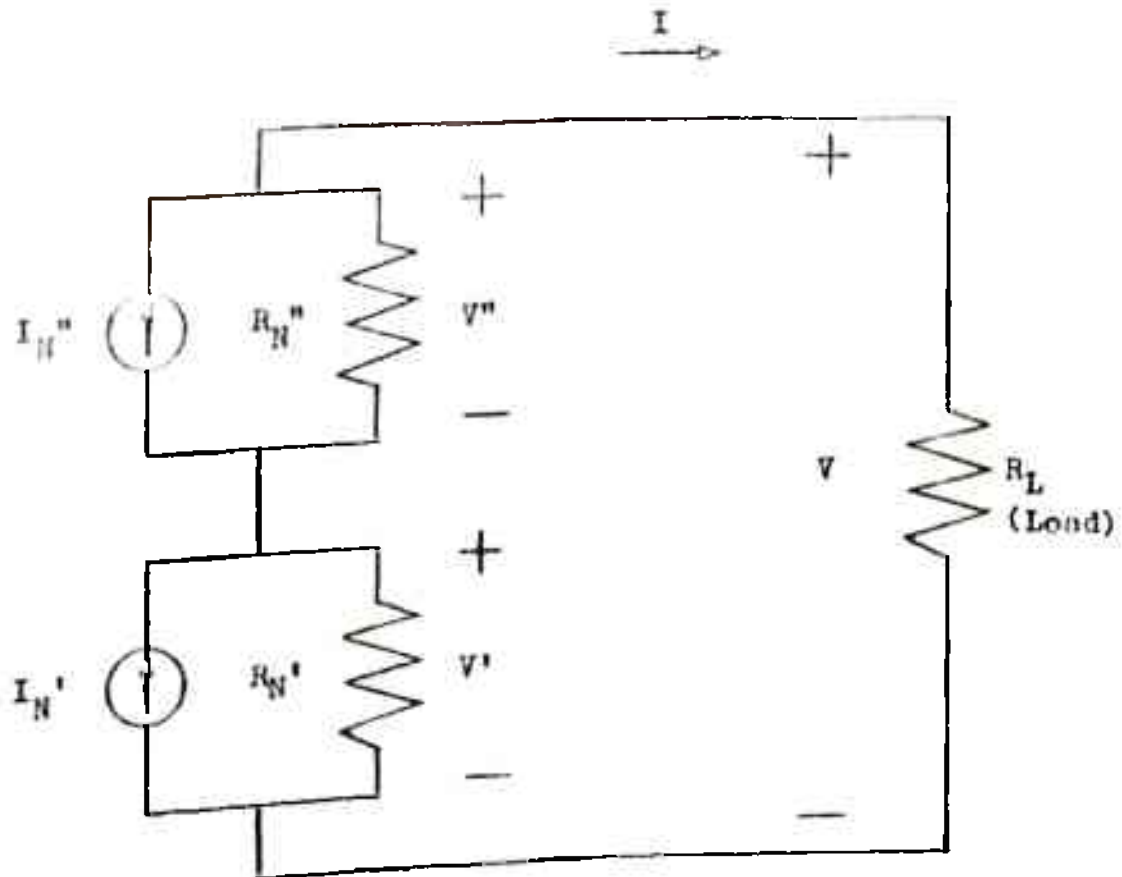


Fig. 3.2 Overall Equivalent Circuit of Series Connection of Two Nonidentical Cells

$$V = V' + V'' = 0.$$

Hence $V' = -V''$

Since $I_{SC}'' > I_{SC}'$, V'' shall be positive.

Hence V' is negative which implies that the cell 1 is operating under reverse bias voltage.¹ Because of this, the cell 1 no longer acts as generator but acts as a load for the other cell. The resultant short circuit current I_{SC}''' is obtained by experimentally measuring and then plotting the reverse characteristics of the cell 1 and taking its mirror image, shown as dotted line in Fig. 3.3. The point of intersection of this line with any segment of the other cell gives V'' . The cell 2 current at $V = V''$ is the resultant short circuit current I_{SC}''' . The negative voltage across cell 1, V' is also shown in the figure. It can be seen from Fig. 3.3 that the reverse voltage across cell 1 goes on increasing as the difference between the V-I characteristics of the two cells become large, V' in fact may approach the reverse break down voltage of the cell. In a large array where a cell may be under shadow or its characteristics has deteriorated, "hot spots" are formed² because of large reverse voltage across one of the cells. The failure of one cell in the array can produce malfunction in the working of the array. To overcome this effect, shunting diodes are normally used.^{1,7,10}

In order to determine the complete V-I characteristics R_L is increased from zero i.e. I is decreased from I_{SC}''' . As

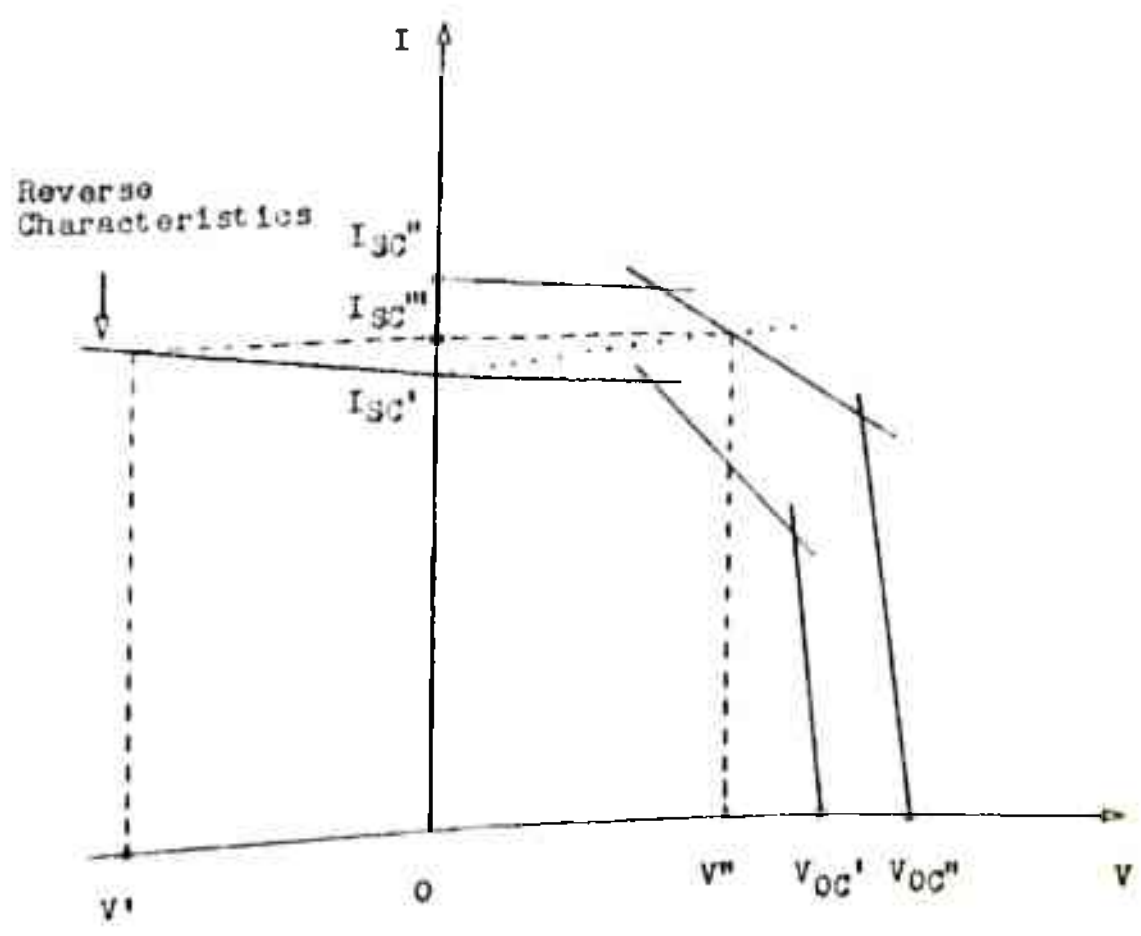


Fig. 3.3 Piece-wise Linear V-I Characteristics and Reverse Characteristics of the Cells

V increases, V'' becomes more positive and V' less negative. At one value of I , V' becomes zero. After this point only, both V' and V'' will be positive. Under the open circuit condition, $V' = V'_{OC}$ and $V'' = V''_{OC}$ resulting in net open circuit voltage $V'''_{OC} = V'_{OC} + V''_{OC}$.

For $0 < I < I'''_{SC}$, the relation between V and I depends upon the slopes of the appropriate segments of the two cells. This procedure is applicable for all combinations of I'_{SC} and I''_{SC} and V'_{OC} & V''_{OC} . If both the cells have identical values of short circuit currents i.e. $I'_{SC} = I''_{SC}$, the resultant short circuit current $I'''_{SC} = I'_{SC} = I''_{SC}$. If $I''_{SC} < I'_{SC}$, the reverse characteristics of the cell 2 can be measured and the above procedure can be adopted to find the resultant V - I characteristics starting from the short circuit current, I'''_{SC} . The following example illustrates the above procedure.

Example

Let us consider two piece-wise linear characteristics of two non-identical cells with the following identities.

$$I'_{SC} < I''_{SC}, \quad I'_2 < I''_2, \quad I'_1 < I''_1, \quad I''_1 < I'_2,$$

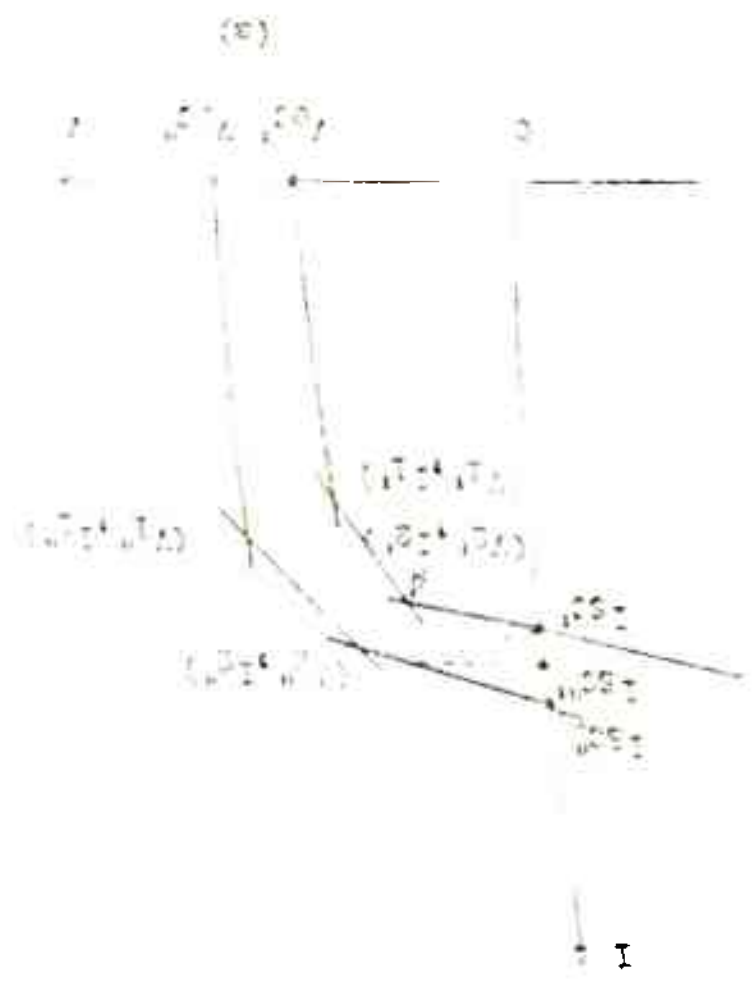
$$I'''_{SC} > I''_2, \quad I''_2 > I'_{SC} \quad \text{and} \quad V''_{OC} > V'_{OC}$$

The characteristics are shown in Fig. 3.4(a). The resultant V - I characteristics of the series combination is shown in Fig. 3.4(b). Table 3.1 gives the equations governing segments VI

(b) ROSS 1-1

Cells

(a) Piece-wise linear



to I. R_r is the reverse resistance of the cell 1 with lower short circuit current. At any point, total voltage across the load, $V = V_A + V_B$.

Table 3.1

Segment	Voltage contribution due to cell 1, V_A	Voltage contribution due to cell 2, V_B
VI	$(I'_{SC} - I)R_r$	$V''_{OC} + I''_1 R''_2 + I''_3 R''_3 - I(R''_1 + R''_2 + R''_3)$
V	$(I'_{SC} - I)R_r$	$V''_{OC} + I''_1 R''_2 - I(R''_1 + R''_2)$
IV	$V'_{OC} + I'_1 R'_2 + I'_2 R'_3 - I(R'_1 + R'_2 + R'_3)$	$V''_{OC} + I''_1 R''_2 - I(R''_1 + R''_2)$
III	$V'_{OC} + I'_1 R'_2 - I(R'_1 + R'_2)$	$V''_{OC} + I''_1 R''_2 - I(R''_1 + R''_2)$
II	$V'_{OC} + I'_1 R'_2 - I(R'_1 + R'_2)$	$V''_{OC} - I R''_1$
I	$V'_{OC} - I R'_1$	$V''_{OC} - I R''_1$

Maximum Power Output

Let us assume that maximum power output in the resultant V-I characteristics lies in segment III (see Fig. 3.4(b)). This segment is governed by segments II of cell 1 and cell 2. Let

$$\begin{aligned}
 V'_{OC} + I'_1 R'_2 &= V'_I \\
 R'_1 + R'_2 &= R'_I
 \end{aligned}$$

$$V_{OC}'' + I_1'' R_2'' = V_{II}''$$

$$R_1'' + R_2'' = R_{II}''$$

So maximum power output

$$\text{due to cell 1, } P_1 = \frac{V_{II}'^2}{4R_{II}'}$$

$$\text{due to cell 2, } P_2 = \frac{V_{II}''^2}{4R_{II}''}$$

$$\text{due to series combination, } P_S = \frac{(V_{II}' + V_{II}'')^2}{4(R_{II}' + R_{II}'')}$$

$$P_1 + P_2 = \frac{V_{II}'^2 R_{II}'' + V_{II}''^2 R_{II}'}{4R_{II}' R_{II}''}$$

Equating $P_1 + P_2$ with P_S , we get

$$\left(1 - \frac{V_{II}' R_{II}''}{V_{II}'' R_{II}'}\right)^2 = 0$$

$$\text{For } P_1 + P_2 = P_S, \quad V_{II}' R_{II}'' = V_{II}'' R_{II}'$$

$$\text{which implies } V_{II}' = V_{II}''$$

$$\text{and } R_{II}' = R_{II}''$$

$$\text{or } \frac{V_{II}'}{R_{II}'} = \frac{V_{II}''}{R_{II}''}$$

which is possible for identical cells only. In other cases,

$$P_1 + P_2 > P_S \quad \text{as } IHS > 0 \text{ always}$$

Hence when two nonidentical cells are connected in series maximum power output $P_S < P_1 + P_2$. This is in agreement with the results presented in literature^{4,6,7}. Similarly, if P_S lies in any other segment of resultant V-I characteristics, it can be shown that always $P_1 + P_2 > P_S$ for nonidentical cells.

3.3.2 Shunt Connection

For the two nonidentical cells connected in shunt, the overall equivalent representation using the linearised equivalent circuit of individual cell (shown in Fig. 3.1) is given in Fig. 3.5. For $R_L = 0$, the current I is given by following relation.

$$I = I_{SC}''' = I_N' + I_N'' = I_{SC}' + I_{SC}'' .$$

Thus, the short circuit current of the combination is the sum of the short circuit currents of the individual cell.

To find the overall open circuit voltage, V_{OC}''' , the voltage source equivalent representation is used. The resultant circuit is shown in Fig. 3.6, where $V_N' = I_N' \cdot R_N'$ and $V_N'' = I_N'' \cdot R_N''$. It is obvious from the Fig. 3.6 that if $R_L = \infty$ (i.e. $I = 0$ and $V = V_{OC}'''$) and $V_N' = V_N''$, then $V_{OC}''' = V_{OC}' = V_{OC}''$ where

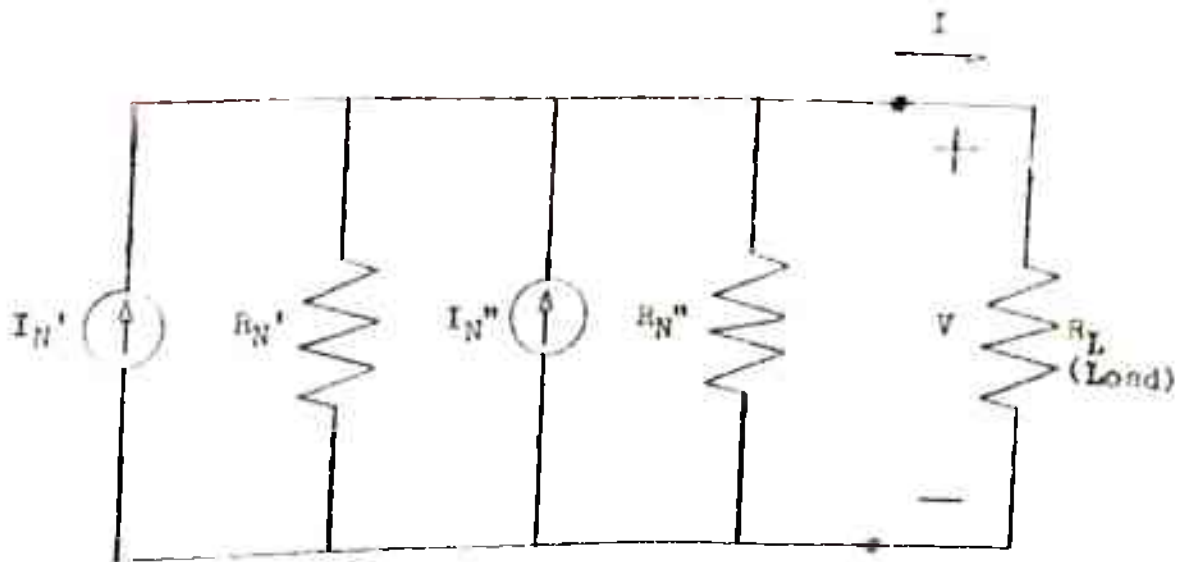


Fig. 3.5 Overall Equivalent Circuit of Cells Connected in Shunt

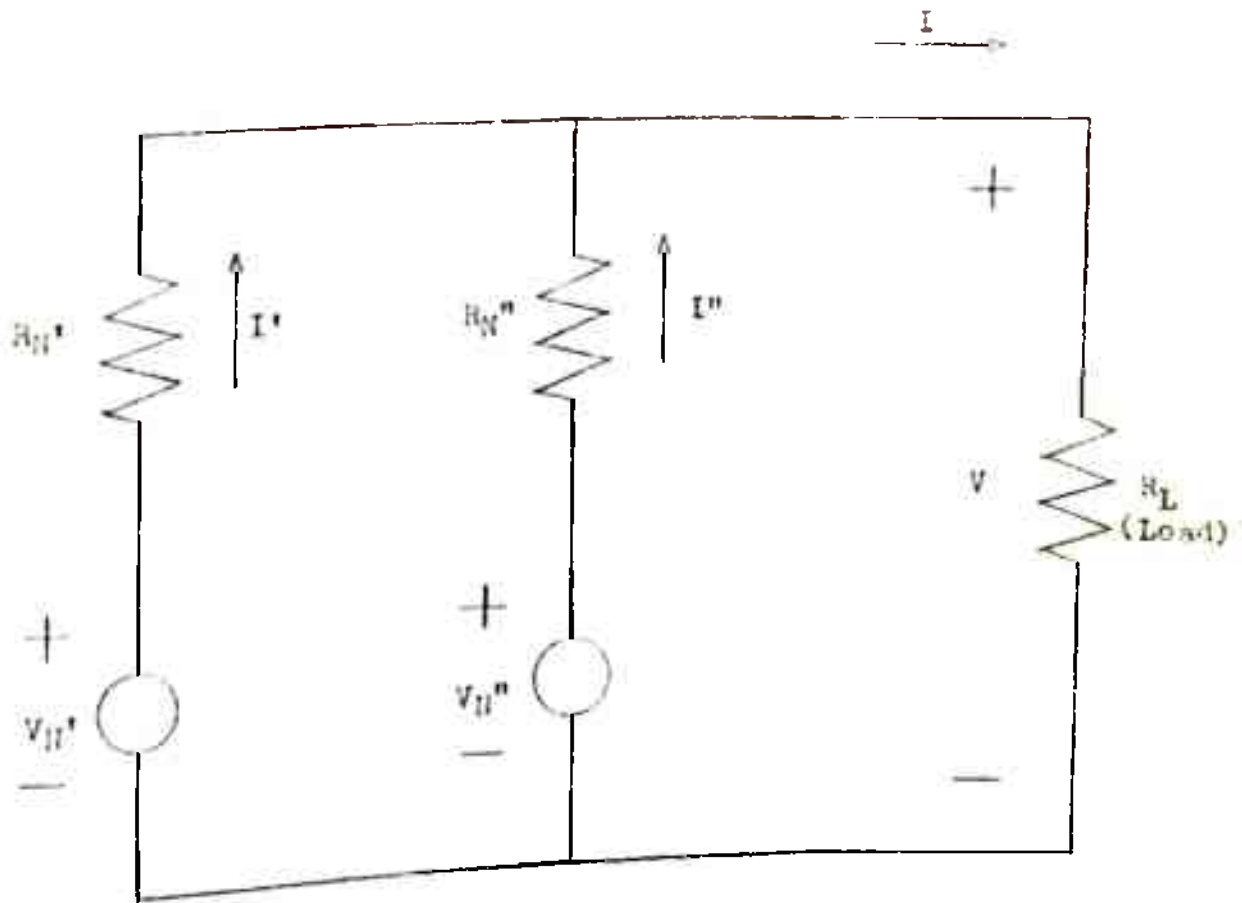


Fig. 3.6 Overall Voltage Source Equivalent Representation of Shunt Connection

$V_{OC}^{\prime} = V_N^{\prime}$ and $V_{OC}^{\prime\prime} = V_N^{\prime\prime}$. If $V_N^{\prime} \neq V_N^{\prime\prime}$, the current flows in the loop consisting of sources V_N^{\prime} and $V_N^{\prime\prime}$ and resistors R_N^{\prime} and $R_N^{\prime\prime}$.

Let $V_{OC}^{\prime} < V_{OC}^{\prime\prime}$. In this case, the loop current flows from $V_{OC}^{\prime\prime}$ through $R_N^{\prime\prime}$ and R_N^{\prime} to V_{OC}^{\prime} , i.e. $I^{\prime\prime}$ is positive and I^{\prime} is negative which results in

$$V_{OC}^{\prime\prime\prime} < V_{OC}^{\prime\prime}$$

$$\text{but } V_{OC}^{\prime\prime\prime} > V_{OC}^{\prime}$$

Similarly if $V_{OC}^{\prime} > V_{OC}^{\prime\prime}$, I^{\prime} is positive and $I^{\prime\prime}$ negative,

$$\text{and } V_{OC}^{\prime\prime\prime} > V_{OC}^{\prime\prime}$$

$$\text{but } V_{OC}^{\prime\prime\prime} < V_{OC}^{\prime}$$

This shows that even if no power is being drained from the combination, energy is being wasted internally. When $V_{OC}^{\prime} < V_{OC}^{\prime\prime}$, cell 1 becomes forward biased and when $V_{OC}^{\prime} > V_{OC}^{\prime\prime}$, cell 2 becomes forward biased.

To find resultant $V_{OC}^{\prime\prime\prime}$ when $V_{OC}^{\prime} \neq V_{OC}^{\prime\prime}$, the forward V-I characteristics of the cell with lower V_{OC} is required. The intersection of mirror image of the forward characteristics with the other cells characteristics give the resultant $V_{OC}^{\prime\prime\prime}$. Fig. 3.7 shows the piece-wise linear characteristics of

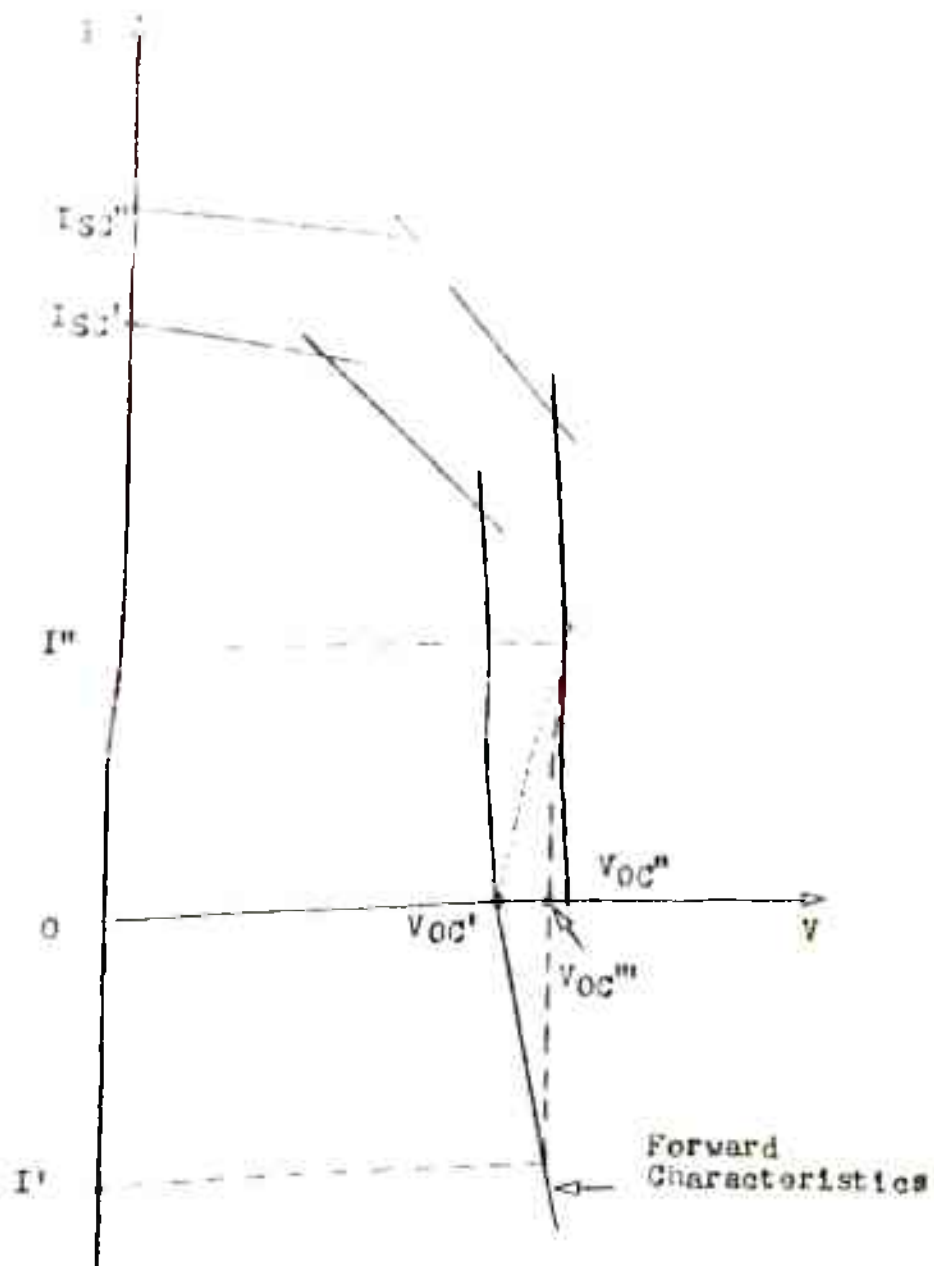


Fig. 3.7 Piece-wise Linear V-I Characteristics and Forward Characteristics of the Cells

two cells and the forward characteristics of a cell leading to the resultant V_{OC}''' . It can be noted that I' is negative. After getting overall open circuit voltage V_{OC}'' , R_L is decreased from ∞ . With decrease in R_L , V decreases. As V decreases, I'' becomes more positive and I' less negative. At one value of V , I' becomes zero. After this value of R_L only, both I' and I'' will be positive. For $V = 0$, $I_{SC}''' = I_{SC}' + I_{SC}''$. For $0 < V < V_{OC}'''$, the relation between V and I depends upon the slopes of the appropriate segments of the two cells. The procedure is further illustrated by an example.

Example

Let us consider two piece-wise linear characteristics of two nonidentical cells with the following identities.

$$V_{OC}' < V_{OC}'' \quad V_1' < V_1'' \quad V_2' < V_2'' \quad V_{OC}''' > V_1''$$

$$V_2'' > V_{OC}' \quad \text{and} \quad I_{SC}' < I_{SC}''$$

Fig. 3.8(a) gives the characteristics of the two cells and Fig. 3.8(b) gives the resultant characteristics of the shunt connection. Table 3.2 gives the equations governing segments I to VI. R_f is the forward resistance of cell 1 with lower V_{OC}' . At any point total current through the load is the sum of two currents i.e.

$$I = I_A + I_B$$

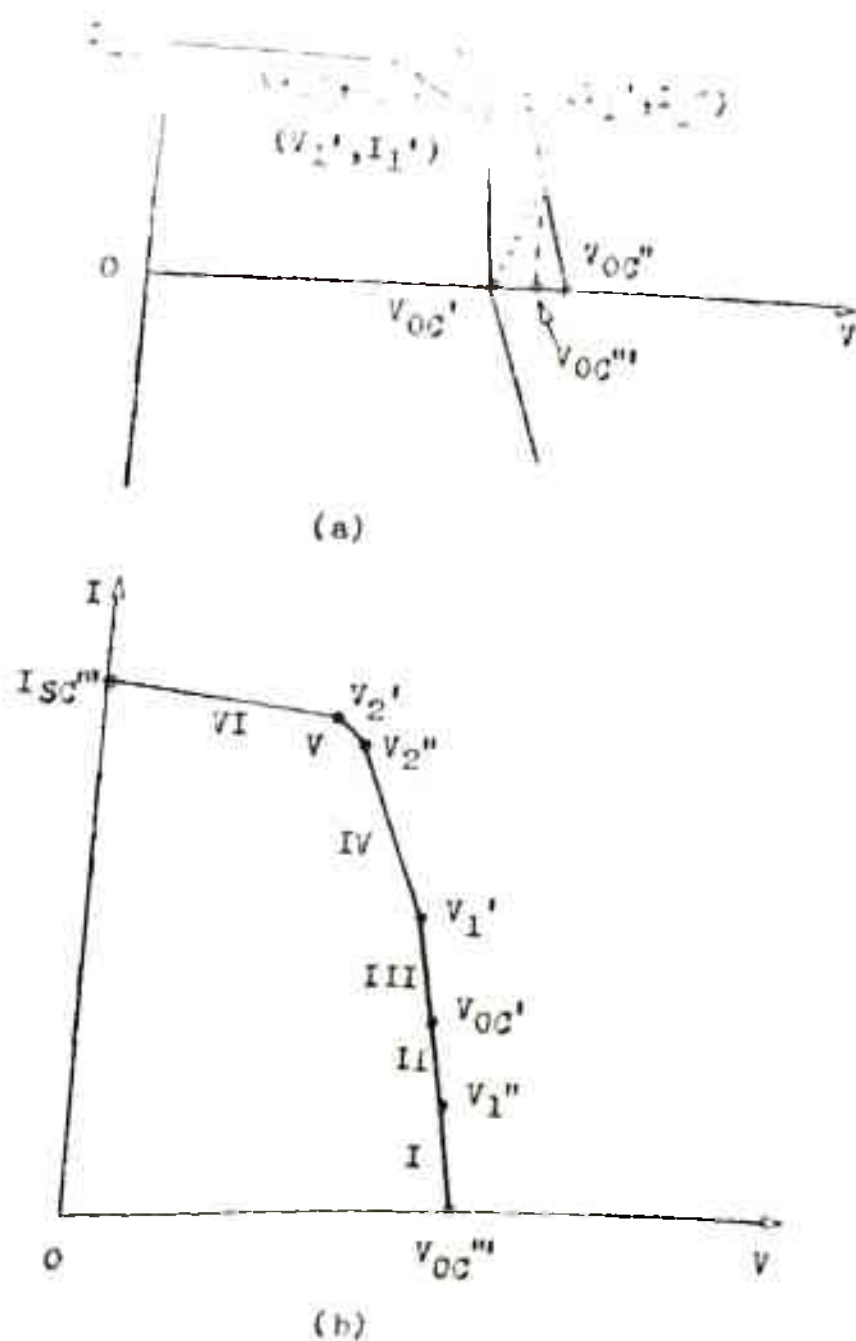


Fig. 3.8 (a) Piece-wise Linear Characteristics of the Individual Cells

(b) Resultant V - I Characteristics of the Shunt Connection

Table 3.2

Segment	Current contribution due to cell 1, I_A	Current contribution due to cell 2, I_B
I	$\frac{(V_{OC}' - V)}{R_f}$	$\frac{(V_{OC}'' - V)}{R_1''}$
II	$\frac{(V_{OC}' - V)}{R_f}$	$\frac{(V_{OC}'' + I_1'' R_2'' - V)}{(R_1'' + R_2'')}$
III	$\frac{(V_{OC}' - V)}{R_1'}$	$\frac{(V_{OC}'' + I_1'' R_2'' - V)}{(R_1'' + R_2'')}$
IV	$\frac{(V_{OC}' + I_1' R_2' - V)}{(R_1' + R_2')}$	$\frac{(V_{OC}'' + I_1'' R_2'' - V)}{(R_1'' + R_2'')}$
V	$\frac{(V_{OC}' + I_1' R_2' - V)}{(R_1' + R_2')}$	$\frac{(V_{OC}'' + I_1'' R_2'' + I_2'' R_3'' - V)}{(R_1'' + R_2'' + R_3'')}$
VI	$\frac{(V_{OC}' + I_1' R_2' + I_2' R_3' - V)}{(R_1' + R_2' + R_3')}$	$\frac{V_{OC}'' + I_1'' R_2'' + I_2'' R_3'' - V}{(R_1'' + R_2'' + R_3'')}$

Maximum Power Output

Let us assume that the maximum power output in the resultant V-I characteristics lies in segment IV (see Fig. 3.8(b)). This segment is governed by segment II of both the cells.

Using the same symbols as in series connection,

$$P_1 = \frac{V_I'^2}{4R_{II}'}$$

$$P_2 = \frac{V_{II}''^2}{4R_{II}''}$$

Max. power output (P_P) due to shunt or parallel connection,

$$P_P = \frac{1}{4} \left(\frac{V_I'}{R_{II}'} + \frac{V_{II}''}{R_{II}''} \right)^2 \cdot (R_{II}' \parallel R_{II}'')$$

Equating $P_1 + P_2$ with P_P we get

$$R_{II}' R_{II}'' (V_I' - V_{II}'')^2 = 0$$

Therefore for $P_1 + P_2 = P_P$, $V_I' = V_{II}''$. This condition is possible only in the case of identical cells.

In other situations, LHS is always greater than zero.

Hence $P_1 + P_2 > P_P$ for a shunt connection of nonidentical cells.

This is in agreement with the results presented by Luque A.^{4,6} Bhaduri A. et. al.⁹ on the other hand have shown that for a certain value of mismatch between two cells, P_P is more than $P_1 + P_2$. This ambiguity seems to be due to the assumptions made in their analysis. A detailed analysis using the diode equivalent

circuit of the solar cell is also presented in Appendix B and it is shown that P_S and P_P can never be greater than $P_1 + P_2$.

3.3.3 Experimental Study

Series Connection

The experimental V-I characteristics of two cells are measured by the method indicated in Ch. 2 (Fig. 2.2). The reverse characteristics of the cell with lower value of I_{SC} are measured by the experimental set up of Fig. 3.9. The V-I characteristics of series combination of the two cells are measured experimentally at same intensity and temperature.

Piece-wise linear characteristics are obtained for each cell and characterising parameters V_1 , I_1 , V_2 , I_2 , V_{OC} , I_{SC} , I_R (Reverse current), V_R (Reverse voltage) are evaluated. The computer program for determining the overall characteristics of the series combination of cells based on the procedure outlined in section 3.3.1 is developed and the resultant characteristics is obtained. Fig. 3.10(a) gives the reverse characteristics of large area cells. Fig. 3.10(b) and (c) give the V-I characteristics of individual cells and the overall V-I characteristics obtained both analytically and using the experimental data respectively.

Fig. 3.11 gives the above characteristics for a series combination of small area cells.

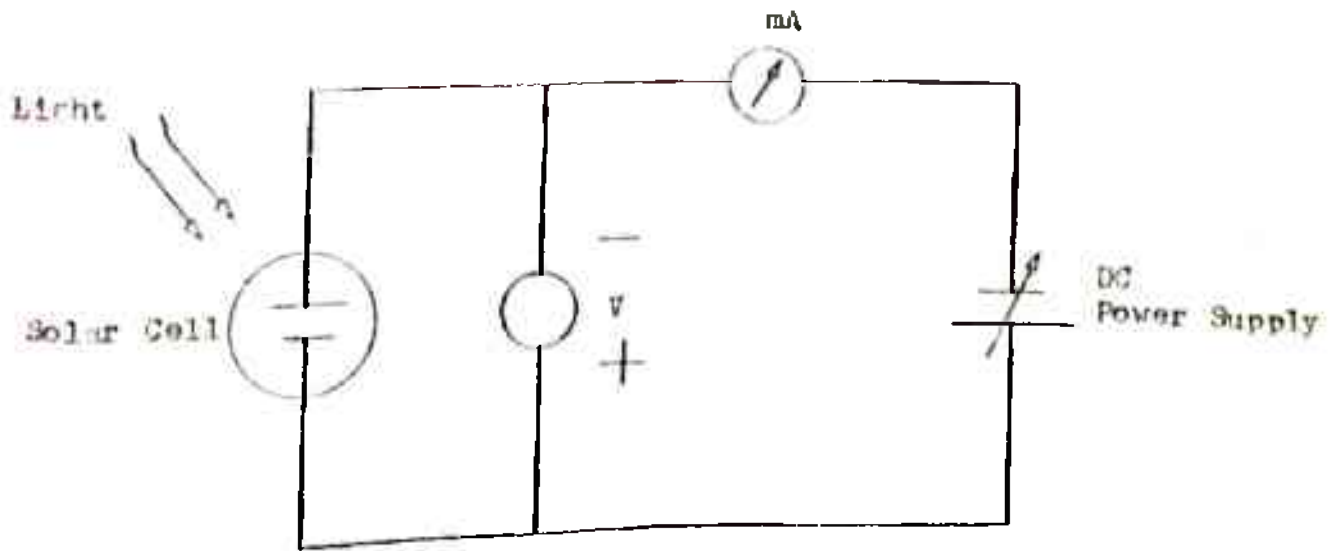


Fig. 3.9 Set up to find Reverse Characteristics of the Cell

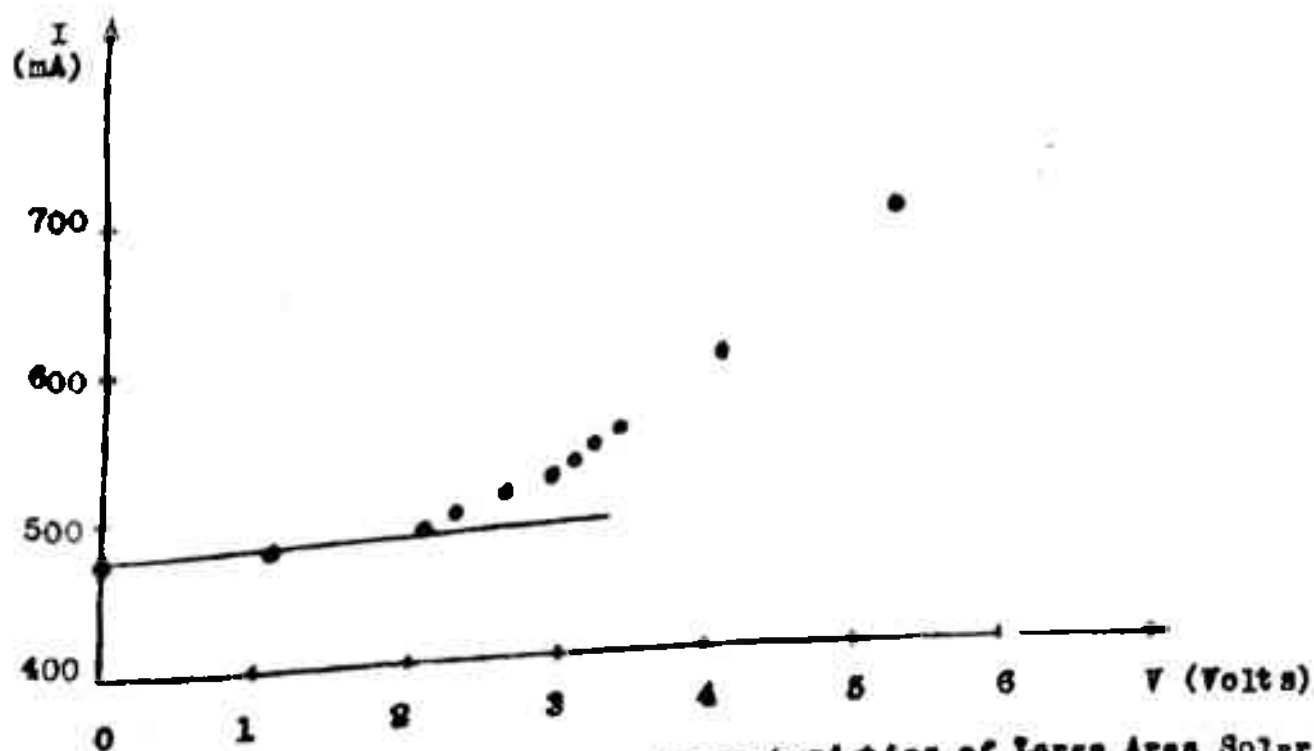


Fig. 3.10 (a) Reverse Characteristics of Large Area Solar Cell

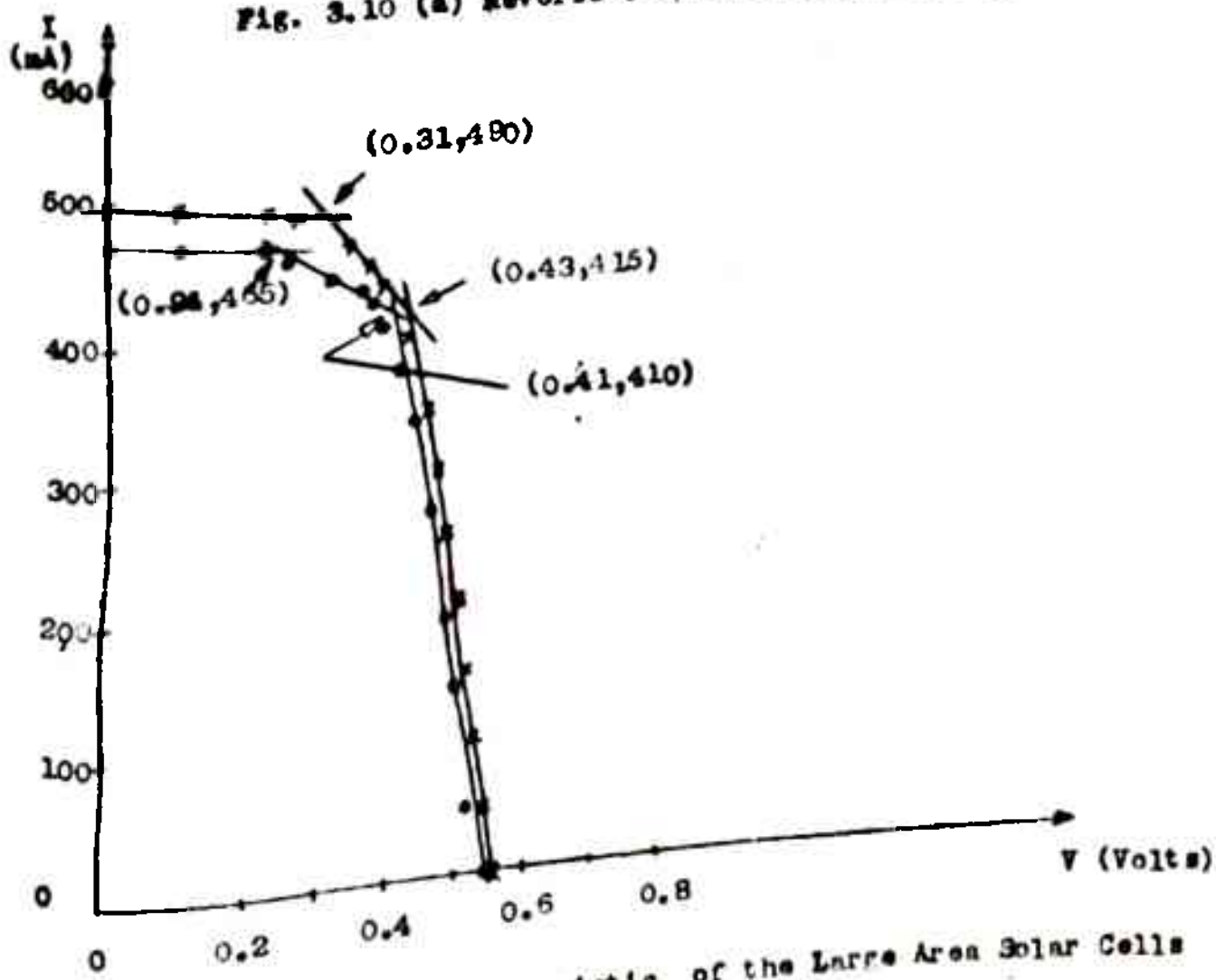


Fig. 3.10 (b) V-I Characteristic of the Large Area Solar Cells

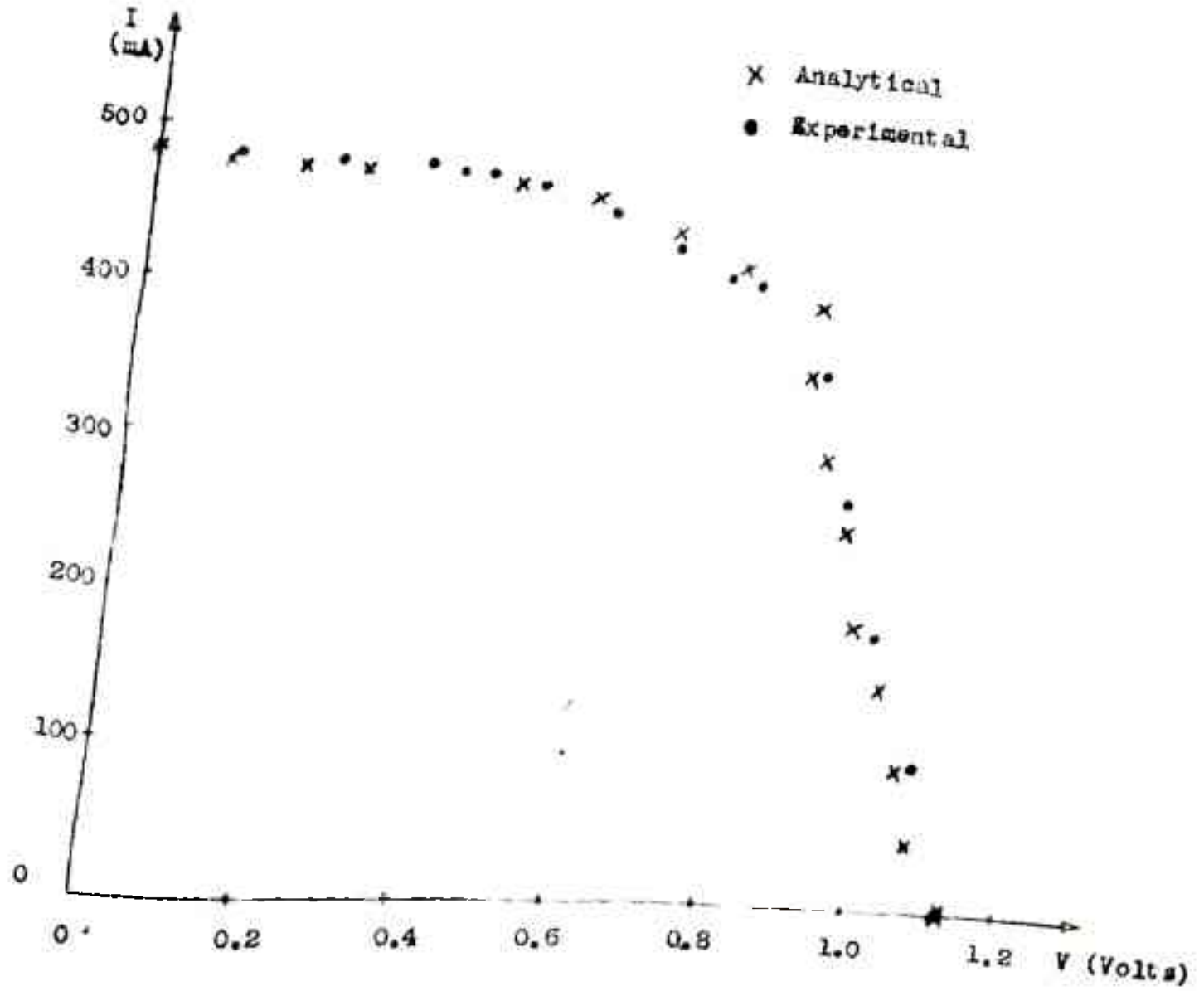


Fig. 3.10 (o) Overall V-I Characteristics of Series Connection of Large Area Cells

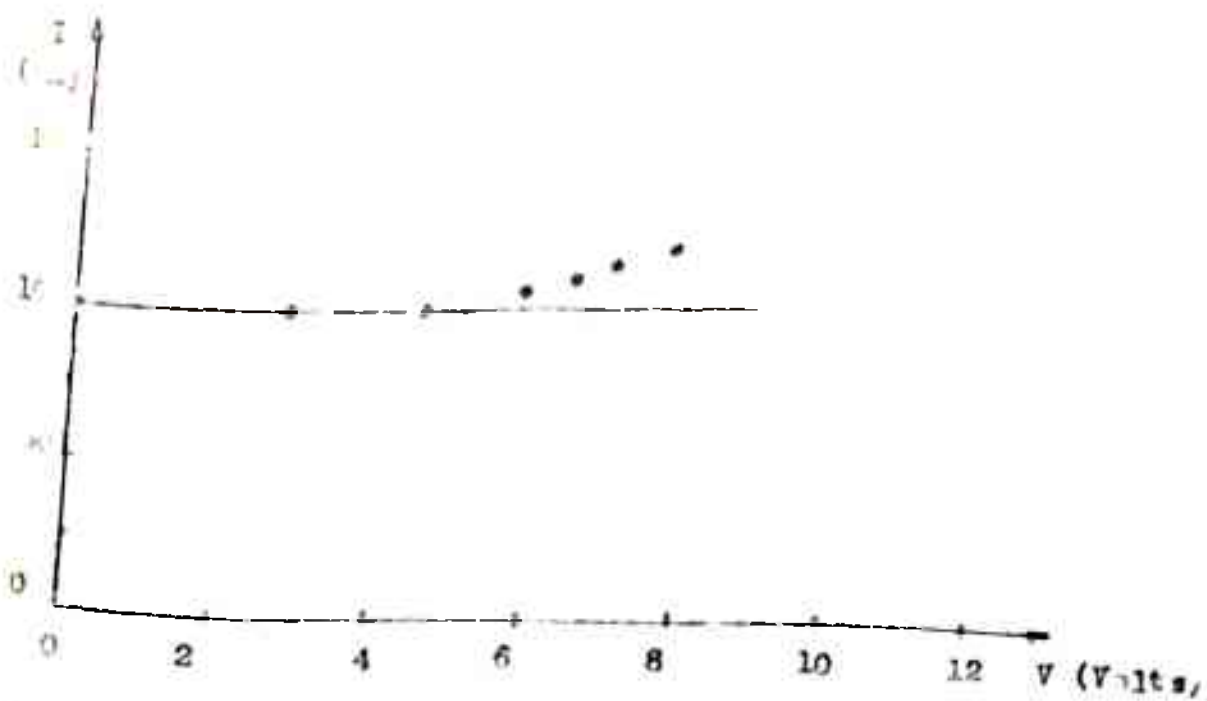


FIG. 3.11 (a) Reverse Characteristics of small Area Solar Cell

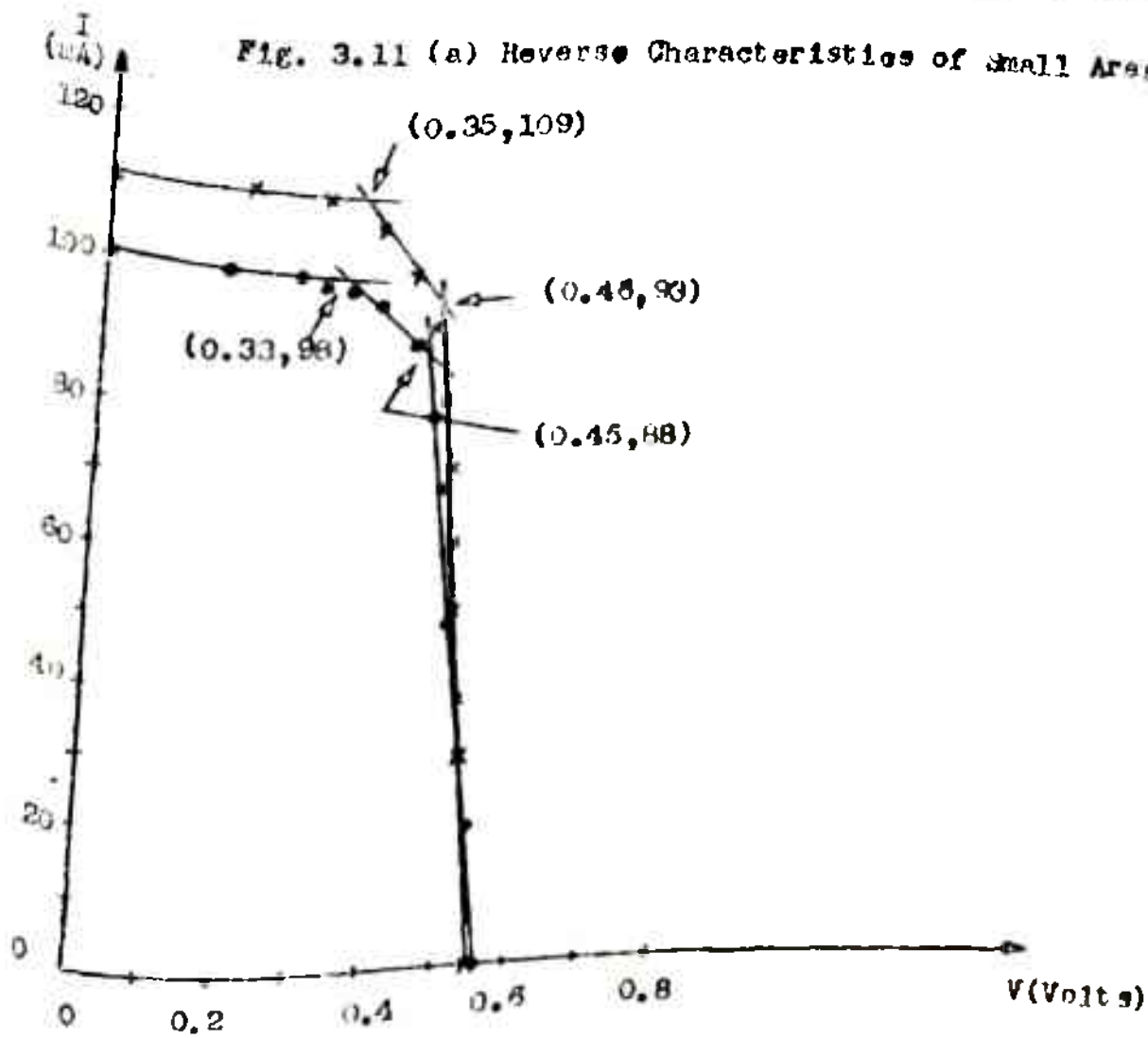


FIG. 3.11 (b) V-I Characteristic of Two Small Area Solar Cells

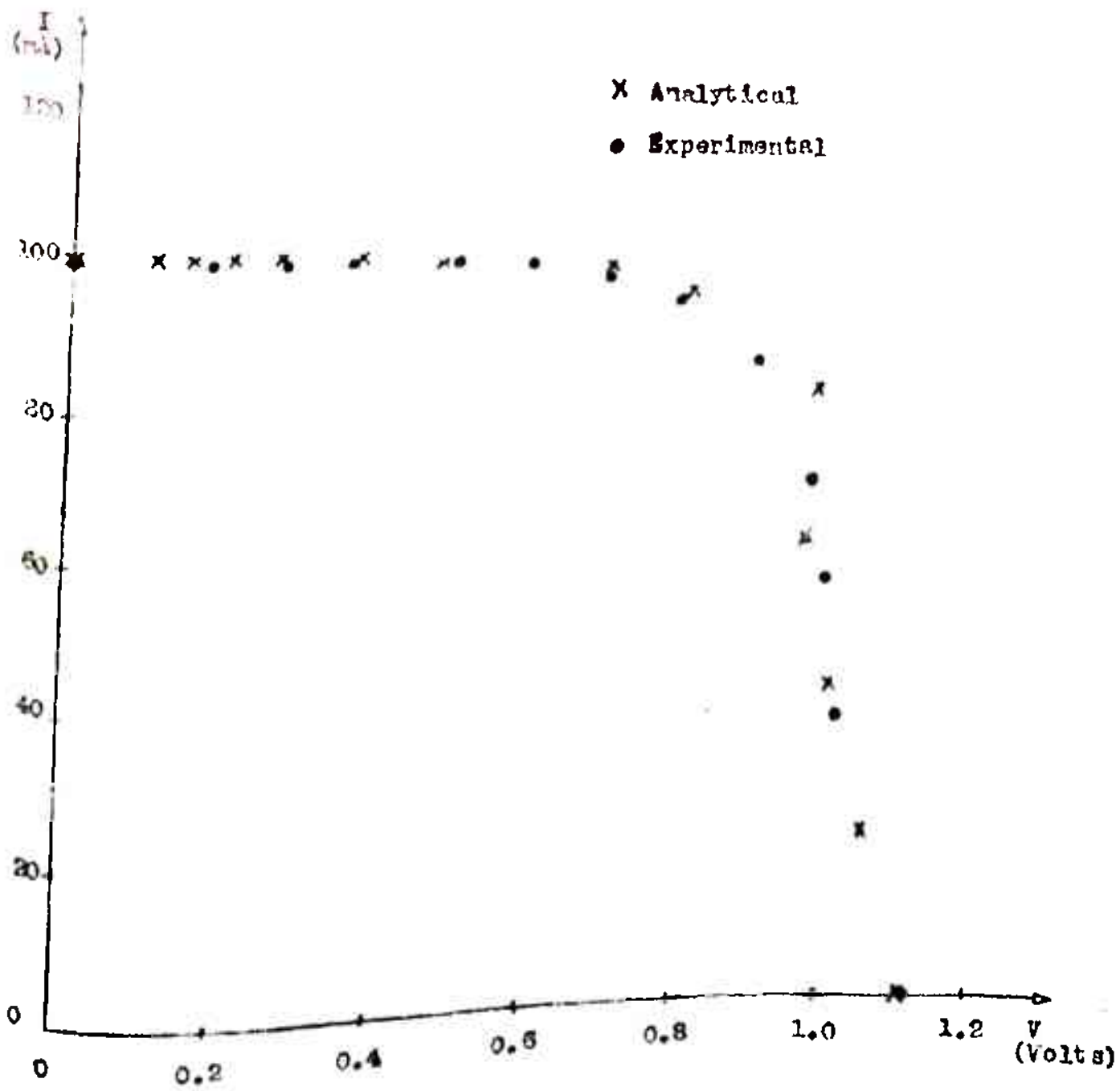


Fig. 3.11 (o) Overall V-I Characteristics of Series Connection of Small Area Cells

For the series combination employing both types of cells, the analytical and experimental overall V-I characteristics match very well. For the combination of large ^{and small} area cells, the maximum power output is given below and it is seen from the observations that P_S is always less than $P_1 + P_2$ as expected from the theory given in sec. 3.3.1.

Series combination of	P_1 (mW)	P_2 (mW)	$P_1 + P_2$ (mW)	P_S (mW)
Large area cells	168.1	178.45	346.55	332.22
Small area cells	39.6	42.78	82.38	81.36

Shunt Connection

In this case, the V-I characteristics of two cells measured using the set up given in Fig. 2.2 are used. The forward characteristics of the cells are obtained using the set-up of Fig. 3.12. The V-I characteristics of shunt connection of the two cells at same intensity and temperature are measured.

After obtaining the piece-wise linear characteristics of individual cell V-I characteristics, the characterising parameters $V_1, I_1, V_2, I_2, V_{OC}, I_{SC}, I_F$ (Forward current) and V_F (Forward voltage) are obtained and the resultant characteristics is derived using the computer program based on the procedure outlined in section 3.3.2.

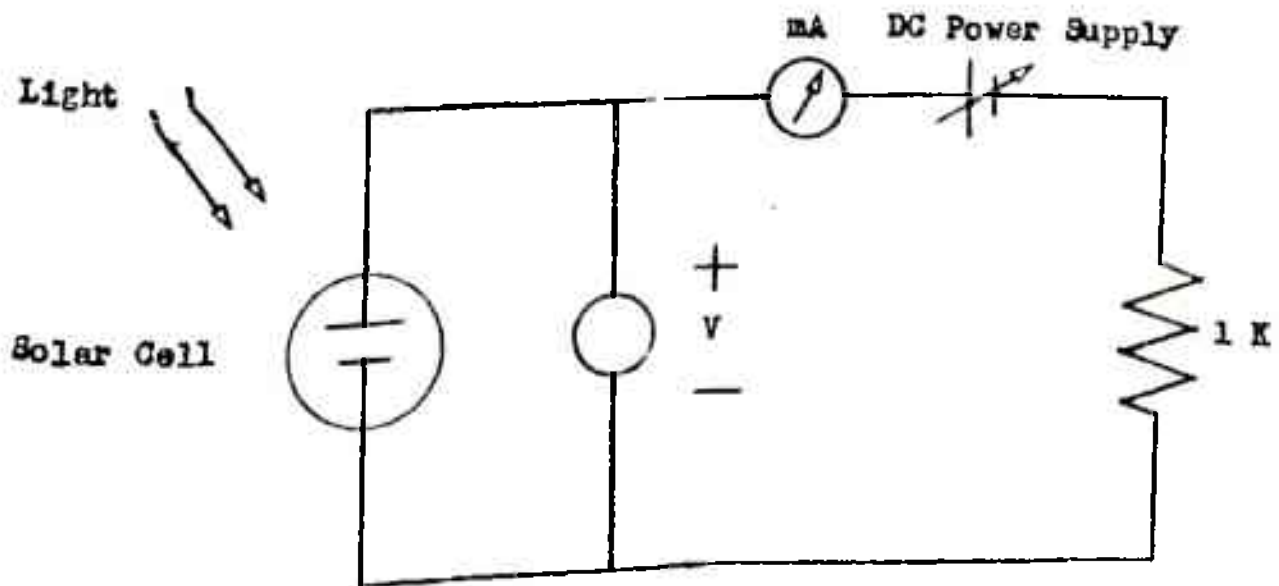


Fig. 3.12 ~~Set~~ up to find Forward Characteristics of the Cell

Figs. 3.13(a), (b) and (c) show the forward characteristics, individual cell V-I characteristics and overall analytical and experimental characteristics respectively for small area cells. The theoretical characteristics matches well with the experimental characteristics. Also the maximum power obtained, P_p for the combination which is equal to 52.24 mW is less than the sum of individual maximum power output which is 52.72 mW. This is in agreement with the discussions given in section 3.3.2.

3.4 Analysis of Solar Cell Array (SCA)

A solar cell array consists of a matrix of series and shunt connected individual solar cells. In the array the number of cells to be connected in series are decided on the basis of the voltage requirements and such series sub-arrays are connected in shunt to satisfy the overall current requirements or vice versa. It has been shown in the literature¹¹ that arrays with large number of series connected cells in comparison with the shunt connected cells have greater reliability.

In order to analytically determine the V-I characteristics of SCA, V-I characteristics of individual cells are experimentally measured. Measurement of the forward and reverse characteristics of each cell to form the array is also carried out.

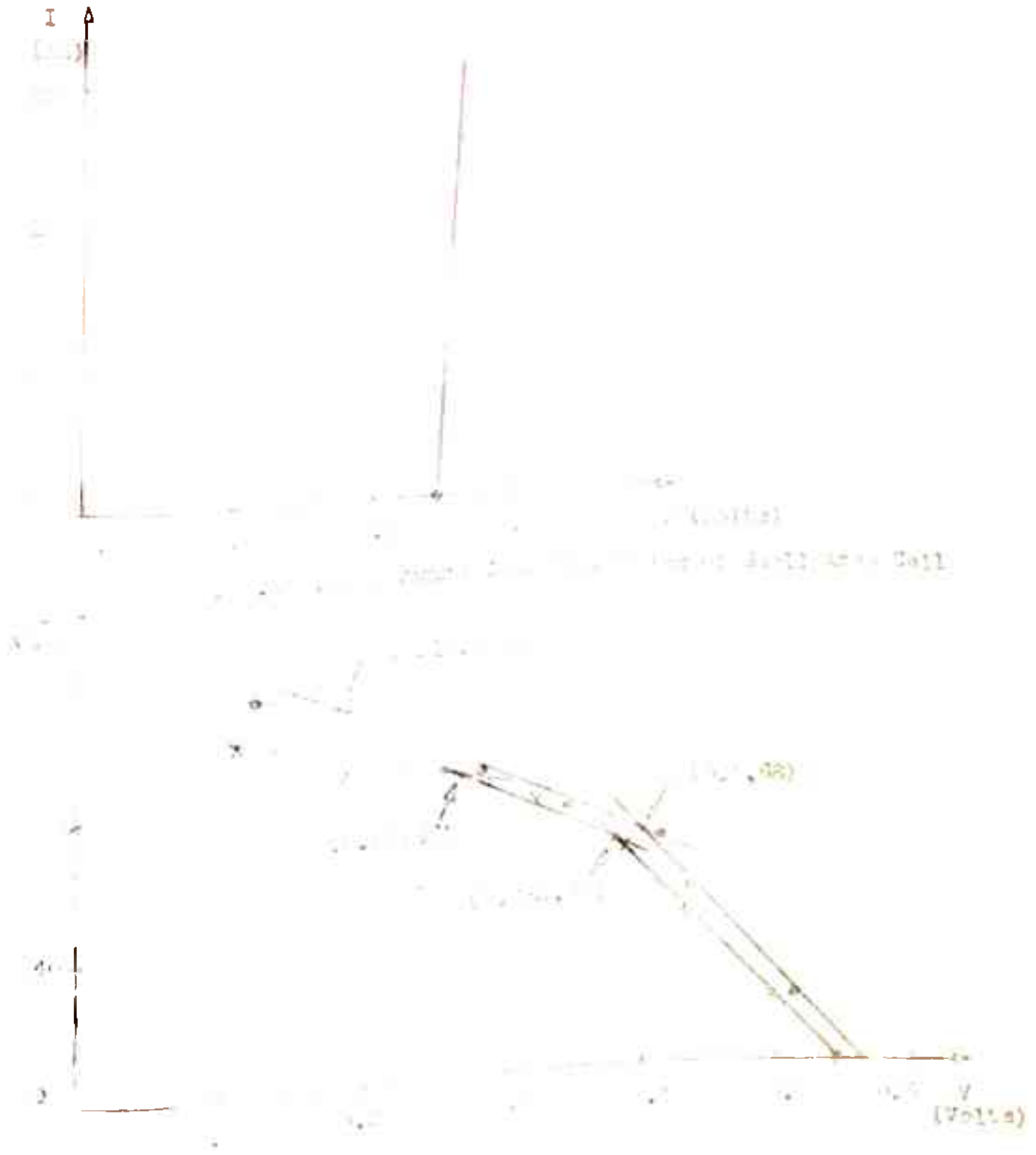


Fig. 5.1.1.1.1. $I-V$ Characteristics of Small Area Cells

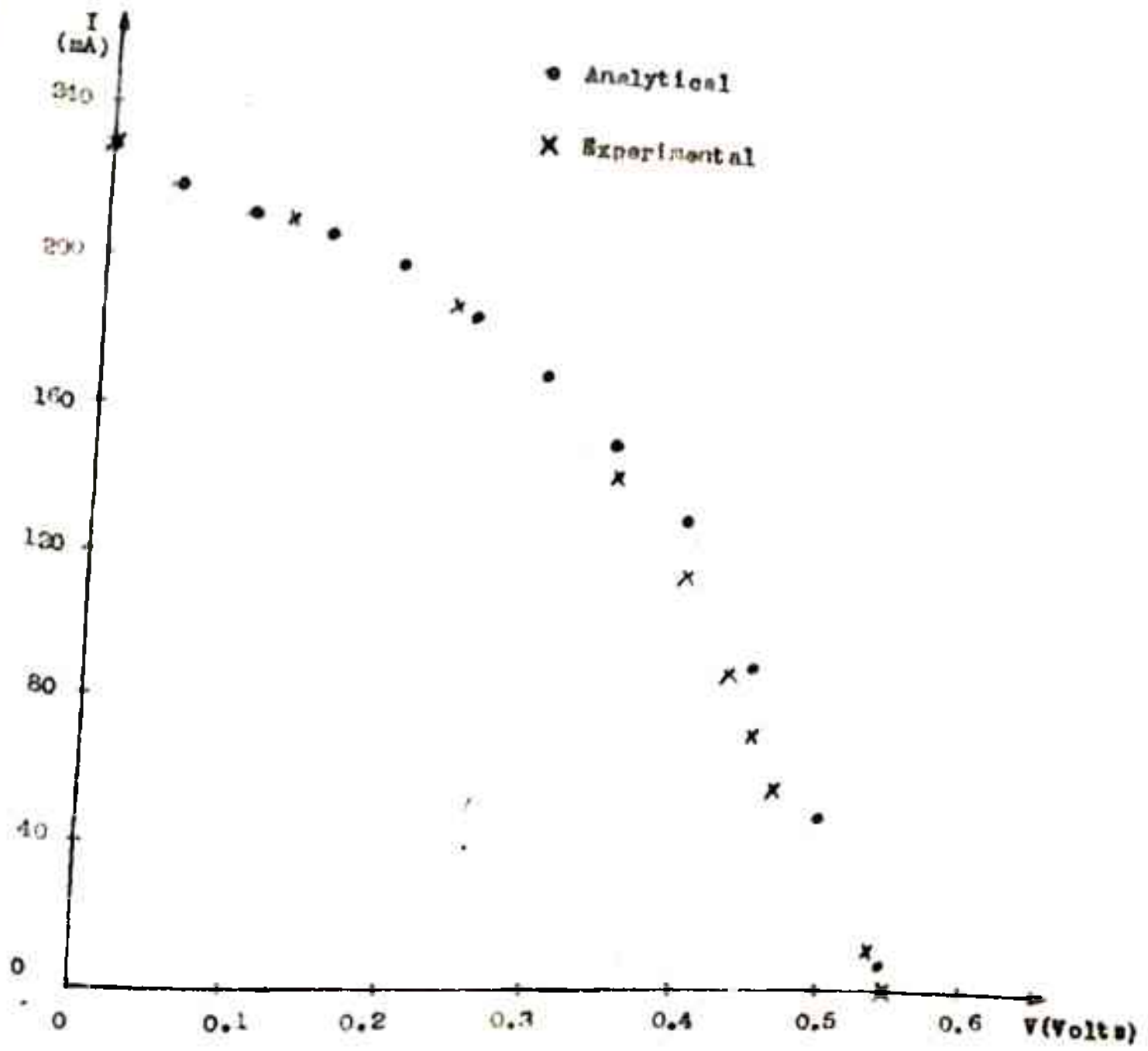


Fig. 3.13 (o) Overall V-I Characteristics of Shunt Connection of Small Area Cells

3.4.1 Sub-array with cells connected in series

The overall V-I characteristics of series connected sub-array is found taking two cells at a time using the procedure outlined in section 3.3.1. As can be seen from Fig. 3.4(b) that starting with three segment piece-wise linear characteristics of each cell, the resultant characteristics has six segments. The six segment characteristics is converted to three segment piece-wise linear characteristics. Using the above three segment V-I characteristics of the combination along with the piece-wise linear characteristics of the third cell, the overall characteristics of the three cell combination is determined and procedure is repeated for other cells in the series sub-array. The procedure for analysing the sub-array having large number of cells connected in series is summarised below.

Step 1: The three segment piece-wise linear V-I characteristics, reverse characteristics and forward characteristics of each cell are experimentally measured.

Step 2: Each cell characterising parameters V_1 , I_1 , V_2 , I_2 , V_{OC} , I_{SC} and R_r (Reverse Resistance) are arranged in the descending order of I_{SC} .

Step 3: Using first two cells data, the resultant characteristics of the series connection is obtained.

Step 4: Resultant characteristics of two cells is again converted to three segment piece-wise linear characteristics.

Step 5: The two cell resultant characteristics and next cell data are considered and the procedure is repeated.

The advantage of arranging cell data in descending order of I_{SC} is that the reverse characteristics of the series combination of the two cells is not required. I_{SC} of the resultant series combination is always greater than or at the most equal to the next cell I_{SC} . As explained in section 3.3.1, for finding the overall I_{SC} of the series connection, the reverse characteristics of the cell with lower value of I_{SC} is only required. This data is already available because to start with the reverse characteristics is to be measured for each cell.

The above illustrated procedure is extended to a sub-array consisting of any number of series connected cells. As the cells are nonidentical, the parameters $V_1, I_1, V_2, I_2, V_{OC}$ and I_{SC} of each cell are different. Different possibilities arise for the variations of two cell parameters, for which the resultant characteristics of the series connection are required. The illustrative example discussed for series connection of two cells in section 3.3.1 shows one possible combination. A computer program which takes care of all the possible combinations of the two cell parameters is developed. This program gives the resultant V-I characteristics of the sub-array formed by series combination of any number of cells. As per the procedure for getting the overall characteristics, there is a need to convert the resultant V-I characteristics of the series connection

obtained into three segments. The computer program also takes care of this step. For this purpose in the resultant V-I characteristics, the first intersection point from V_{OC} (e.g. I_1' of Fig. 3.4(b)) is taken as (V_1, I_1) and third intersection point starting from V_{OC} (e.g. I_2' of Fig. 3.4(b)) is taken as (V_2, I_2) . This results in a minimum error.

Experimental study

The experimental V-I characteristics of ten small area cells are obtained and the characterising parameters of each cell are determined. Table 3.3 gives the list of parameters of the ten cells. The parameter values are fed to the computer and the resultant characteristics is obtained by using the general procedure. The overall characteristics thus obtained is shown in Fig. 3.14 along with the experimentally measured characteristics of sub-array consisting of series combination of ten cells. From this figure it is obvious that both the analytical and experimental characteristics are very close to each other.

Table 3.3 also gives the maximum power output of each cell and also the total maximum power output due to these cells obtained by adding the maximum power output of individual cells. The maximum power output of the sub-array from the analysis is $P_S = 210.59 \text{ mW}$. Clearly P_S is less than the sum of individual maximum power output of each cell. This is in agreement with the discussions of section 3.3.1.

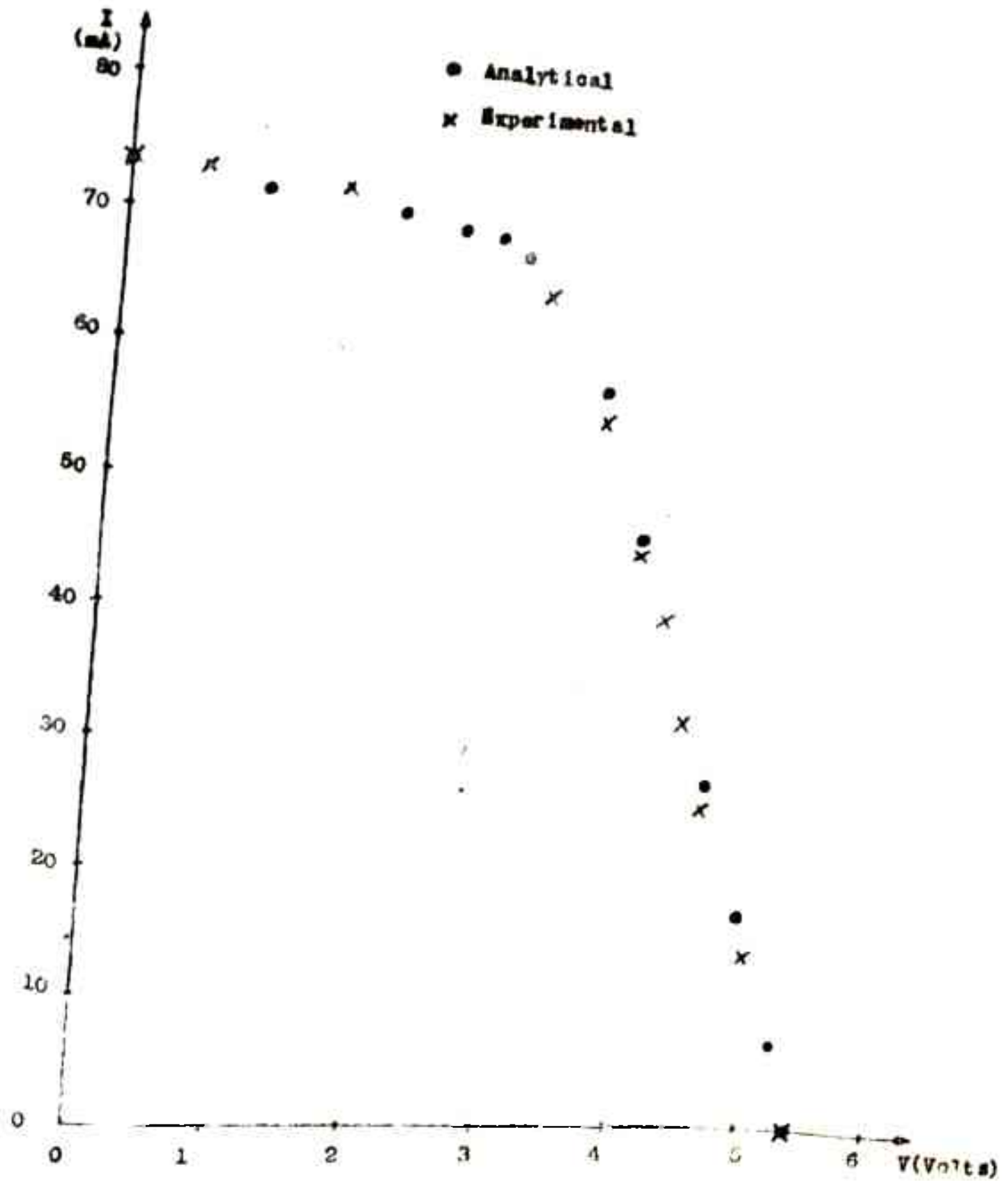


Fig. Overall V-I Characteristics of Series Connection of Ten Small Area Cells

Table 3.3

Parameter	Cell									
	1	2	3	4	5	6	7	8	9	10
V_1 (Volts)	0.28	0.41	0.29	0.375	0.385	0.42	0.40	0.255	0.36	0.28
V_2 (Volts)	0.195	0.295	0.145	0.20	0.37	0.29	0.25	0.19	0.21	0.15
I_{SC} (mA)	85	83	81	77	77	77	77	76	75	69
V_{OC} (Volts)	0.545	0.545	0.55	0.55	0.55	0.54	0.54	0.545	0.525	0.54
I_1 (mA)	72	68	68	69	74	62	61	70	62	54
I_2 (mA)	83	81	80	76	75	73	75	75	74	67
I_P (mA)	90	88	86	82	82	82	82	81	80	74
V_P (Volts)	2.64	2.64	2.64	2.64	2.64	2.64	2.64	2.64	2.64	2.64
P_M (mW)	20.16	27.88	19.72	28.50	28.49	26.04	24.40	17.85	22.32	15.12

Maximum power output of sub-array of ten series connected cells = 230.48 mW.

3.4.2 Determination of Solar Cell Array (SCA) V-I Characteristics

After determining the characteristic of all series sub-arrays, the composite V-I characteristics of the SCA consisting of shunt connection of such sub-arrays is obtained. The procedure for obtaining the resultant characteristics of sub-arrays connected in shunt is identical to that of the sub-array having cells in series, as already explained. However, as the resultant V_{OC} is to be obtained first, the forward characteristics of each sub-array is also required. To start with, the forward resistance of each cell to be used in the array is measured. The forward resistance of each sub-array with cells in series is the sum of forward resistances of individual cells. Therefore, the sub-arrays parameters are arranged in descending order of V_{OC} rather than of I_{SC} . The overall forward resistance of each sub-array is obtained and the procedure given in section 3.4.1 is followed. The computer program in this case also takes care of all possible combinations of each sub-array parameters and it also includes the procedure for the conversion of each resultant V-I characteristics into three segment characteristics.

The procedure to determine the composite characteristics of an $n \times m$ SCA consisting of a series sub-array of n number of cells in series and m such sub-arrays connected in shunt, is summarised below.

Step 1: Three segment piece-wise linear characteristics for each cell are obtained and the characterising parameters of each cell V_1 , I_1 , V_2 , I_2 , I_{SC} and V_{OC} are recorded.

Step 2: Reverse and forward characteristics of each cell are obtained.

Step 3: The resultant characteristics of each series sub-array is determined.

Step 4: Forward resistance of each series sub-array is calculated.

Step 5: Characteristics of each series sub-array is approximated to the three segment piece-wise linear characteristics and the characterising parameters are noted.

Step 6: The resultant characteristics of the parallel connection of m series sub-arrays is determined to yield the composite characteristics of the SCA.

Experimental Study

The experimental study on a 5×2 solar cell array is carried out. The V-I characteristics of each cell forming the series sub-array of five cells are measured experimentally and therefrom three segment piece-wise linear characteristics for each cell are derived. The reverse and forward characteristics of each cell are also measured. Table 3.4 gives the characterising parameters of individual cells of each sub-array.

Table 3.4

Parameter	Sub-array I					Sub-array II				
	Cell					Cell				
	1	2	3	4	5	1	2	3	4	5
V_1 (Volts)	0.300	0.295	0.375	0.375	0.47	0.380	0.420	0.440	0.465	0.385
V_2 (Volts)	0.115	0.200	0.240	0.240	0.35	0.370	0.270	0.250	0.315	0.270
I_{SC} (mA)	79	78	68	67	60	65	60	46	43	43
V_{OC} (Volts)	0.539	0.526	0.534	0.518	0.529	0.510	0.527	0.510	0.526	0.507
I_1 (mA)	56	66	46	52	40	50	36	30	32	35
I_2 (mA)	73	76	64	64	58	62	57	44	42.5	42
I_R (mA)	81	80	70	69	62	67	62	48	45	45
V_R (Volts)	2.030	1.740	2.130	1.340	2.100	1.000	1.030	2.240	3.840	1.090
I_F (mA)	20	20	20	20	20	20	20	20	20	20
V_F (Volts)	0.579	0.556	0.562	0.553	0.559	0.552	0.561	0.547	0.560	0.540

For each series sub-array, the resultant V-I characteristics are obtained first, using the general procedure discussed in section 3.4.1. The analytical and experimental values of V_{OC} and I_{SC} for the series sub-array I and II are given in Table 3.5.

Table 3.5

Sub-array	V_{OC} (Volts)		I_{SC} (mA)	
	Analytical	Experimental	Analytical	Experimental
I	2.646	2.62	61.02	61.00
II	2.58	2.58	43.32	44.00

These parameters of the sub-array I and II thus obtained are used in the computer program based on the general procedure for the evaluation of characteristics of the shunt connection of the series sub-arrays. The composite characteristics of the 5×2 array is determined and is given in Fig. 3.15 along with the experimental measured V-I characteristics.

Table 3.6 lists the maximum power output of individual cell, sub-array I and sub-array II. The maximum power output of the 5×2 SCA analytically obtained is 156.65 mW whereas the maximum power output obtained from the results of the individual sub-arrays i.e. $P_{SI} + P_{SII}$ equals 164.94 mW verifying the earlier conclusions.

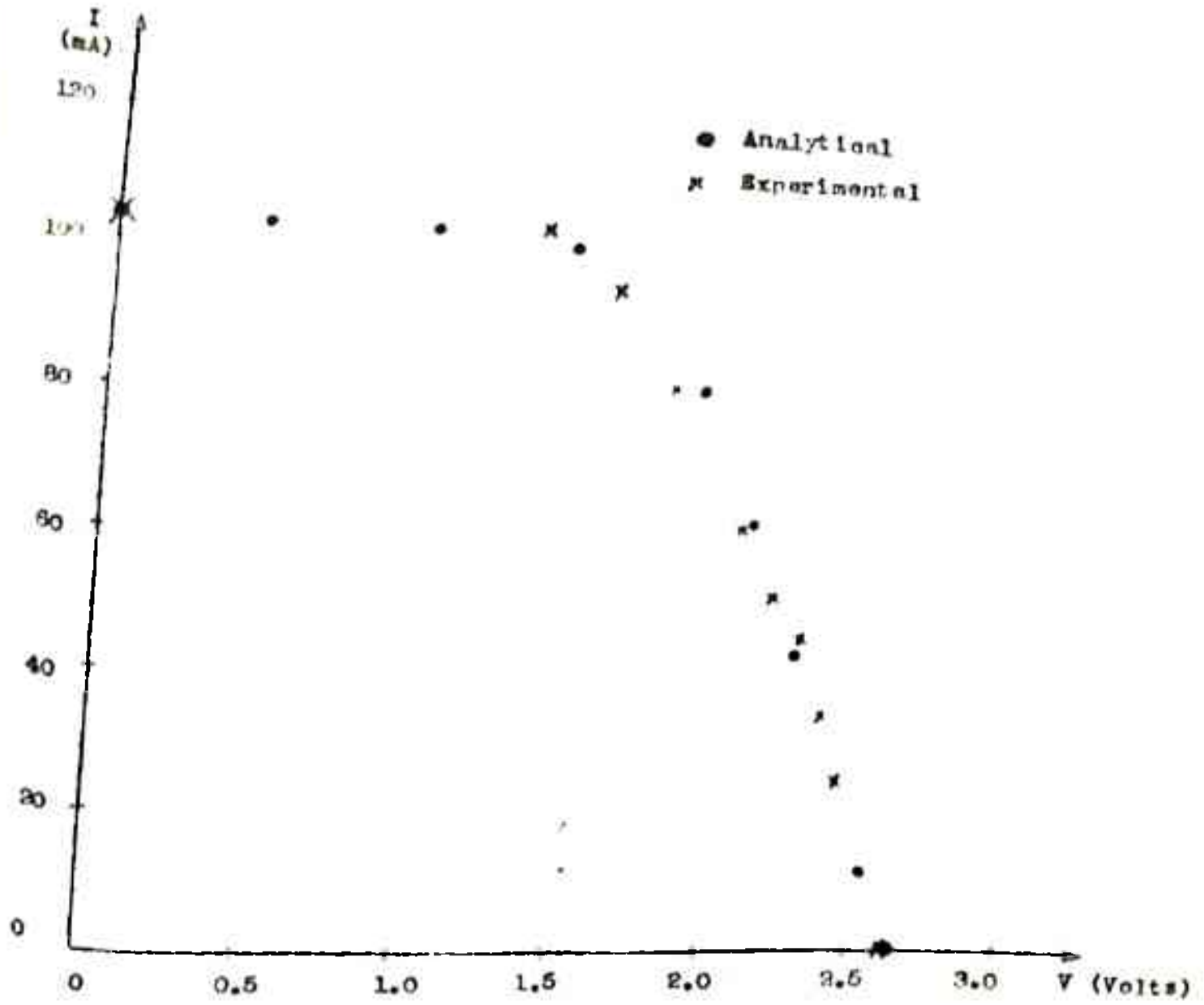


Fig. 3.15 Composite V-I Characteristics of a 5 x 2 Array

Table 3.6

Sub-array	Maximum power output in mW						
	P_1	P_2	P_3	P_4	P_5	$\sum_{i=1}^5 P_i$ (Experimental)	P_S (Analytical)
I	16.80	19.47	18.00	19.50	20.35	94.12	89.93
II	19.10	15.39	13.22	14.88	13.48	76.07	75.01

3.5 Variation of Array Parameters with Intensity and Temperature

The variation of the resistances offered by each linear segment corresponding to the V-I characteristics of a cell has been presented in Chapter 2. In this section, the variation of these resistances of a series sub-array with intensity and temperature is presented and therefrom the behaviour of the SCA with intensity and temperature is established.

3.5.1 Variation of R_I , R_{II} and R_{III} with Intensity Keeping Temperature Constant

Ten small area solar cells are mounted on a hollow rectangular aluminium pipe made of 1 mm thick sheet. (Dimensions $610 \times 25 \times 12 \text{ mm}^3$) as shown in Fig. 3.16 with proper electrical insulation between the cells.

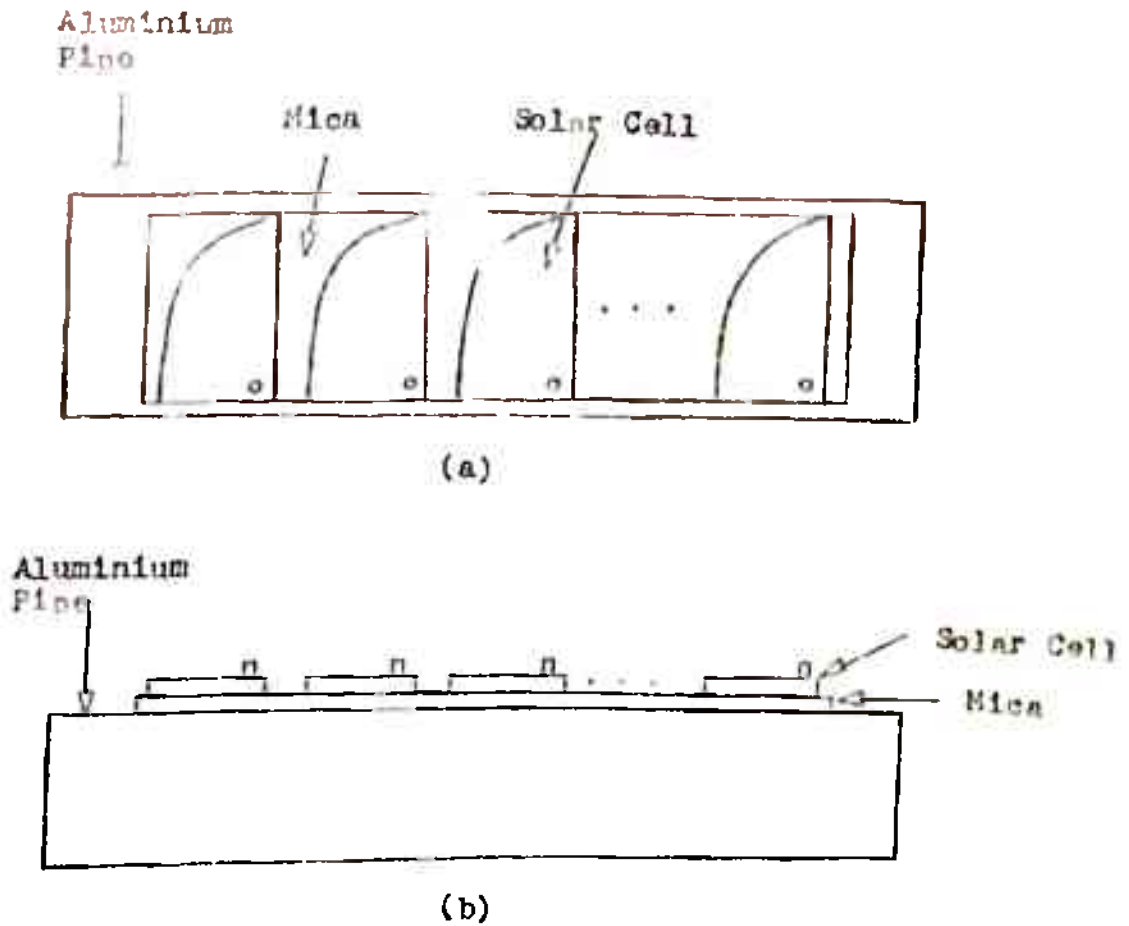


Fig. 3.16 Mounting of Solar Cells on Aluminium Pipe
 (a) Top View (b) Cross-sectional View

An uniformly illuminated cylindrical nontracking concentrator model no. U3 developed at BTS¹² and shown in Fig. 3.17 is used for getting the concentrated sunlight. The material used in the concentrator is plain anodised aluminium sheet.

The maximum concentration specified is 7.6 but due to reflection losses etc., the concentration of the order of 2.7 is obtained in the experiment.

To maintain constant temperature, water cooling is used. The temperature is monitored by using copper constantan thermocouple and is measured by Honeywell's potentiometer.

Fig. 3.18 shows the measured V-I characteristics of the array without concentrator (Curve A) and with concentrator (Curve B). Table 3.7 lists the intersection points, R_I , R_{II} , R_{III} , P_M and I_M for each curve.

In Chapter 2, it has been shown that R_I , R_{II} and R_{III} decrease with intensity nonlinearly. The same trend is also expected for the array because the array behaviour is decided by each single cell characteristics. The resistances R_I and R_{III} of the array are directly related with the single cell R_I and R_{III} . Therefore as R_I and R_{III} for single cell decrease with intensity, the array R_I and R_{III} should also decrease with intensity. This is verified from the experimental results given in Table 3.7. R_{II} of the overall array characteristics is given

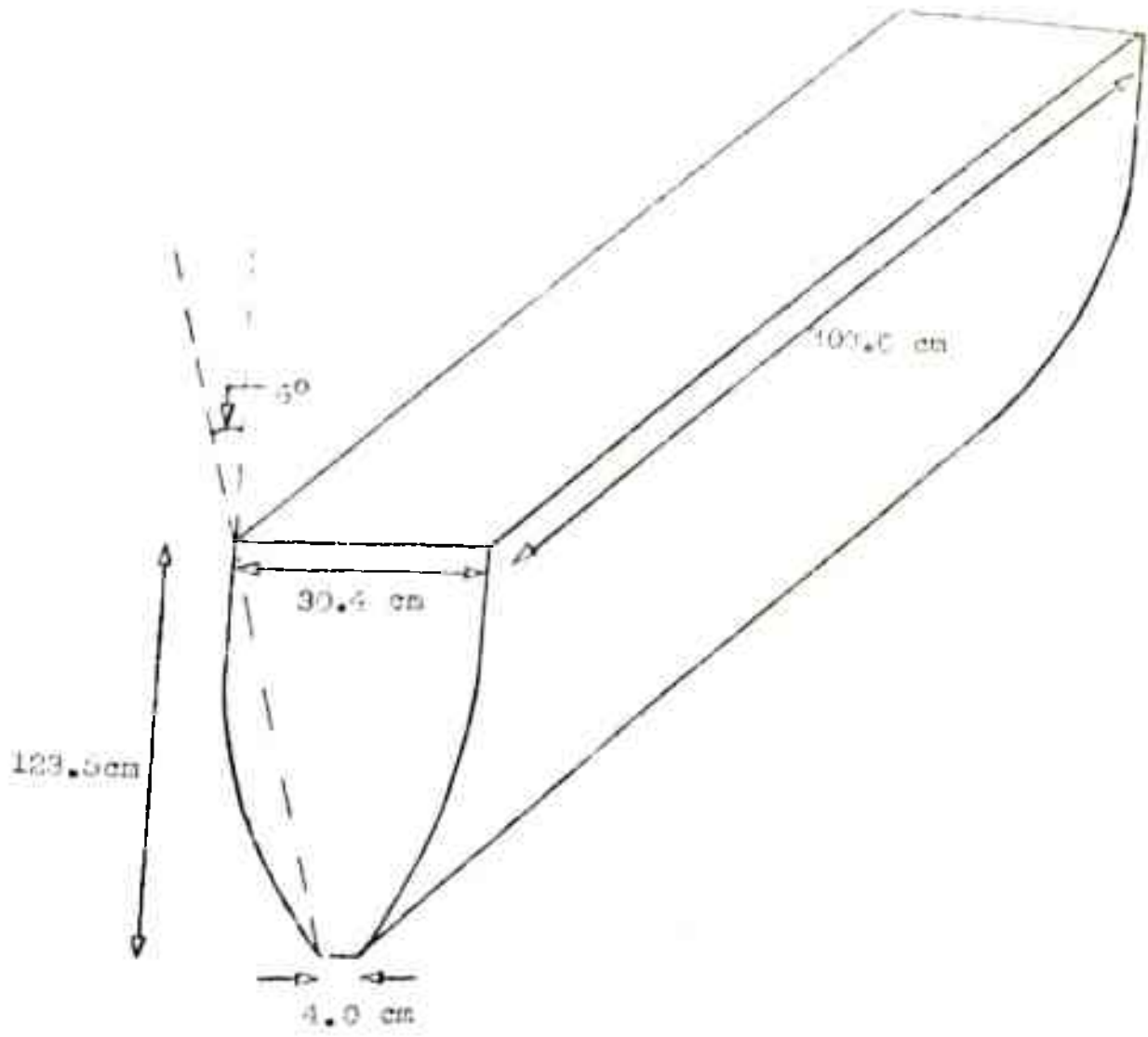


Fig. 3.17 Uniformly Illuminated Cylindrical Nontracking Concentrator

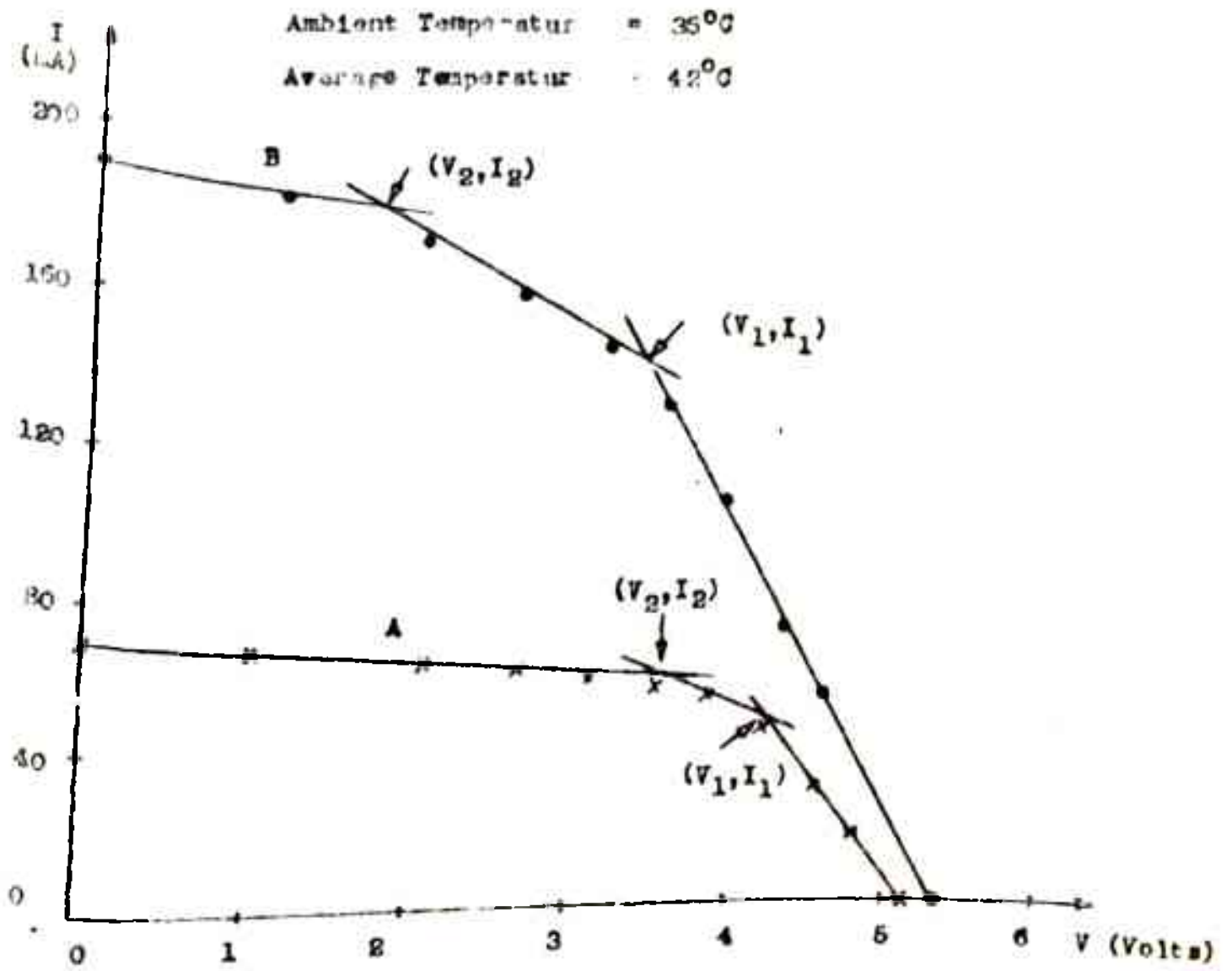


Fig. 3.18 Measured V-I Characteristic of the Array

Table 3.7

Curve	V_{OC} (Volt)	I_{SC} (Amp)	(V_1, I_1) (Volt, Amp)	(V_2, I_2) (Volt, Amp)	R_I (Ohms)	R_{II} (Ohms)	R_{III} (Ohms)	P_{II} (Watt)	I_M (Amp)
A	5.14	0.07	(4.2, 0.048)	(3.6, 0.06)	19.5833	50.0000	360.0000	0.216	0.06
B	5.32	0.19	(3.4, 0.14)	(1.7, 0.18)	13.7143	42.5000	173.0000	0.476	0.14

by the ratio of P_M and I_M^2 . As P_M and I_M for each cell increase with intensity and since denominator is I_M^2 , R_{II} of each cell decreases with intensity. The variation of R_{II} of the array with intensity should also follow the same trend. This is exactly shown in Table 3.7.

The above discussion holds true only if the illumination is uniform. Infact, in the present experiment, as the dimensions of the concentrator used are much large as compared to the dimensions of the array, the assumption of uniform illumination perfectly holds.

3.5.2 Variation of R_I , R_{II} and R_{III} with Temperature Keeping Intensity Constant.

The performance of a series sub-array consisting of six small area cells with temperature keeping the intensity constant is experimentally studied.

Fig. 3.19 shows the V-I characteristics at three temperatures 25°C , 49°C and 77°C and Table 3.8 gives the measured values of V_{OC} , I_{SC} and calculated values of R_I , R_{II} , R_{III} , P_M , V_M and I_M . As temperature increases, R_I of the sub-array increases whereas R_{II} and R_{III} of the sub-array decrease. The variation of R_I , R_{II} and R_{III} with temperature is explained on the basis of the known variation of these parameters for a single cell.

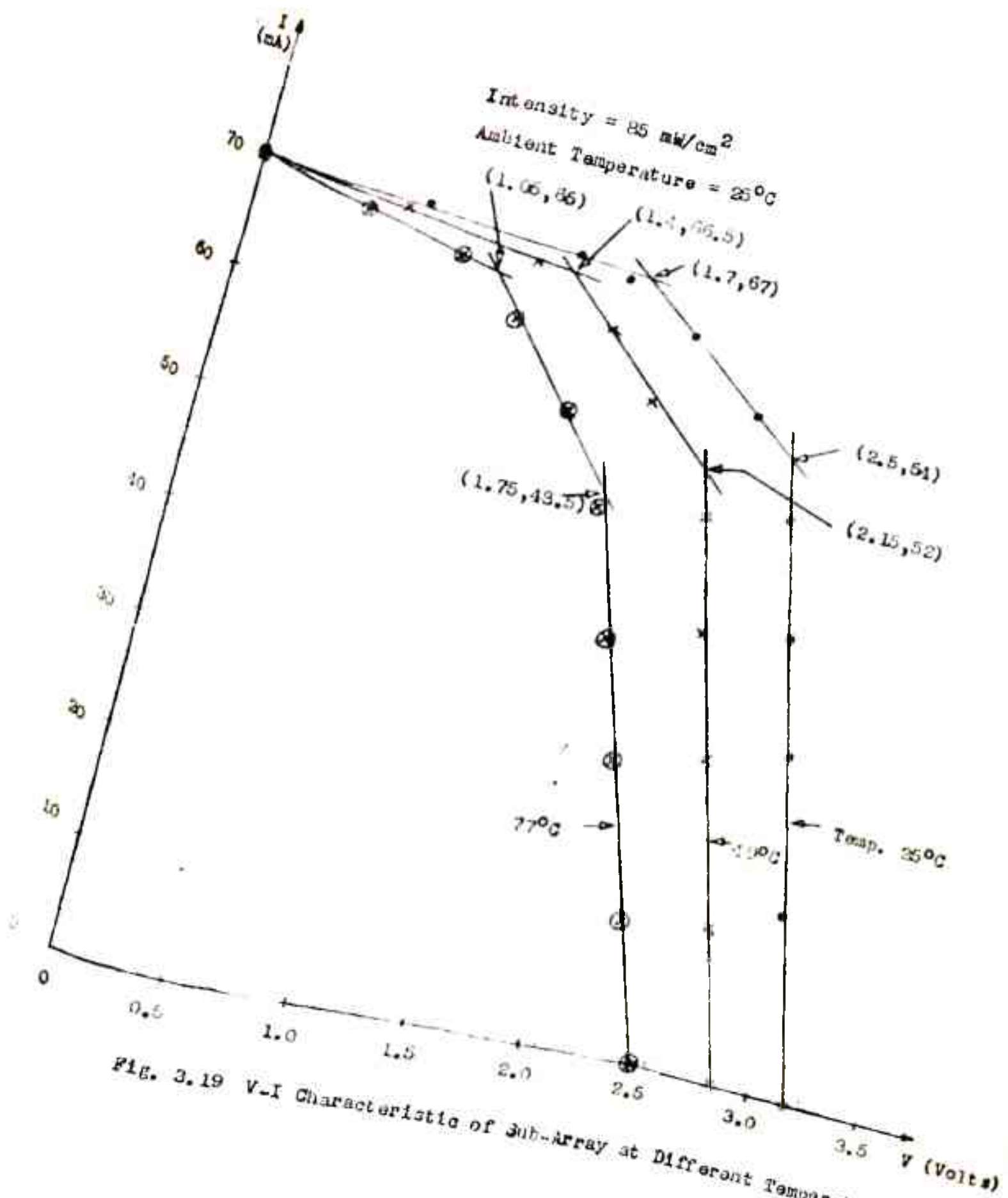


Fig. 3.19 V-I Characteristic of Sub-Array at Different Temperatures

Table 3.8

Temperature	V_{OC} (Volts)	I_{SC} (Amp.)	R_I (Ohms)	R_{II} (Ohms)	R_{III} (Ohms)	P_M (Watts)	V_M (Volts)	I_M (Amp.)
25°C	3.1700	0.0700	12.4074	61.5385	566.6667	0.1350	2.5700	0.0540
49°C	2.8400	0.0700	13.2692	51.7241	400.000	0.1118	2.1500	0.0520
77°C	2.4900	0.0700	15.2577	42.4242	210.0000	0.0849	1.750	0.0485

It is shown in Chapter 2 that R_I increases and R_{II} and R_{III} decrease with increase in temperature. Since the sub-array employs cells in series, these parameters of the array are also expected to vary with temperature in a similar manner. Thus R_I should increase, R_{II} and R_{III} should decrease with temperature. This is duly verified from Table 3.8.

3.6 Conclusions

In this Chapter, V-I characteristics of a solar cell array has been determined analytically using piece-wise linear approximation of V-I characteristics of individual solar cells in the array. The procedure for the determination of V-I characteristics of an array has been first illustrated using a combination of only two solar cells. Both series and shunt combinations of the cells have been studied. It is shown that the determination of V-I characteristics of the combination of two identical cells is straight forward and the maximum power output of the series as well as shunt combination of two identical cells is twice of the individual cell maximum power output.

The analytical determination of V-I characteristics of both series and shunt connections of nonidentical cells has been discussed in detail. It is shown that the resultant short circuit current of a series combination of two nonidentical cells is not the minimum of the two but lies between the short circuit currents

of the two cells. Exact determination of this current for the combination has been illustrated. Similarly, the determination of exact open circuit voltage when two nonidentical cells are connected in shunt is explained. The hot spot formation in series connection of cells and wastage of power in shunt connection has also been discussed. Maximum power output calculations has been done both for series and shunt combinations of the cells.

It is shown that the maximum power output of the series or shunt combination can never be greater than the sum of the maximum power outputs of the individual cell. The performance of the combination has also been studied experimentally and a close agreement between analytical and experimental results has been obtained.

The method to evaluate the V-I characteristics of a sub-array consisting of large number of cells in series has been outlined and also verified experimentally. The procedures for the determination of V-I characteristics of a series sub-array and shunt connection of these sub-arrays yield the general procedure to get V-I characteristics of a solar cell array of any size. Experimental verification of the performance of the array has also been carried out. It is concluded that the piece-wise linear approximation of the V-I characteristics of individual cells is good enough for the analytical determination of the V-I characteristics of a solar cell array.

The performance of a solar cell array at high intensities and high temperatures has also been studied both analytically and experimentally. An uniformly illuminated cylindrical non-tracking concentrator fabricated at BITS has been employed in the experimental study. It is shown that the variation of the array characterising parameters, R_I , R_{II} and R_{III} with intensity and temperature follows the same trend as observed in the case of a single solar cell.

In the next chapter, the design of a microprocessor based system for characterisation of a solar cell and solar cell array is presented.

.....

REFERENCES

1. Ranschenbach, H., "Electrical Output of Shadowed Solar Arrays", *IEEE Transactions on Electron Devices*, Vol. ED-18, 1971, p 483.
2. Watkins, J.L. and Burgess, E.L., "The Effect of Solar Cell Parameter Variation on Array Power Output", Conference records on 13th IEEE Photovoltaic Specialists Conference, Washington, 1978, p 1061.
3. Goldstein, L.H. and Cage, G.R., "PVSS-Photovoltaic System Simulation Program", *Solar Energy*, Vol. 21, 1978, p 37.
4. Luque, A. et al, "Connection Losses in Photovoltaic Arrays", SUN II, Proceedings of the International Solar Energy Society, Georgia, 1979, p 1851. Also *Solar Energy*, Vol. 25, 1980, p 17
5. Bany, J. et al, "The Influence of Parameter Dispersion of Electrical Cells on the Array Power Output", *IEEE Transactions on Electron Devices*, Vol. ED 24, 1977, p 1032.
6. Luque, A. and Lorenzo, E., "The Effect of Dispersion of the Characteristics of Solar Cells in Large Systems", *Solar Energy*, Vol. 22, 1979, p 187.
7. Ross, R.G. Jr., "Interface Design Considerations for Terrestrial Solar Modules", Conference records of 12th IEEE photovoltaic Specialists Conference, Louisiana, 1976, p 801.

3. Lahiri, R. et al., "An Experimental Study of Series Combination of Solar Cells", Conference records on 13th IEEE Photovoltaic Specialists Conference, Washington, 1978, p 1080.
9. Bhaduri, A., et al., "Electrical Characteristics of Solar Cell Series/Parallel Combinations", Proceedings of National Solar Energy Convention, 1980, p 406.
10. Diamond, R.M. and Steele, E.D., "Solar Arrays with Integral Diodes", Solar Cells, Proceedings of the International Colloquium, Toulouse, France, 1970, p 407.
11. Bogomolny, A. et al., "Reliability Simulation of a Large Solar Cell Battery", Proceedings of Photovoltaic Solar Energy Conference, Luxembourg, 1977, p 1261.
12. Gupta, A. et al., "Design and Testing of a Uniformly Illuminating Nontracking Concentrator", Solar Energy, Vol. 27, 1981, p 387.
